KINETIC CHARACTERIZATION AND NEWLY DISCOVERED INHIBITORS FOR VARIOUS CONSTRUCTS OF HUMAN T-CELL LEUKEMIA VIRUS-I PROTEASE AND INHIBITION EFFECT OF DISCOVERED MOLECULES ON HTLV-1 INFECTED CELLS

By

AHU DEMIR

A DISSERTATION PRESENTED TO THE GRADUATE SCHOOL
OF THE UNIVERSITY OF FLORIDA IN PARTIAL FULFILLMENT
OF THE REQUIREMENTS FOR THE DEGREE OF
DOCTOR OF PHILOSOPHY

UNIVERSITY OF FLORIDA

2010

ProQuest LLC.
789 East Eisenhower Parkway
P.O. Box 1346
Ann Arbor, MI 48106 - 1346

To my beautiful mom

ACKNOWLEDGMENTS

I would like to express my deepest appreciation to my mentor, Professor Ben M. Dunn, for allowing me to work with him on this project and for the independent work environment he provided. I would not be able to finish my dissertation without his guidance and support. I would secondly like to thank my co-advisor and committee member Dr. Gail Fanucci. Her support and ideas have lead and helped me a lot in my research. I would also like to thank other committee members Dr. Nicole Horenstein, Dr. Thomas Lyons and Dr. Nicolo' Omenetto for their guidance and expertise. Their suggestions were invaluable to the progress of this project. Thanks to Dr. Rob McKenna who was willing to participate in my final defense committee in the last year. I would also like to thank the members of the Dunn laboratory, in particular Dr. Melissa R. Marzhan for her support and invaluable scientific advice and her friendship that has made many days bearable and even enjoyable.

Additionally, I would like to thank those that provided technical support during my work, including Mr. Alfred Y. Chung. I would also like to thank Dr. David Ostrov and his lab for his help for computational studies, Dr. Alexander Wlodawer and his lab for his great collaboration and for all the help he provided, and Dr. Tomozumi Imamichi and Dr. Raphael Oguariri for their help and support for cell assays.

I would specifically love to thank my mom who has never stopped believing in me, who has supported me and actually inspired me to accomplish my dreams, who made me a strong woman and made me believe that I can move the world if I try hard enough. I would not have been where I am or who I am without her. I would like to thank my father for his love. I hope he is proud of me; if he is watching as said. I could not have

made it without my brother who helped me and supported me throughout. He has always been a good objective supporter.

Last, but certainly not least I want to thank to my friends Meryem Demir and Aysun Altan for listening to all of the complaints, for giving me advice and always being there for me. There is no way I would have finished without them. I also want to thank Dacia Kwiatkowski, painful part of PhD was much more fun with her. Thanks to the many others I cannot finish writing who contributed my beautiful days during my Ph.D. work in Gainesville.

TABLE OF CONTENTS

LIST OF TABLES

LIST OF FIGURES

LIST OF AMINO ACID ABBREVIATIONS

Alanine	Ala	A
Arginine	Arg	R
Asparagine	Asn	N
Aspartic Acid	Asp	D
Cysteine	Cys	C
Glutamic Acid	Glu	E
Glutamine	Gln	Q
Histidine	His	H
Isoleucine	Ile	I
Leucine	Leu	L
Lysine	Lys	K
Methionine	Met	M
Phenylalanine	Phe	F
Proline	Pro	P
Serine	Ser	S
Threonine	Thr	T
Tryptophan	Trp	W
Tyrosine	Tyr	Y
Valine	Val	V

LIST OF ABBREVIATIONS

BME	2-β-mercaptoethanol
ºC	degrees centigrade
$CaCl_2$	calcium chloride
ddH_2O	double-distilled water
DNA	deoxyribonucleic acid
dNTPs	deoxyribonucleotide triphosphate
DDT	dichlorodiphenyltrichloroethane
EDTA	ethylenediaminetetraacetic acid
Etot	total amount of enzyme
FPLC	Fast Protein Liquid Chromatography
g	gram(s)
HAART	Highly Active Antiretroviral Therapy
HIV-1	Human Immunodeficiency Virus-1
hr:	hour(s)
IPTG:	isopropyl-B–D-1-thiogalactopyranoside
k_{cat}:	turnover number (maximum number of enzymatic reactions catalyzed per second)
K_m	Michaelis constant
L	liter(s)
LB	Luria Broth
LSB	Laemmeli sample buffer
M	molar
mg	milligram

$MgCl_2$	magnesium chloride
mL	milliliter(s)
mM	millimolar
NaCl	sodium chloride
NaOH	sodium hydroxide
ng	nanograms(s)
nM	nanomolar
OD	optical density
PCR	polymerase chain reaction
PIs	Protease Inhibitors
BLV	Bovine leukemia virus
MuLV	Mmurine leukemia virus
SIV	Simian immunodeficiency virus
FIV	Feline immunodeficiency virus
EIAV	Equine infectious anemia virus
RSV	Rous sarcoma virus
mwco	Molecular weight cut off

Abstract of Dissertation Presented to the Graduate School
of the University of Florida in Partial Fulfillment of the
Requirements for the Degree of Doctor of Philosophy

KINETIC CHARACTERIZATION AND NEWLY DISCOVERED INHIBITORS FOR VARIOUS CONSTRUCTS OF HUMAN T-CELL LEUKEMIA VIRUS-I PROTEASE AND INHIBITION EFFECT OF DISCOVERED MOLECULES ON HTLV-1 INFECTED CELLS

By

Ahu Demir

December 2010

Chair: Gail Fanucci
Cochair: Ben Dunn
Major: Chemistry

Discovered in 1980, HTLV-1 (Human T-cell Leukemia Virus-1), was the first identified human retrovirus and is shown to be associated with a variety of diseases including: adult T-cell leukemia lymphoma (ATLL), tropical spastic paraparesis/HTLV-1 associated myelopathy (TSP/HAM), chronic arthropathy, uveitis, infective dermatitis, and polymyositis. The mechanism by which the virus causes disease is still unknown. HTLV-1 infection has been reported in many regions of the world but is most prevalent in Southern Japan, the Caribbean basin, Central and West Africa, the Southeastern United States, Melanesia, parts of South Africa, the Middle East and India. Approximately 30 million people are infected by HTLV-1 worldwide, although only 3-5% of the infected individuals evolve Adult T-cell Leukemia (ATL) during their life and the prognosis for those infected is still poor.

The retroviral proteases (PRs) are essential for viral replication because they process viral Gag and Gag-(Pro)-Pol polyproteins during maturation, much like the PR from Human Immunodeficiency Virus-1 (HIV-1). Various antiviral inhibitors are in clinical use and one of the most significant classes is HIV-1 PR inhibitors, which have used for

antiretroviral therapy in the treatment of AIDS. HTLV-1 PR and HIV-1 PR are homodimeric aspartic proteases with 125 and 99 residues, respectively. Even though substrate specificities of these two enzymes are different, HTLV-1 PR shares 28% similarity with HIV-1 PR overall and the substrate binding sites have 45% similarity.

In addition to the 125-residue full length HTLV-1 PR, constructs with various C-terminal deletions (giving proteases with lengths of 116, 121, or 122 amino acids) were made in order to elucidate the effect of the residues in the C-terminal region. It was suggested that five amino acids in the C-terminal region are not necessary for the enzymatic activity in Hayakawa et al. 1992. In 2004 Herger et al. had suggested that 10 amino acids at the C-terminal region are not necessary for catalytic activity. A recent paper suggested that C-terminal residues are essential; and that catalytic activity lowers upon truncation, with even the last 5 amino acids necessary for full catalytic activity (*1*).

The mutation L40I has been made to prevent autoproteolysis and the W98V mutation was made to make the active site of HTLV-1 PR similar to HIV-1 PR. We have characterized C-terminal amino acids of HTLV-1 PR as not being essential for full catalytic activity. We have discovered potential new inhibitors by *in silico* screening of 116-HTLV-1 PR. These small molecules were tested kinetically for various constructs including the 116, 121 and 122-amino acid forms of HTLV-1 PR. Inhibitors with the best inhibition constants were used in HTLV-1 infected cells and one of the inhibitors seems to inhibit gag processing.

CHAPTER 1
INTRODUCTION

Retroviruses

Retroviruses are a large family of RNA enveloped viruses. The mechanism of retroviral transcription differs from other organisms in that RNA is reverse transcribed into DNA which is integrated into the host genome then translated to proteins. Retroviral virions are 100 nm in diameter and packaged in 10 kilo bases double stranded RNA (*2, 3*).

Retroviruses have recently been classified into two groups; simple and complex viruses, based on their genome organization (*2*). Simple viruses include Gag (group antigen), which encodes for; the matrix, capsid and nucleocapsid protein, Pol (polymerase), which encodes for reverse transcriptase and integrase and Env (envelope), which encodes for surface and transmembrane proteins such as glycoprotein gp45 and gd20 (*4*). Complex viruses include extra non-structural genes besides Gag, Pol and Env (*2*). Although Murine Leukemia Virus (MLV) is a simple virus, Human Leukemia Virus-1 (HTLV-1) and Human Immunodeficiency Virus (HIV-1) are complex viruses because of their regulatory genes tax and tat, respectively. Beside the recent classification, retroviruses have been combined in three groups as oncoviruses, lentiviruses and spumaviruses according to morphology of the virions as well as the genomic structures. Not all the oncoviruses cause tumor formation and they are classified morphologically into three sub-groups as B-, C- and D-type particles (*5*). HTLV-1 is an oncovirus (*2*). Lentiviruses are associated with slow disease with long latent period such as HIV-1 and HIV-2 (*6, 7*). Spumaviruses, are known as foamy

viruses, cause pathogenic changes in the infected cell (*7*). Feline foamy virus is an example of spumavirus type (*6*).

HTLV-1

HTLV-1 is a C-type oncovirus, and is classified as a complex virus. According to the The International Committee on Taxonomy of Viruses (http://www.ncbi.nlm.nih.gov/ICTVdb/), it is classified in the *Retroviridae* group and Deltaretrovirus subgroup with Bovine Leukemia Virus (BLV-1), Simian T-lymphotropic Virus-1-2 and 3 (STLV-1, 2, 3) (*8*). HIV-1 is in the Lentiretovirus subgroup, and thus differs from HTLV-1. HIV-1 is non-oncogenic, while HTLV-1 is oncogenic. HIV-1 has a conical capsid, while HTLV-1 has a spherical capsid (*9*).

Discovered in 1980, HTLV-1 (Human T-cell Leukemia Virus-1), was the first identified human retrovirus and is associated with a variety of diseases including: adult T-cell leukemia lymphoma (ATLL) (*10*), tropical spastic paraparesis/HTLV-1 associated myelopathy (TSP/HAM) (*11*), chronic arthropathy (*12*), uveitis (*13*), infective dermatitis (*14*), and polymyositis (*15, 16*).

HTLV-1 infection has been reported in many regions of the world but is most prevalent in Southern Japan (*17*), the Caribbean basin (*18, 19*), Central and West Africa (*20-23*), the Southeastern United States, Melanesia (*19*), parts of South Africa, the Middle East and India (*19, 24, 25*). (Figure 1-1) HTLV-1 subtype A, known as cosmopolitan subtype, is found in many endemic areas like Japan, the United States and Europe (*26*). Subtype B, D and F are found in Central Africa; subtype F in Central and South Africa; and subtype C in Asia (*26*). Approximately 30 million people are infected by HTLV-1 worldwide, and though only 3-5% of the infected individuals evolve ATL in their life, the prognosis for those infected is still poor (*27, 28*).

History and Discovery

HTLV-1 was first isolated from a cutaneous lymphoma patient on 1980 by Gallo (*29-32*). It was detected in T-cells of a patient who had mycosis fungoides. The newly recognized ATL was described by Uchiyama on 1977 (*10*), and this research suggested ATL antigen expressed by cell lines from ATL patients was recognized by antibodies in all serum of ATL patients. Anti-ATLA (adult T-cell leukemia virus-associated antigen) was detected in 1982; and another isolation was reported in 1981 (*33*). It was shown that both human T-cell leukemia virus (HTLV) and adult T-cell leukemia virus (ATLV) isolates were identical based on gene-specific probes (*34*).

Global Implications

Table 1-1 shows the countries that have the most prevalent HTLV-1 infection. Japan is the country with the highest level of HTLV-1 infection at 10% of the population, followed by the Caribbean with 6%, and sub-Saharan Africa with 5% HTLV-1 infection (*19, 25*). Most of the data of HTLV-1 prevalence rate is from selected populations, general population information is rare in these studies (*25*). The implications in Europe and United States are due to immigration or sexual contact with people from endemic areas (*25*).

Transmission

HTLV-1 is transmitted primarily in three ways: mother–infant (mainly through breastfeeding) (*35*), sexual contact (*36*) and infected blood transmission (*37, 38*). Even though there is no case, transmission through saliva might be possible because of presence of proviral DNA and HTLV-1 antibodies (*39*). For all three routes, infected cells must be passed from the infected individual because the living HTLV-1 infected cells are essential for infection that occurs primarily with cell-cell contact (*40, 41*). The HTLV-1

infected cell and another cell form biological synapses, and viral RNA is transmitted to the target cell. Although HTLV-1 can infect almost any mammalian cell in vitro, it can only infect T-cells in vivo for an unknown reason (*42*). The transmission mechanism of HTLV-1 is not clearly understood *in vivo* or *in vitro* (*43*).

Prevention and Treatment

The median survival of adults with T-cell leukemia and lymphoma (ATLL) is determined as 1 year despite advances in both chemotherapy and supportive care. Cyclophosphamide (inhibits cell division, brand name **c**ytoxan), adriamycin (doxorubicin/ **h**ydroxydoxorubicin), vincristine (**o**ncovin, inhibits cell division), and **p**rednisolone drug therapy (CHOP) is one of the methods that has been used for treatment of ATLL patients and results in either complete remission (CR) or partial remission (PR). The more potent chemotherapy, consisting of VCAP (vincristine, cyclophosphamide, and adriamycin, which prevents RNA or DNA replication, and prednisolone), AMP (doxorubicin, ranimustine [MCNU], and prednisolone), and VECP (vindesine, etoposide, carboplatin, and prednisolone), improves the prognosis of ATL (*44*). However, the overall prognosis of ATL is still poor despite intensive chemotherapy (*45*). Another combination that had been used is zidovudine plus interferon (ZDV/IFN which is a HIV-1 RT inhibitors) that gives a better CR result when it is used for the first-line therapy (*46*). Zidivudine is a drug used for HIV therapy.

There are 6 classes of more than 20 approved antiretroviral drugs used to cure AIDS. Nucleoside/nucleotide reverse transcriptase inhibitors (NRTIs), non-nucleoside reverse transcriptase inhibitors (NNRTIs), protease inhibitors (PIs), fusion inhibitors (FIs), CCR5 antagonists, and integrase strand transfer inhibitors (INSTI) are the 6 different classes of drugs. Two NRTIs plus either one NNRTI or a PI are the most extensively

studied combination regimens (*47*). Even though NNRTI-, PI- and INSTI-based regimens are equal alternatives according to current guidance, there are selected patients whom PI-based regimen seems to show the best result considering toxicity and dosing of the regimens (*48*). Introducing PIs to HIV treatment combinations in 1996 has predominantly lowered the morbidity and mortality due to HIV infection (*48*). The addition of an inhibitor of HTLV-1 PR might have the same kind of beneficial effect seen with HAART in HIV therapy.

The poor prognosis of HTLV-1 infection is associated with high lactate dehydrogenase (LDH) level (*49*). Most of the HTLV-1 infected patients are not able to be treated because of drug resistant leukemia cells (*50, 51*). P-glycoprotein was found to be overexpressed in various multidrug resistant cell lines (*52-54*). Bone marrow transplantation (BMT) has been successfully used to cure ATL (*55*). Allogeneic hematopoietic stem cell transplantation (allo-HSCT) provides sustained long-term survival for patients with adult T-cell leukemia/lymphoma (*56*). There is a case report which suggests unrelated cord blood transplantation (UCBT) should be a therapeutic option for ATL patients who do not have suitable donors and those who urgently require treatment (*57*). All of these treatments need to be studied further.

There is no specific drug treatment for HTLV-1. Anti-HIV or anti-cancer regimens have been used as chemotherapic treatment of ATLL (*51*). There are studies on discovering drugs targeting HTLV-1 PR, reverse transcriptase (RT), integrase (IN) based on the success of antiretroviral treatment of AIDS and most extensively Tax proteins. Tax is a transcriptional activator viral genes, it transforms and immortalizes the T-cells (*58*). Despite the fact that Tax is essential for viral replication, 50% of ATLL patients lose

the ability to produce Tax due to mutations (*59-62*). RT and IN exist in low amounts (5-10 fold less) in the HTLV-1 virion compared to PR; because two frameshifts are necessary to produce Gag-Pro-Pol polyprotein while one frameshift is Gag-Pro necessary for (*63-66*). Therefore HTLV-1 PR is one of the best drug targets for ATLL patients (*67*).

Genome and Structure

HTLV-1 virus particles (80-100 nm in diameter) are enveloped viruses which target CD_4^+ receptor on the host cell and replicates via a proviral DNA intermediate. The HTLV-1 is a single stranded RNA virus; its genome is approximately 9 kb (*68*). It has Gag, Pol, Pro and env genes and uniquely a pX region at the end of the 3' region. pX encodes for tax and rex which are involved in regulation and synthesis and processing of RNA of the virus as shown in Figure 1-2 (*68*). Similar to other retroviruses; Gag encodes for matrix (MA), about 14 kDa, capsid (CA), which provides the core for genomic RNA, is about 24 kDa and nucleocapsid (NC) which is about 12-15 kDa (*69*). Pro encodes for protease (PR) of about 14 kDa that is essential for viral maturation (*70*); and pol encodes for reverse trascriptase (RT, ≈62kDa), which provides the reverse transcription, and integrase (IN,) which helps the viral DNA integrate into host genome. Env encodes for surface protein (SU) about a 60 kDa and transmembrane protein (TM) about 21 kDa. Env proteins help virion to go into the cell (*2, 24*). (Figure 1-3) After protease cleavage which is necessary for maturation, capsid undergoes a morphological change from circle to pentagonal shape (*71, 72*). (Figure 1-3)

Life Cycle

Despite the fact that the mechanism by the virus causes which disease and how is still unknown, steps within the viral replication cycle have been shown to be critical for the development of mature, infectious HTLV-1(*73*).

The virus particle attaches to $CD4^+$ receptor with the gp120 and then enters the cell. (Figure 1-4) The virus releases its RNA and with the help of reverse transcriptase (RT), this single stranded RNA is transcribed into double stranded DNA in the cell cytoplasm. Then this viral DNA is transported into the nucleus of the cell where it is inserted into the host cell DNA with integrase (IN). This form of retrovirus is called a provirus (*74*). Provirus is transcribed by the host-cell RNA polymerase, generating viral RNA. The host-cell machinery translates the viral RNA into proteins. Proteins and RNA assemble into virions that eventually bud from the host cell membrane. These new virions mature and continue the cycle of infection (*9*). (Figure 1-4)

Gag and Gag/Pol Processing

The sequence of Gag-Pro-Pol is shown in Figure 1-5. Ribosomal frameshifting is a process that uses one mRNA to translate more than one protein by changing the reading frame at a specific site or sites. The genes of the most retroviruses are translated as a single polypeptide by ribosomal frameshifting. This process occurs at the overlapping reading frame. There are two frameshifts for HTLV-1: one is in the -1 direction within the Gag-Pro overlap and one is in the Pro-Pol overlap to synthesize Gag, Gag-Pro, and Gag-Pro-Pol polyproteins (*65, 75*). Gag, Gag-Pol processing essential for viral maturation (*76*).

HTLV-1 Protease

Proteases are enzymes that catalyze the hydrolysis of proteins, belong to hydrolases group of enzymes according to the Nomenclature Committee of the International Union of Biochemistry and Molecular Biology. They are classified in four groups depending on the type reaction they catalyze, catalytic site residues and relation of the origin of the structure. MEROPS (http://merops.sanger.ac.uk/) is an online

database which is a source to get information about proteases (such as name, identifier, gene name, organism and substrates) or their protein inhibitors (*77*). Proteases are divided further in three categories based on peptidase, family based on their sequences and clan according to their evolutionary origin. The most common classification is based on their catalytic residues which are combined in five subgroups: aspartic acid, serine, cysteine, metalloproteases and unknown or mixed active site proteases.

HTLV-1 protease belongs to the aspartic acid protease family; which catalyzes an acid-base mechanism (*78*). An enzyme bound water molecule attacks the amide bond to form a tetrahedral intermediate; then the conjugate base aspartate attacks to the intermediate to take the hydrogen so the amide nitrogen is expelled as the leaving group (*78*). (Figure 1-6)

The retroviral proteases (PRs) are essential for viral replication because they process viral Gag and Gag-(Pro)-Pol polyproteins during maturation, much like the PR from HIV-1 (Human Immunodeficiency Virus-1) (*62, 79, 80*). Various antiviral inhibitors are in clinical use and one of the most significant classes are HIV-1 PR inhibitors, which have proved to be an invaluable component of antiretroviral therapy in the treatment of AIDS (*81*). HTLV-1 PR and HIV-1 PR are homodimeric aspartic proteases with 125 and 99 residues, respectively, in the monomers. Even though substrate specificities of these two enzymes are different, HTLV-1 PR shares 28% homology with HIV-1 PR overall and the substrate binding sites have 45% homology (*82*).

Structure

HTLV-1 PR (116 residues) has been crystallized by Mi Li in 2005 (*27, 83*). (Figure 1-7) The protease was co-crystallized with Ac-Alanine-Proline-Glycine-Valine-Statin-Valine-Methionine-Histidine-Proline inhibitor and the structure was refined at 2.5 Å

resolution. It had three homodimeric molecules per unit. When the structure was superimposed with 7 other retroviral proteases, it was seen that the flap, active site and the dimerization regions were conserved; while the elbow region of the proteases were divergent (*83-88*). (Figure 1-8) One of the different features of HTLV-1 PR compared to the other retroviruses is the presence of the two water molecule between the tips of the flaps (*83*). There are extra additional amino acids at the C-terminal region of HTLV-1 protease compared to other aspartic acid proteases; it is only similar to Bovine Leukemia Virus-1 (BLV-1) PR (*83-89*). (Figure 1-9)

Substrate

Natural substrate cleavage sites are shown in Table 1-2 (*90*). Even though natural cleavage sites of HTLV-1 PR and HIV-1 PR are similar, their substrate specificities are different (*82*). Based on cross reactivity of PRs using a vaccinia virus, it was determined that HTLV-1 PR was able process BLV Gag protein, but not HIV-1 PR Gag protein (*91*). This result shows there are other effects on PR cleavage beside the primary amino acid sequence.

There is a nomenclature for naming the sub-sites of the substrate and the enzyme (*92*). (Figure 1-10) The cleavage bond is called the scissile bond and the amino acid next to it on the left is called P1 amino acid and to the right is called the P1' amino acid; the numbers increase getting further away from the bond. The same procedure is applied for enzyme subsites that interact with each amino acid of a substrate or an inhibitor as S1 and S1' (*27*).

All retroviral PRs prefer hydrophobic large residues at the P1 subsite; and HTLV-1 PR prefers a hydrophobic P4 amino acid. S1/S1' The Trp98 has a drastic effect on the H-bonding and binding of inhibitor because of its big side chain. Four residues are

identical, and two are different in the S1 and S1' pockets in 7 retroviral proteases. This subsite is large and hydrophobic (*27, 68, 73*). S2/S2' Beside Met37, all the other residues are the same or similar. This subsite is large and hydrophobic. In subsites S3/S3' 3 amino acids are different out of 6 amino acids. Trp98 has a big effect based on its side chain. Subsites S4/S4' are hydrophobic and subsites S5/S5' are hydrophilic (*27, 68, 73*).

Inhibitors

Even though, HTLV-1 PR is significantly similar to HIV-1 PR, they have different inhibitor specificity (*73, 93, 94*). According to the literature and our experiments; it was determined that clinically used HIV-1 PR inhibitors have no or little inhibition effect on HTLV-1 PR (*73*). Based on the crystal structure of 116-residue HTLV-1 PR; the steric effect of Trp98 and Leu57 side chains might prevent possible inhibitor-protease interactions (*27*).

Although HTLV-1 PR is an aspartic acid protease, pepstatin; which is an aspartic acid protease inhibitor has a low inhibition effect on HTLV-1 PR (K_i ≤100 μM) (*95*). The best inhibitor for HTLV-1 PR is JG-365, a HIV-1 PR inhibitor, with K_i of 6.0 nM (*93*). The second most efficient inhibitor is a peptide inhibitor with K_i of 38 nM, followed by a non-peptide inhibitor MES13-099 with K_i of 243 nM (*93, 96*). The cleavage products of (30-180 μM) APQVLNphVMHPL synthetic peptide by 1-5 μM protease were measured by C18 column by eluting with a linear gradient of 30-45% acetonitrile (0.1% TFA) and was monitored at 210 nm for these two inhibitors (*93*). Buffer including 100 mM sodium citrate, 5 mM EDTA, 1 mM DTT, and 1 M NaCl, pH 5.3) was used and the reactions were incubated at 37 °C for 5 min (*93*).

There are a couple of novel inhibitors (KNI-10729 and KNI-10516 that give 79% and 86 % inhibition at 50 nM concentration, respectively) found by Dr. Wlodawer's lab recently (*83*). The hydrolysis of the (0.2 mM) substrate fluorescent substrate(H-Lys ([7-methoxycoumarin-4-yl]acetyl)-APQVL–(p-nitrophenylalanine)–VMHPL-OH) by 1 µg protease was determined in 0.2 M citrate buffer (pH 5.3), 1 mM dithiothreitol, 1 M NaCl, 5 mM EDTA, 6% v/v glycerol, and 2% v/v DMSO solution at different inhibitor concentrations, and the reaction proceeded at 37ºC for 30 min, then the reaction was terminated with 20% aqueous trichloroacetic acid (15 lL). IC50 value was calculated by measuring the hydrolyzed substrate fragments and/or non-hydrolyzed substrate by probit model HPLC using a YMC-Pack Pro C18 column (linear gradient: 5–35% CH3CN in 0.1% aqueous TFA; 1.0 mL/min; 215 nm; 40ºC), and the calculated from standard curves of the areas under the peaks at 6, 10, and 13 min by probit model (*97*).

The structures of the inhibitors are shown in Figure 1-11.

Table 1-1. Percent prevalence of countries which are highly infected by HTLV-1 PR

Country	Prevalence
Japan (*98*)	10%
Caribbean (*14*)	6%
sub-Saharan Africa (*99*)	5%
Iran and Melanesia (*100*)	<5%
Europe and USA (*101*)	0.01–0.03%

Table 1-2. Cleavage junction sequence of HTLV-1 PR

Cleavage junction	HTLV-1 amino acid sequence
MA/CA	PQVL/PVMH
CA/NC	TKVL/VVQP
Gag/PR	ASIL/PVIP
PR/Pol	PVIL/PIQA
Pro/RT	PAVL/GLEL
RT-RH/IN	VLQL/SPAD

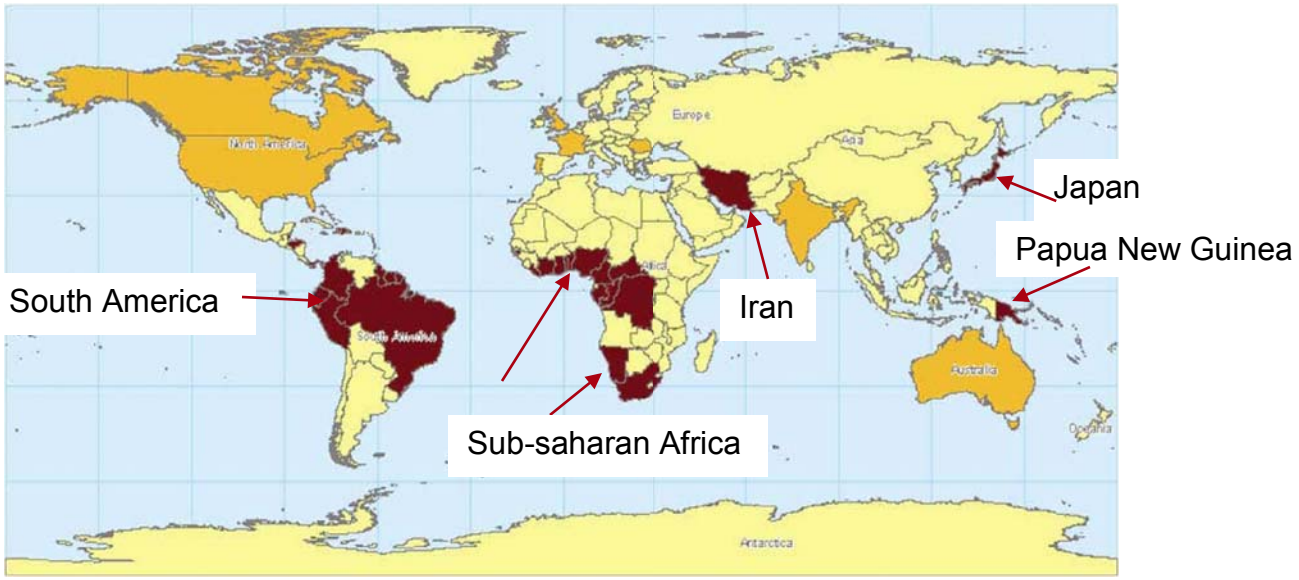

Figure 1-1. World map showing HTLV-1 endemic areas. Countries prevalence between 1-5% are shown in dark brown, less than 1% in orange (adapted from Proietti, F. A et al. 2005).

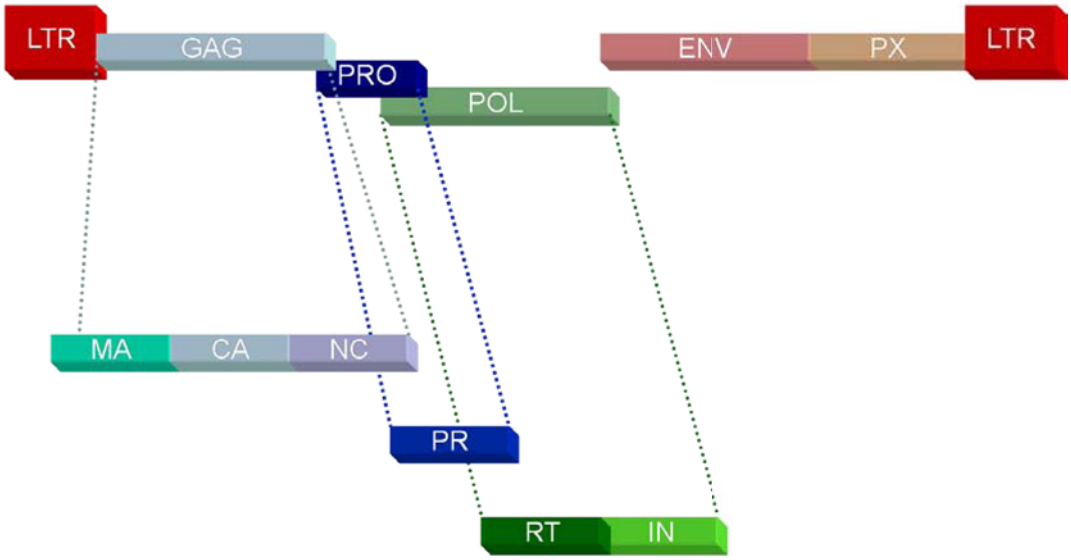

Figure 1-2. HTLV-1 genome cartoon picture. Gag, Pro, Pol, , Env and Px open reading frames are shown in various color and they are flanked by long terminal repeats shown in red (adapted from Shuker, S. B. et al. 2003).

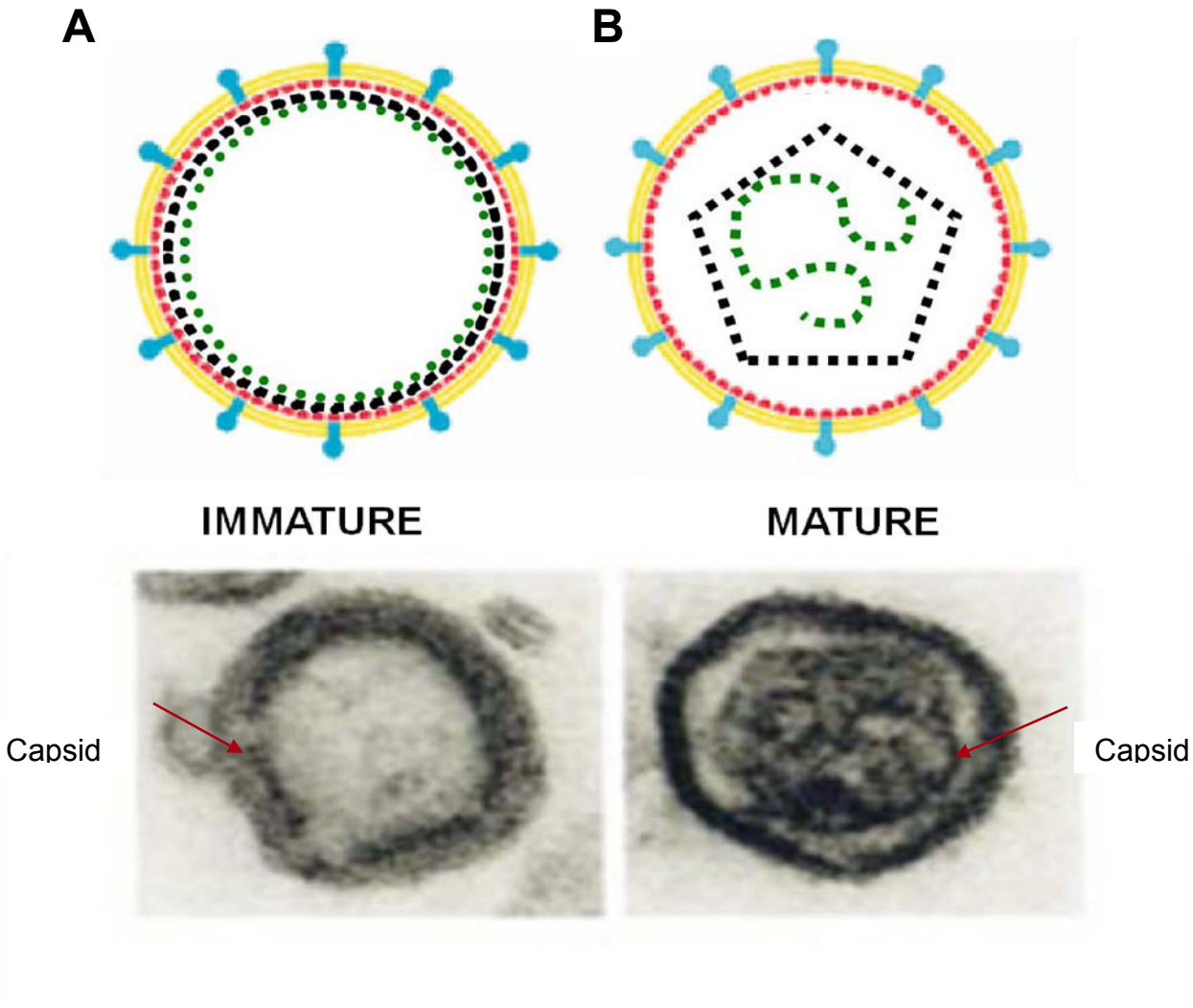

Figure 1-3. HTLV virion. A) Immature B) Mature. Lipid bilayer is shown in yellow, matrix (MA) is shown in red, capsid (CA) in black, NC in green. The electromicrograph of the mature and immature form of HTLV-1 is shown under the cartoon representation (adapted from Jiang, F. et al. 2000, and Briggs, J. A. 2004).

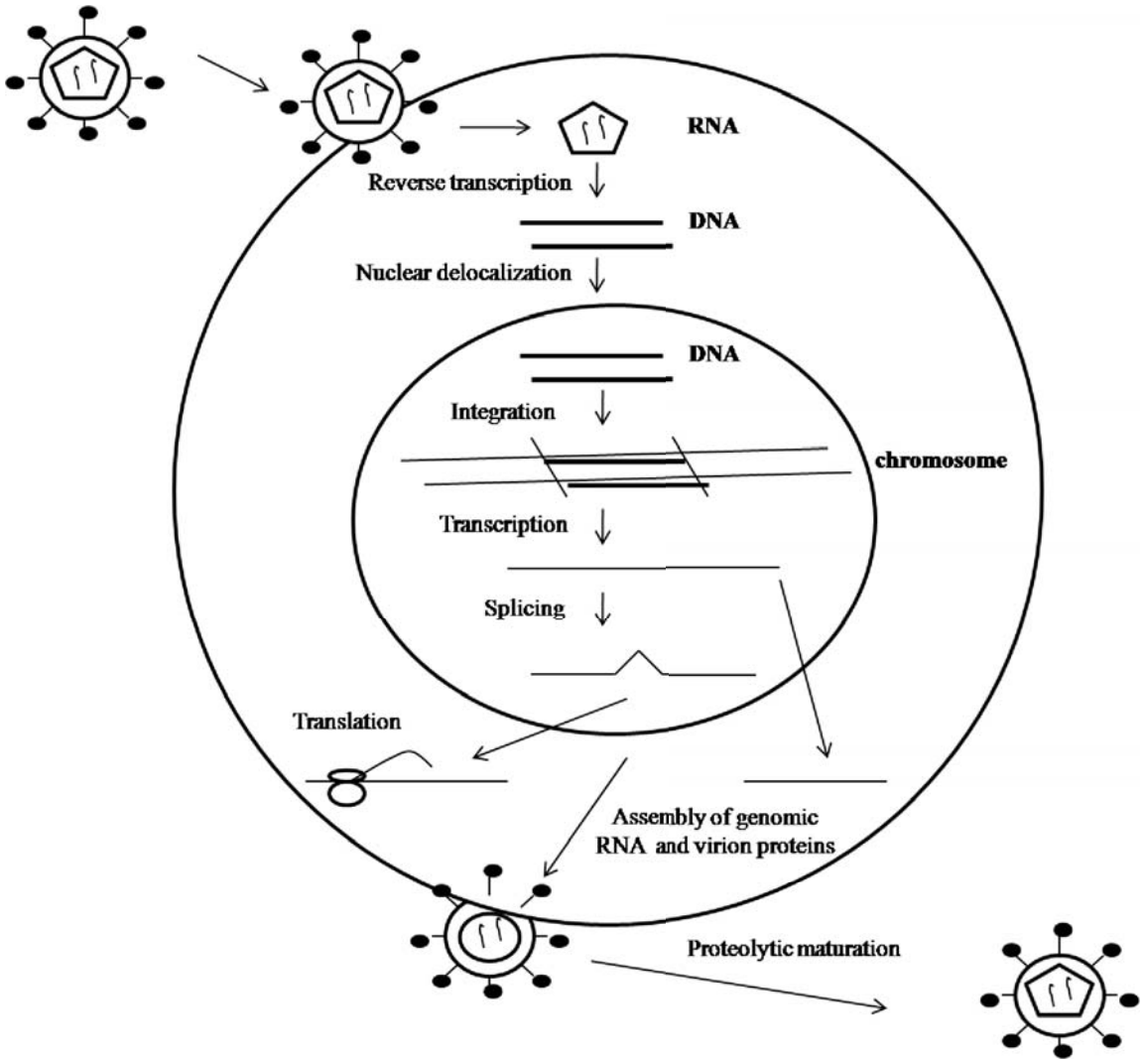

Figure 1-4. Retrovirus life cycle (adapted from Coffin, J. M. H. et al. 1997).

MGQIFSRSASPIPRPPRGLAAHHWLNFLQAAYRLEPGPSSYDFHQLKKFLKIALETPVWICPINY
SLLASLLPKGYPGRVNEILHILIQTQAQIPSRPAPPPPSSSTHDPPDSDPQIPPPYVEPTAPQVL
PVMHPHGAPPNHRPWQMKDLQAIKQEVSQAAPGSPQFMQTIRLAVQQFDPTAKDLQDLLQYLCSS
LVASLHHQQLDSLISEAETRGITGYNPLAGPLRVQANNPQQQGLRREYQQLWLAAFAALPGSAKD
PSWASILQGLEEPYHAFVERLNIALDNGLPEGTPKDPILRSLAYSNANKECQKLLQARGHTNSPL
GDMLRACQAWTPKDKTKVLVVQPKKPPPNQPCFRCGKAGHWSRDCTQPRPPPGPCPLCQDPTHWK
RDCPRLKPTIPEPEPEEDALLLDLPADIPHPKNLHRGGGLTSPPTLQQVLPNQDPTSILPVIPLD
PARRPVIKAQIDTQTSHPKTIEALLDTGADMTVLPIALFSSNTPLKNTSVLGAGGQTQDHFKLTS
LPVLIRLPFRTTPIVLTSCLVDTKNNWAIIGRDALQQCQGVLYLPEAKRPPVILPIQAPAVLGLE
HLPRPPEISQFPLNPERLQALQHLVRKALEAGHIEPYTGPGNNPVFPVKKANGTWRFIHDLRATN
SLTIDLSSSSPGPPDLSSLPTTLAHLQTIDLKDAFFQIPLPKQFQPYFAFTVPQQCNYGPGTRYA
WRVLPQGFKNSPTLFEMQLAHILQPIRQAFPQCTILQYMDDILLASPSHADLQLLSEATMASLIS
HGLPVSENKTQQTPGTIKFLGQIISPNHLTYDAVPKVPIRSRWALPELQALLGEIQWVSKGTPTL
RQPLHSLYCALQRHTDPRDQIYLNPSQVQSLVQLRQALSQNCRSRLVQTLPLLGAIMLTLTGTTT
VVFQSKQQWPLVWLHAPLPHTSQCPWGQLLASAVLLLDKYTLQSYGLLCQTIHHNISTQTFNQFI
QTSDHPSVPILLHHSHRFKNLGAQTGELWNTFLKTTAPLAPVKALMPVFTLSPVIINTAPCLFSD
GSTSQAAYILWDKHILSQRSFPLPPPHKSAQRAELLGLLHGLSSARSWRCLNIFLDSKYLYHYLR
TLALGTFQGRSSQAPFQALLPRLLSRKVVYLHHVRSHTNLPDPISRLNALTDALLITPVLQLSPA
DLHSFTHCGQTALTLQGATTTEASNILRSCHACRKNNPQHQMPQGHIRRGLLPNHIWQGDITHFK
YKNTLYRLHVWVDTFSGAISATQKRKETSSEAISSLLQAIAYLGKPSYINTDNGPAYISQDFLNM
CTSLAIRHTTHVPYNPTSSGLVERSNGILKTLLYKYFTDKPDLPMDNALSIALWTINHLNVLTNC
HKTRWQLHHSPRLQPIPETHSLSNKQTHWYYFKLPGLNSRQWKGPQEALQEAAGAALIPVSASSA
QWIPWRLLKRAACPRPVGGPADPKEKDHQHHG

Figure 1-5. Gag-Pro-Pol sequence of HTLV-1. Matrix is shown in dark blue (130 amino acids), capsid is shown in green (214 amino acids), nucleocapsid is shown in light blue (105 amino acids), protease is shown in red (125 amino acids), reverse transcriptase is shown in blue (563 amino acids) and integrase is shown in orange (300 amino acids)

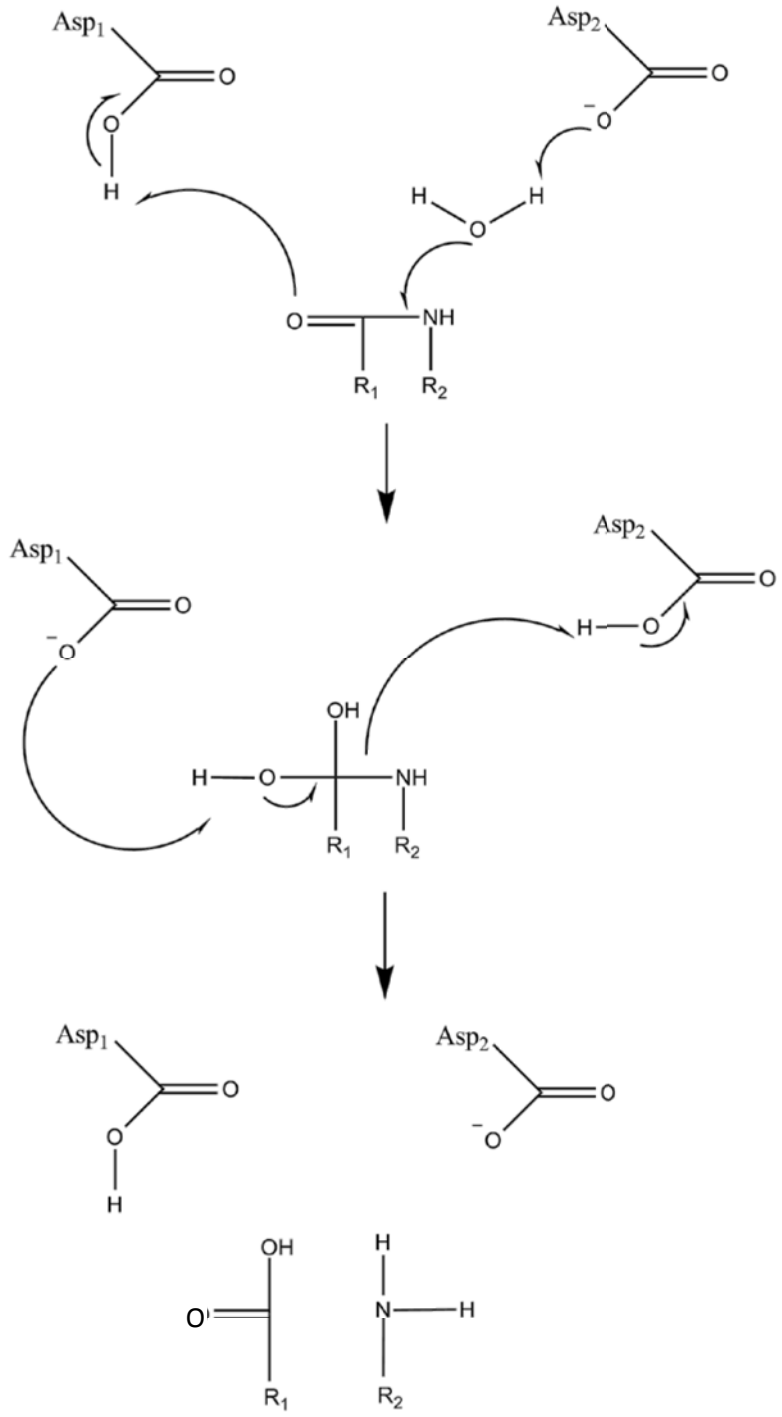

Figure 1-6. Mechanism of aspartic acid protease-catalyzed peptide cleavage (adapted from Liu, H. et al. 1996).

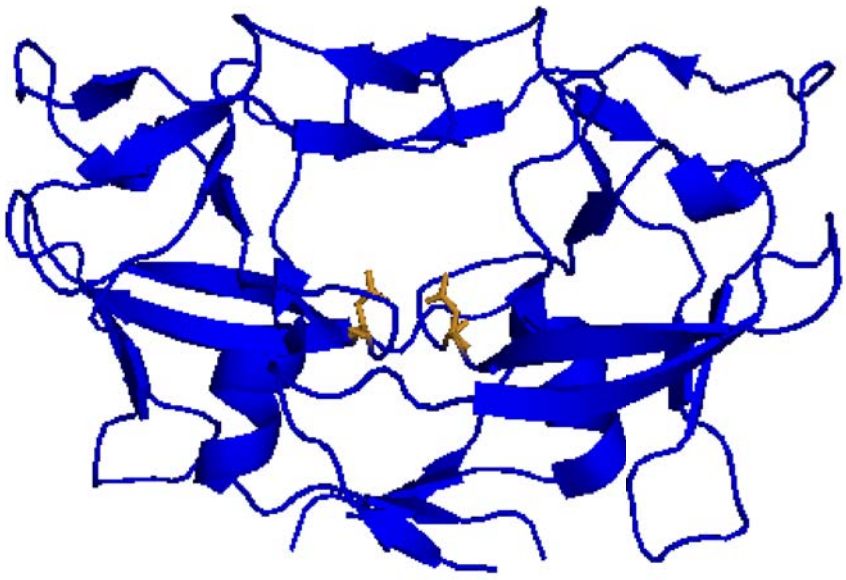

Figure 1-7. Cartoon of the crystal structure of 116-residue HTLV-1 PR (PDB#2B7F). Aspartic acid residues are shown in orange sticks (adapted from Satoh, T. et al. 2010).

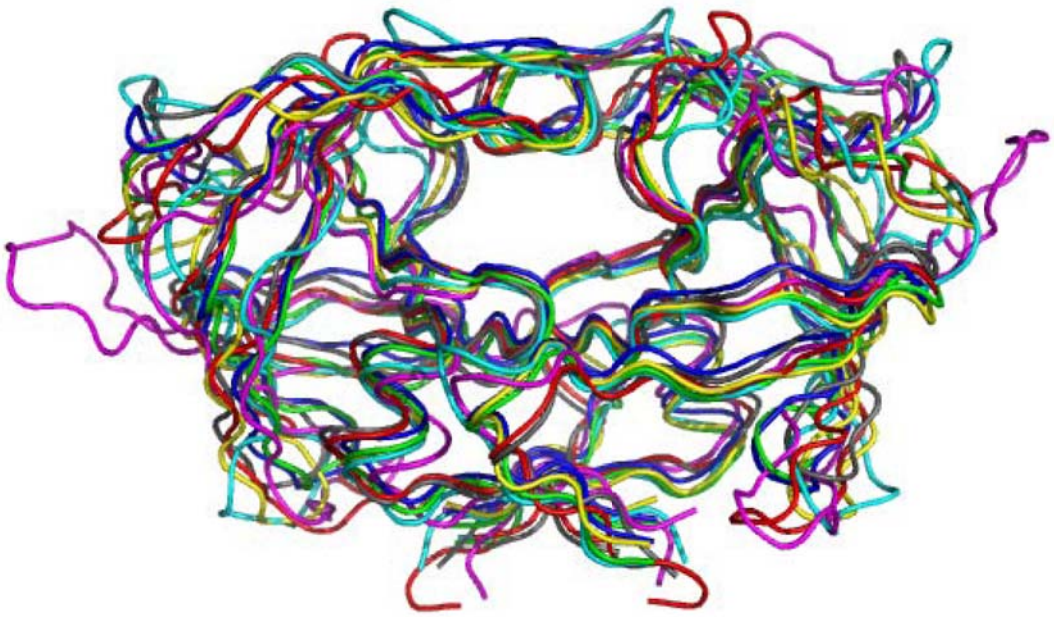

Figure 1-8. Superposition of seven retroviral PRs shown in ribbon representation.HTLV-1 PR is colored blue (PDB#3LIY); HIV-1 PR (PDB#2FLE), green; HIV-2 PR (PDB#3EBZ), dark blue; SIV PR (PDB#2SAM), gray; RSV PR (PDB#2RSP), magenta; EIAV PR (PDB#2FMB), yellow; and FIV PR (PDB#4FIV), red.

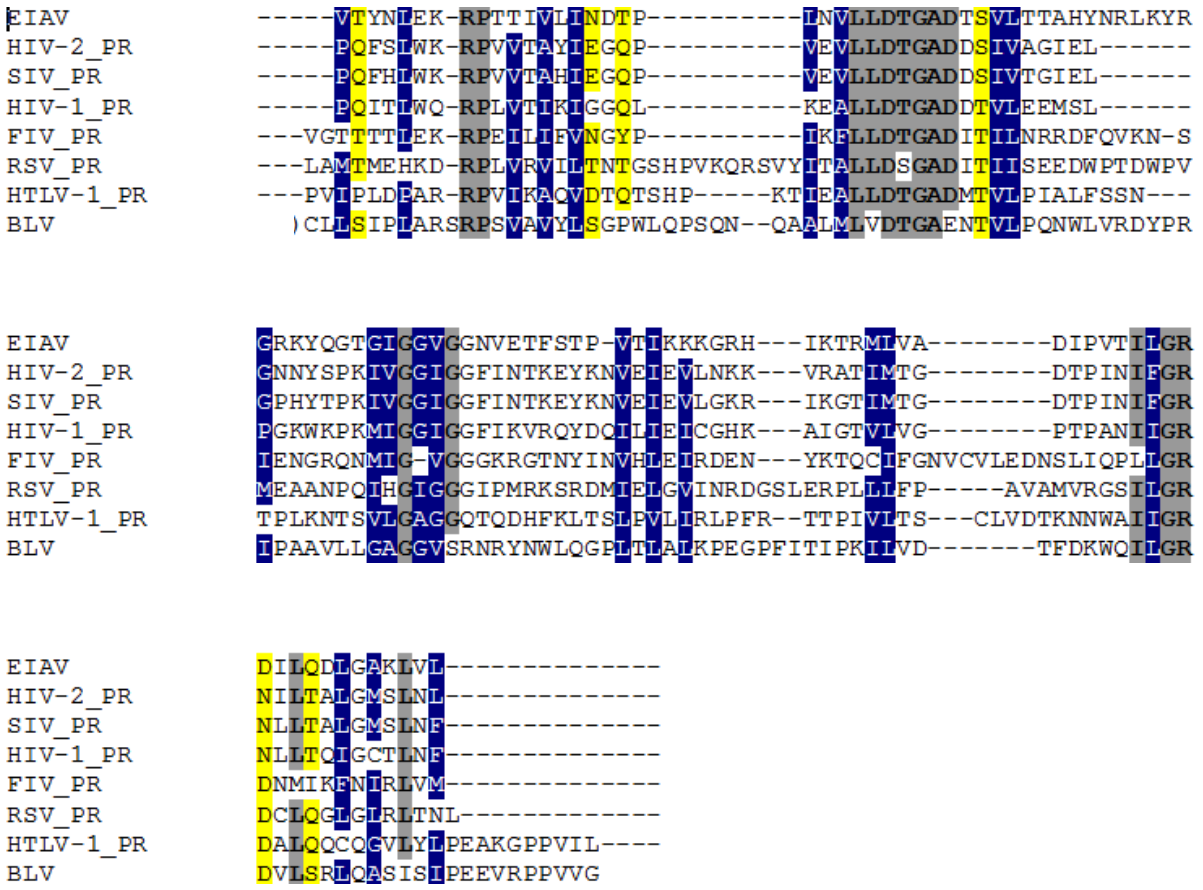

Figure 1-9. Sequence Alignment of the Leukemia Retrovirus Proteases with Retroviral Proteases of Known Structure (besides BLV). The alignment for HIV-1, HIV-2, SIV, FIV, EIAV, and RSV proteases was generated based on the reported structures (PDB IDs: HIV-1, 2FLE; HIV-2, 3EBZ; SIV, 2SAM; FIV, 4FIV; EIAV, 2FMB; and RSV, 2RSP). Hydrophobic residues are indicated in blue, hydrophilic residues in yellow.

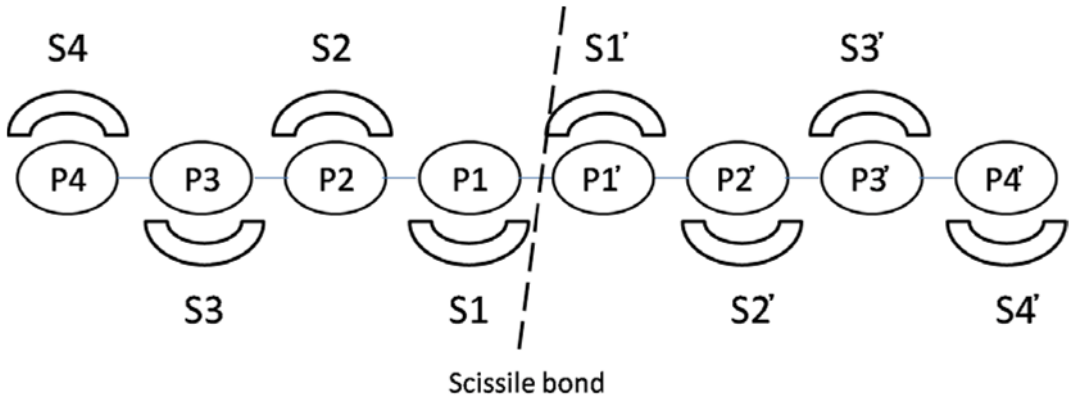

Figure 1-10. Nomenclature of enzyme and substrate subsites (adapted from Schechter, I. et al. 1967).

.

A **B**

R1: Ac-Ser-Leu-Asn R2: Ile-Val-OMe R1: H-Pro-Val-Ile R2: $CH_2C_6H_4I$

C

D

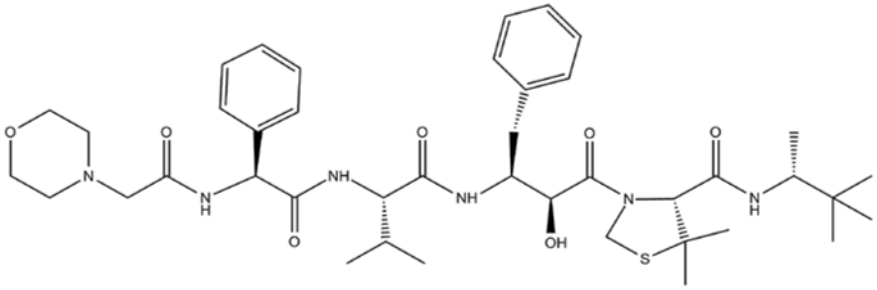

E

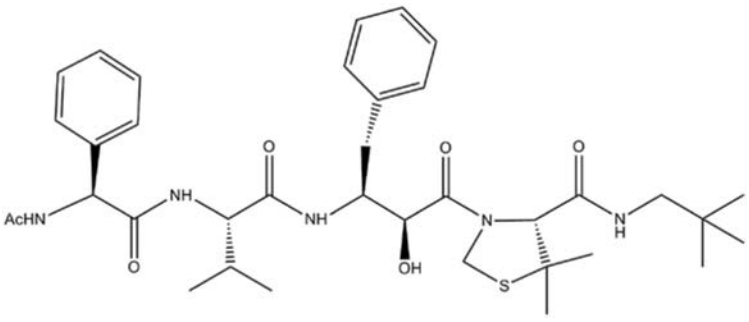

Figure 1-11. Structures of the best inhibitors of HTLV-1 PR. A.JG-365, B.Compound 31,C. MES13-099, D.KNI-10729, E.KNI-10516

CHAPTER 2
MATERIALS AND METHODS

Site Directed Mutagenesis

The HTLV-1 PR gene, which was obtained from NIH, was cloned into a pET11a vector (Novagen) using the restriction sites NdeI (NEB) and BamHI (NEB). To make the truncated forms of HTLV-1 PR, a stop codon has been introduced after the appropriate amino acid coding sequence. Complementary primers (Invitrogen) were designed according to the coding and non-coding DNA strand. The reactions were carried out using the Site Directed Mutagenesis Protocol (Stratagene) with 18 cycles of amplification using melting step at 98°C for 3 min followed by an annealing step at 55°C for 1 min, and extension at 72°C for 7 min, then the reaction temperature was dropped to 4°C. To remove template DNA, 1 mL of the restriction enzyme Dpn1 (10 µL /mL) was added to the PCR reaction and the mixture was incubated at 37°C for 1 hr. Successful mutagenesis was confirmed by sequencing (ICBR Core, University of Florida, Gainesville, Florida).

Transformation

Transformation was done with using chemically component cells and One Shot Top 10 (Invitrogen) protocol with some modifications. 2.5 µL of the DNA (32.5 ng/µL) of interest was mixed with 25 µL of cell stock and the mixture was kept on ice for 30 min. The reaction mixture was then heat shocked in a 42ºC water bath for 45 s. The reaction mixture was replaced on the ice immediately for 15 min. Next, 100 µL of SOC media (2.0% Tryptone, 0.5% Yeast Extract, 10 mM NaCl, 2.5 mM KCl, 10 mM $MgCl_2$, and 20 mM glucose, pH 7) were added to the reaction tube and placed in an incubator rotating at 250 rpm at 37°C for an hour. 75 µL of the cell culture were spread onto LB plates

containing ampicillin (50 µg/mL). Plates were incubated at 37°C overnight to promote colony growth. A colony was randomly picked the next day and grown overnight (16 hours) in 10 mL of LB with ampicillin (50 μg/mL). The plasmid DNA was checked by sequencing to verify the correct amino acid sequence and mutations. Transformation into BL21(DE3) Rosetta pLysS cells (Invitrogen) was done with the same method as above with addition of chloramphenicol (34 μg/mL) as well as ampicillin (50 µg/mL).

Protein Expression

LB medium (10 g Bacto-tryptone, 5 g yeast extract, 10 g NaCl in 1L water at pH 7.5) was used for expression. The expressions were initiated with a 4% inoculation from overnight cultures of cells grown in LB media supplemented with 50 μg/mL of ampicillin for BL21 Star DE3 cells or 50 μg/mL of ampicillin and 34 μg/mL of chloramphenicol for BL21 Star DE3 Rosetta pLysS cells. Expression cultures were grown overnight for ~16 hr. When the optical density reached 0.8, protein expression was induced with final concentration of 1 mM isopropyl b-D-thiogalactopyranoside. The cells were allowed to grow for an additional 3 – 4 h and then pelleted by centrifugation at 10000 x g for 10 min (*102*). Cell pellets were stored at -20 º C (*95*).

Inclusion Bodies Extraction

Cell pellets stored at -20°C overnight were thawed and resuspended in buffer (10 mM Tris pH 7.5, 5 mM EDTA) and DNase I was added to a final concentration of 0.1 mg/mL. SLMAminco French Pressure Cell at 1000 psi was used to break cells. After lysing the cells, urea was added to solution to 0.5 M final concentration and stirred for 30 min. Cells were centrifuged at 5000 x g for 10 min. The procedure was repeated until

a clear supernatant was obtained (*27*). Pelleted inclusion bodies (IB) were stored at -80º C. Samples of IB were run on SDS-PAGE gels.

Enzyme Purification and Refolding

The inclusion bodies were solubilized in buffer B (8 M urea, 10 mM Tris-HCl pH 7.5, 5 mM EDTA). All urea solutions were de-ionized by ion exchange to remove cyanates. Solubilized inclusion bodies were loaded onto a Q Sepharose Fast Flow column (Pharmacia) equilibrated with buffer C (6 M urea, 10 mM Tris-HCl pH 7.5, 5 mM EDTA). As the pI of HTLV-1 PR is predicted to be 8.89, it did not bind to the Q Column. The flow through from the column was collected and adjusted to pH 4.0 with acetic acid. Various pH's, as pH 3, 4, and 5, have been tried, pH 4.0 resulted the best yield. (data not shown) The pH adjusted solution was then loaded onto a Sepharose Fast Flow SP column (Pharmacia) equilibrated in buffer D (6 M urea, 20 mM sodium acetate pH 4.0, 5 mM EDTA) (*102*). The PR that bound to the column was eluted with 0.4 M NaCl. Rapid dilution with excess of 10 mM formic acid was used to refold the purified HTLV-1 PR. Size exclusion chromatography was used to determine purification and folding success. Purification of HTLV-1 PR was determined by 18% sodium dodecyl sulfate polyacrylamide gel electrophoresis (SDS).

Kinetic Assays

The enzyme concentrations for HTLV-1 PR preparations were determined by Bradford assay (BioRad) and optical density (OD) reading at 280 nm of the stock solutions after concentrating the purified PR using Amicon ultrafiltration devices (Amicon Ultra-15, Millipore). The chromogenic substrate A-P-Q-V-L*Nph-V-M-H-P-L, which mimics the natural Gag/Pol MA/CA cleavage site, was synthesized by ICBR Core Facility at UF. This substrate was used to assay enzyme activity in 2 X incubation buffer

(0.5 mM potassium phosphate pH 5.6, containing 10% glycerol, 2 mM EDTA, 10 mM dithiothreitol, 2 M NaCl) at 37 °C (*103*). Various NaCl concentrations were used to determine the optimum ionic strength and 2 M was selected based on the highest protease activity. (Data not shown) The enzyme mixture and the substrate were incubated separately at 37 °C for 3 minutes before mixing them and monitoring cleavage of the substrate at 302 nm using a Cary 50 Bio Varian spectrophotometer equipped with an 18-cell multitransport system. The initial rate data for each assay was plotted versus substrate concentration to obtain the characteristic Michaelis-Menten curve. The experimental curve was then fit to the following equation by using Sigma Plot:

$$v = \frac{V_{max} * S}{(K_m + S)} \qquad (3\text{-}1)$$

A non-linear Marquardt analysis was used to determine K_m and V_{max} for the substrate.(*104*) In the above formula v is the rate of product formation, V_{max} is the maximum velocity, S is the substrate concentration, and K_m is the Michaelis-Menten constant, which has the unit of molarity. Every enzyme has a distinct K_m value for a certain substrate. The K_m value of an enzyme represents the substrate concentration required to reach the half of the maximum velocity (V_{max}), is a measure of the concentration of the substrate required for an effective catalysis. The rate of the reaction was derived from the measured change of absorbance per unit time (ΔA/s). The conversion factor was determined by using the exact concentrations of substrate, as determined by amino acid analysis. The initial values of the absorbance (i.e., before substrate cleavage at time zero), and after the completion of substrate cleavage (i.e., after 2 hours) were measured by UV Spectrometry four different substrate

concentrations. A graph was then plotted using the absorbance change versus substrate concentrations. The conversion factor is derived from the slope of the graph that converts the ΔA/s to μM/s. The conversion factor used in this assay is 0.00123 determined by Dr. Roxana Coman..

The k_{cat} values were determined using the following equation:

$$k_{cat} = \frac{V_{\max}}{E_{tot}} \tag{3-2}$$

k_{cat} is the turnover number of the enzyme which is a measure of its maximal catalytic activity. The reciprocal k_{cat} is the time required by an enzyme molecule to turn over one substrate molecule. E_{tot} is the total enzyme concentration in this formula, it was calculated by OD reading at 280 nm; the absorptivity coefficient is 14,000 L/mol.cm (*90*).

Determination of K_i and Relative Vitality Values

Various inhibitors are used to provide information about the active site of the protein. Inhibition was measured as a decrease in the rate of substrate cleavage in the presence of inhibitor over time.

After fitting the Michaelis-Menten curve in the absence of inhibitor, the assay is repeated twice in the presence of two different concentrations of inhibitor. The curves are then simultaneously fit to the following equation:

$$v = \frac{V\max}{(1 + K_m/S) * (1 + I/K_i)} \tag{3-3}$$

to determine K_i values of classical (non-tight binding) competitive inhibitors. In the above equation, v is the rate of product formation, V_{max} is the maximum velocity, K_m is the Michaelis-Menten constant, S is the concentration of the substrate, I is the

concentration of inhibitor and K_i is the inhibition constant which is expressed in units of molarity. The graphs were fit in the cases of uncompetitive and noncompetitive inhibitor type of equations, and the best fits were obtained with the competitive inhibitor fit. K_m and K_{cat} were determined for each inhibitor: in order to check the precision of the assay, they were repeated under the same conditions and found to be reproducible. Although no numerical values of the error bars were determined in these assays, but the K_m values were very close to each other for each enzyme preparations. K_m value was determined and reproduced in the same range even after freezing and thawing. While determining the K_i values for each inhibitor, a consistent K_m value was reproduced.

Novel Protease Inhibitors

In silico screening of over 140,000 compounds available from the National Cancer Institute Developmental Therapeutics Program was done by docking these small molecules into the active site of the HTLV-1 PR based on the crystal structure of the 116-residue HTLV-1 PR available in the Protein Data Bank (PDB 2B7F) using DOCKv5.2.(*105*) The small molecules are available on the NCI website. (http://dtp.nci.nih.gov/index.html) (*106*). After water molecules were removed from the structure each compound was docked as a rigid body. The interactions between molecules are estimated by calculating approximate molecular mechanics interaction energies as implemented by the force field function in the DOCK program and compounds were ranked based upon predicted van der Walls and electrostatic interactions. A van der Waals surface representation of the model was generated using the program dms and the method of Richards (*107*). Spheres characterizing the potential target sites of the protein were generated using the program sphgen. Subset selection of spheres was performed using sphere select to within 6 Å of the target site.

Electrostatic grid files and bump filters were generated around the target site using the program grid with 10 Å buffers. The AMBER force field was used for vDW calculations. Docking was performed using DOCK6.0 (*108*), and all software programs referenced are distributed with the package. A database of 250,251 small molecules derived from the National Cancer Institute (NCI) Developmental Therapeutics Program (DTP) plated set (*109*) was used for the docking calculations. A maximum of 5000 orientations was searched for each small molecule in the lig and database. All docking calculations were performed on the University of Florida High-Performance Computing cluster. The best 40 compounds were selected and obtained from the National Cancer Institute. The stock solution was obtained by dissolving in 100% DMSO to a final concentration 50 mM and stored at room temperature.

ELISA and Western Immunoblotting Assays

MT-2 cells were obtained from the AIDS Research and Reference Reagent Program (*110, 111*) National Institute of Allergy and Infectious Disease (Rockville, MD) and maintained in complete RPMI-1640 medium (Invitrogen) as previously described (*112, 113*). MT-2 cells were seeded at 4 x 10^5 cells per ml and cultured for 4 or 24 hrs at 37^{o}C in the presence or absence of 5, 10 or 50 μM of selected inhibitors. Total cell lysates were obtained using RIPA lysis buffer (25 mM Tris-HCl pH 7.6, 150 mM NaCl, 1% NP-40, 1% sodium deoxycholate and 0.1 % SDS) containing protease inhibitor (Sigma-Aldrich) and phosphate inhibitor (Thermo Scientific, Rockford, IL) Total cellular protein amount was measured with the BCA Protein Assay Kit (Thermo Scientific). Western blotting was performed as previously described (*112, 113*). Briefly, samples containing a total of 30 μg of total cellular protein were loaded onto a 4-12% SDS-Bis-Tris Gels (Invitrogen) and subsequently transferred onto a 0.45 μM nitrocellulose

membrane (Invitrogen). Membranes were probed with anti-HTLV-1 p19 monoclonal antibody (Zeptometrix, Buffalo, NY). The primary antibody was detected with horseradish peroxidase (HRP)-conjugated anti-mouse IgG (GE HealthCare, Piscataway, NJ, USA). The membranes were stripped using restore Western stripping buffer (Thermo Scientific,) and re-probed with monoclonal anti-β-actin (Santa Cruz Biotechnology, Santa Cruz, CA, USA) as internal control. Signals were detected using the enhanced chemilumnescence Western blotting detection reagent (GE HealthCare).

MT-2 cells were seeded at 4 x 10^5 cells per ml and incubated in the presence or absence of 5 or 50 μM of selected inhibitors for 1 or 2 days. Levels of HTLV-1 p19 production in culture supernatants were quantified using enzyme-linked immunosorbent assay kits for p19 (Zeptometrix, Buffalo, NY) according to the manufacturer's instructions.

Cell growth was estimated by counting the cells using a hemocytometer or a machine counter. Cell viability was determined by counting the viable cells by staining with trypan blue. All the cell assays were done at NCI-Frederick facility in Dr. Tomozumi Imamichi’s laboratory.

CHAPTER 3
EXPRESSION, PURIFICATION AND REFOLDING OF HTLV-1 PR

The optimum methods and conditions for expression, purification and refolding of HTLV-1 PR have been investigated such as the most efficient *E-coli* cell line, method to lyse the bacterial cells, purification method determined to be ion exchange chromatography, pH for ion exchange chromatography, NaCl concentration for the most active protease and the refolding method determined to be rapid dilution.

The most efficient *E. coli* cell line was selected as Rosetta™*(*DE3*)*pLysS Competent Cells that enhance the expression of eukaryotic proteins that contain codons rarely used in *E. coli*. The pLysS plasmid encodes T7 phage lysozyme, BL21(DE3)pLysS is lysogenic for λ-DE3, which contains the T7 bacteriophage gene I. Because pLysS strains express T7 lysozyme, which further suppresses basal expression of T7 RNA polymerase before the induction, they stabilize pET recombinants encoding target proteins that affect cell growth and viability. T7 lysozyme lowers the background expression level of target genes under the control of the T7 promoter but does not interfere with the level of expression achieved after IPTG induction. Rosetta™*(*DE3*)*pLysS cell strains supply tRNA genes for AGG, AGA, AUA, CUA, CCC, GGA which are the rare codons used in *E. coli* on a Col-E1 compatible chloramphenicol-resistant plasmid. This cell strain has yielded higher expression efficiency of HTLV-1 PR, therefore the assays have continued by this cell strain selection.

The pET 11a vector was selected as an expression vector. (Figure 3-1) Various constructs were cloned into pET11a by using Nde1 and BamH1 restriction enzymes. Digestion products from pET 11a vector and insert HTLV-1 PR are shown in Figure 3-2,

and cut vector and insert were ligated for 1 h, and then transformed into TOP 10 cells. (See Chapter 2)

The 116-residue L40I and W98V amino acids substituted HTLV-1 PR in pET 11a vector and 125-residue L40I amino acids substituted HTLV-1 PR in pET 19b vector were provided from NIH. The L40I substitution was used to prevent autoproteolysis and the W98V substitution was introduced to make the active site region of HTLV-1 PR similar to HIV-1 PR (Figure 3-3). The 125-residue HTLV-1 PR was cloned in pET 11a vector of *E. coli.* Stop codons were introduced at the 121 and 122 residues to get various construct lengths. The primers are shown in Figure 3-4. The PCR reactions were conducted on as mentioned in the experimental procedure. (See Chapter 2) Various concentrations of DNA from 0.1 to 0.5 ng were used as template. A gradient was used for annealing temperature between 43-60ºC. After the PCR reaction was finished, a DNA gel was run to determine PCR products. (Figure 3-5) PCR products which have the correct band were transformed in Rosetta™*(*DE3*)*pLysS *E. coli* cells.

After cloning and site directed mutagenesis (SDM), DNA sequences were checked for correct frame locations of ribosome binding sites and restriction sites for protein translation. (Figure 3-6)

The concentration of 1 mM IPTG was picked as the optimum concentration to induce expression of the gene based on literature (*114*). Different expression times were tried as shown in Figure 3-6. Because there was no significant change between 3 h and 6 h, 3 h of expression was selected.

The French Pressure Cell, Bug buster (Novagen) and sonication methods were used to break cells. Resuspension buffer (10 mM Tris pH 7.5, 5 mM EDTA, 0.5 M

urea) was added twice to wash the pellet and the samples centrifuged at 8000 rpm for 10 min. (Figure 3-7) French pressure cell treatment gave the best yield as 2 g of inclusion bodies (IBs) were obtained compared to 1g of IBs obtained with Bug buster and sonication.

After solubilizing IBs in buffer B (8 M urea, 10 mM Tris-HCl pH 7.5, 5 mM EDTA), Q Sepharose Fast Flow column (Pharmacia) equilibrated with buffer C (6 M urea, 10 mM Tris-HCl pH 7.5, 5 mM EDTA) was used to purify the protease from proteins that have lower pIs. The Q column flow through was adjusted to pHs 3, 4, and 5 as well as buffer D (6 M urea, 20 mM sodium acetate, 5 mM EDTA) to apply to a SP column (Pharmacia). pH 4 gave the best purification for HTLV-1 PR. Various concentrations (0.3, 0.4, 0.5 M) of NaCl was used to elute the protease of the SP column. 0.4 M NaCl gave the best elution yield. The SDS-PAGE gel of the purification of one of the constructs was shown in Figure 3-8.

Many conditions have been tried for refolding of HTLV-1 PR. For the first condition the purified protease was dialyzed against 20 mM PIPES, pH7.0, containing 2 mM DTT, 1 mM EDTA, 150 mM NaCl and 10% glycerol at 25 C for 3, 5 ,8 h and 16 h. (Figure 3-9) None of the time points gave any active protein, so folding was not accomplished. Overnight dialysis resulted in precipitation of the protease. No active protease was obtained. Dialysis against 50 mM sodium acetate buffer (pH 5.0) containing 100 mM NaCl at 0°C for 3, 5, 9 and 24 h was used in an attempt to get folded protease, but this method failed as well. (Figure 3-10) As mentioned in Kadas et al.; subsequent dialysis against 25 mM formic acid (pH 2.8) at 0°C for 6 h followed by dialysis against 50 mM sodium acetate buffer (pH 5.0) containing 100 mM NaCl at 0°C overnight was tried; also

yielded inactive protease. After testing them by Size Exclusion Chromatography and kinetic assays; none of these conditions provided correctly folded, active HTLV-1 PR.

Only 10x rapid dilution of purified protein in 10 mM formic acid gave active, correctly folded HTLV-1 PR. This result was confirmed by size exclusion chromatography in Figure 3-11.

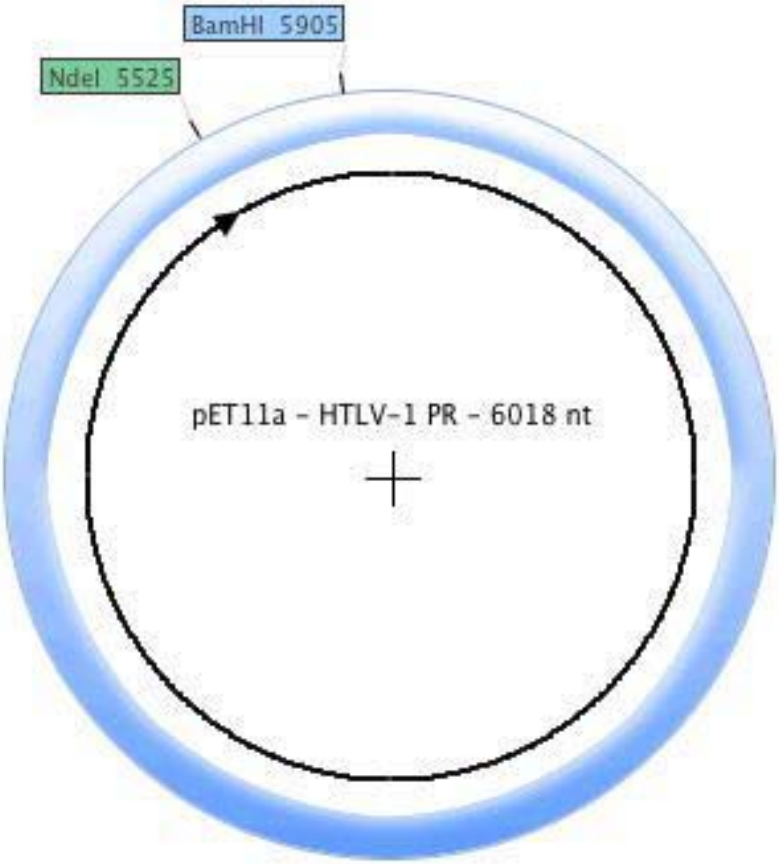

Figure 3-1. The expression vector pET11a (Novagen).

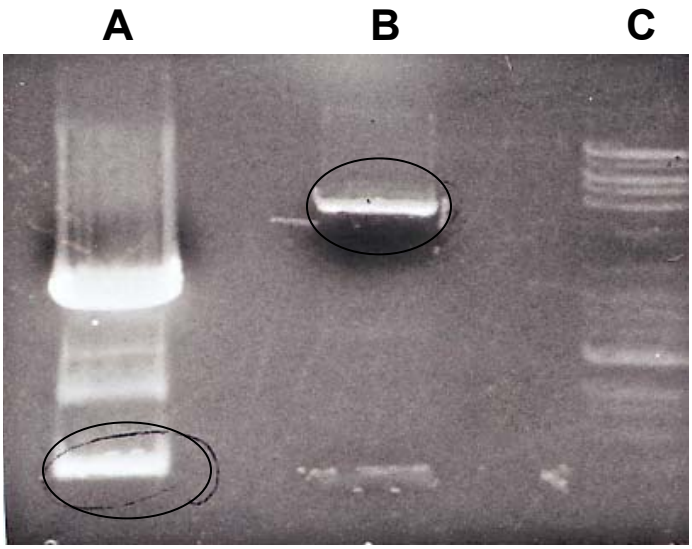

Figure 3-2. DNA gel picture of cloning. Lane A represents the cut insert of 121-residues HTLV-1 PR, lane B the cut vector of pET 11a and the lane C the molecular weight marker (1 kb DNA Ladder (NEB).

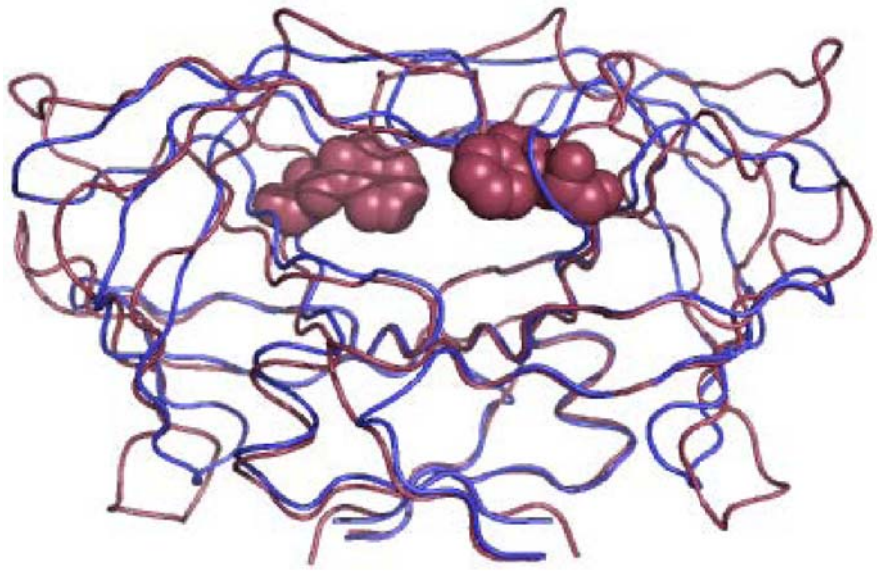

Figure 3-3. Alignment of HIV-1 PR and HTLV-1 PR. W98V amino acid substitution is shown in pink spheres, HTLV-1 PR is shown in pink and HIV-1 PR in blue colors.

L40I
Upper GCAGACATGACAGTCATTCCGATAGCCTTGTTC
Lower GAACAAGGCTATCGGAATGACTGTCATGTCTGC

121 HTLV-1 PR
Upper GGCAAAAGGGCCGTAAGTAATCTTG
Lower CCGTTTTCCCGGCATTCATTAGAAC

122 HTLV-1 PR
Upper GGCAAAAGGGCCGCCTTAAATCTTG
Lower CCGTTTTCCCGGCGGAATTTAGAAC

Figure 3-4. Primers for 121, 122-residue and L40I mutation of HTLV-1 PR.

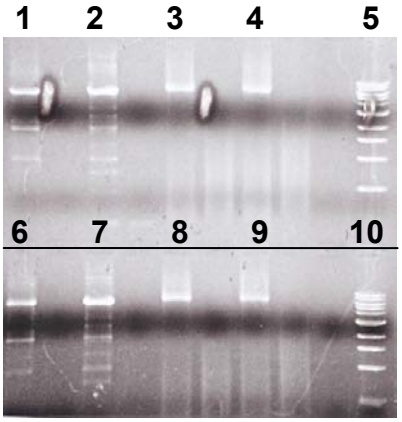

Figure 3-5. DNA gel picture of PCR products. Lane 1 is 0.5 ng 121-residue HTLV-1 PR elongation temperature at 52°C, Lane 2 100 pg 121-residue HTLV-1 PR elongation temperature at 52°C, Lane 3 is 0.5 ng 121-residue HTLV-1 PR elongation temperature at 43°C, Lane 4 is 100 pg 121-residue HTLV-1 PR elongation temperature at 43°C. Lane 6 is 0.5 ng 122-residue HTLV-1 PR elongation temperature at 52°C, Lane 7 100 pg 122-residue HTLV-1 PR elongation temperature at 52°C, Lane 8 is 0.5 ng 122-residue HTLV-1 PR elongation temperature at 43°C, Lane 9 is 100 pg 122-residue HTLV-1 PR elongation temperature at 43°C. Lane 5 and Lane 10 is 1 kb DNA ladder (NEB).

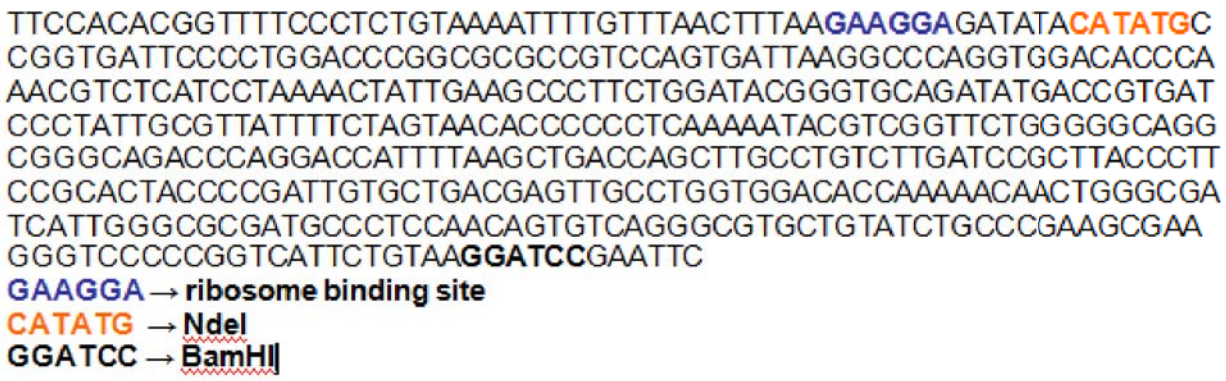

Figure 3-6. DNA sequence of HTLV-1 PR vector used in these studies.

1

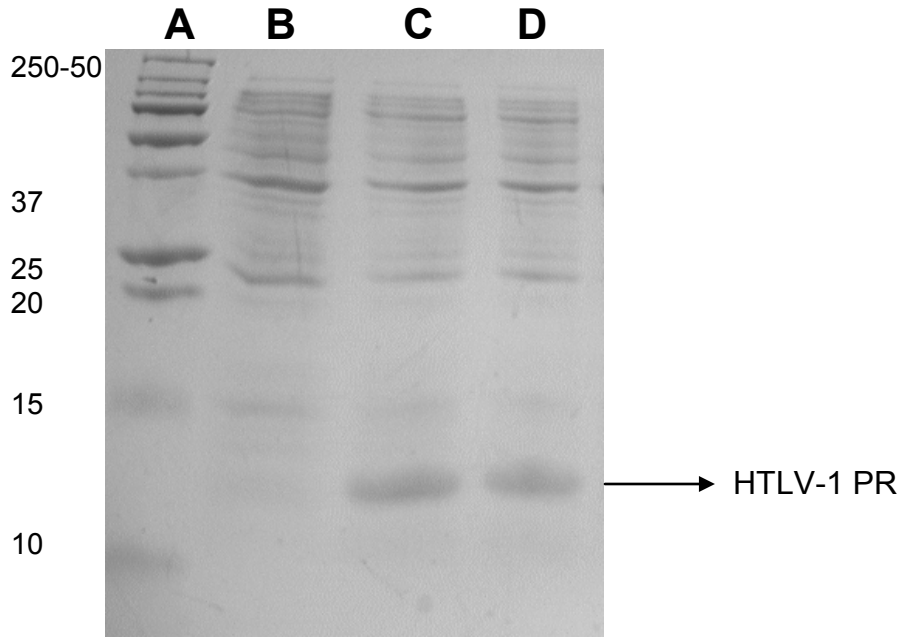

2

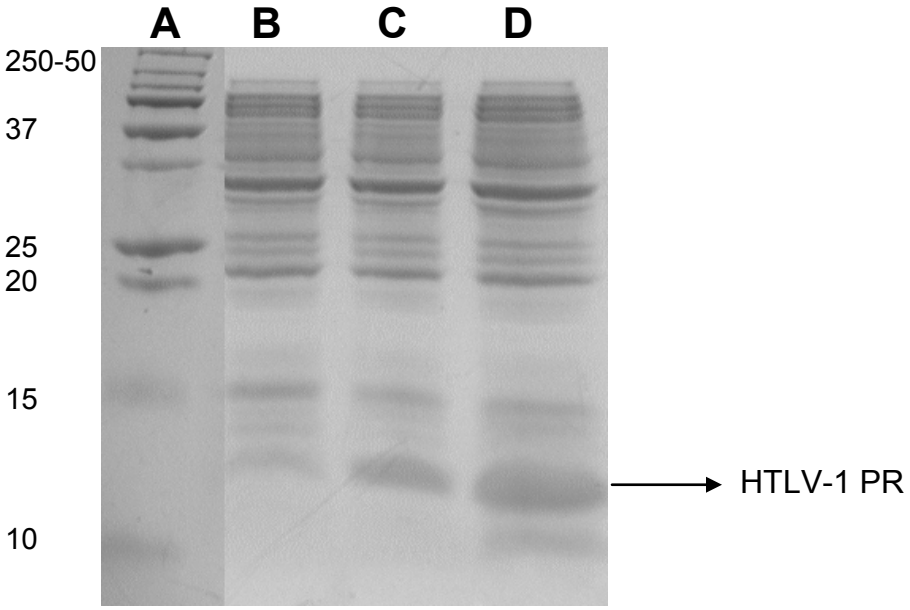

Figure 3-7. SDS PAGE (18%) gel of expression. 1. 116-residue HTLV-1 PR. 2. 121-residue HTLV-1 PR. Lane A represents the Precision Plus Ladder (Biorad), lane B before IPTG induction, lane C 3 h after IPTG induction and lane D 6 h after IPTG induction.

1

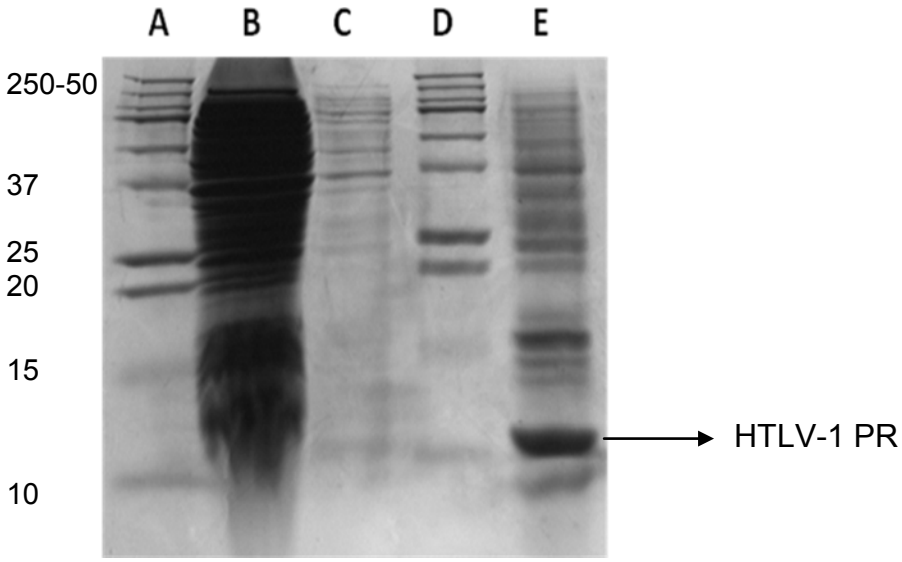

2

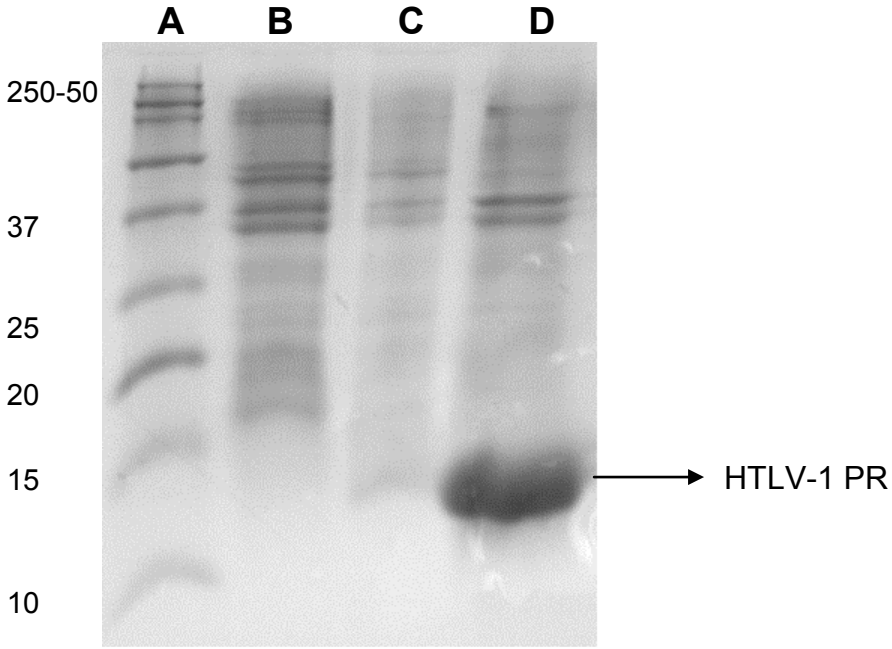

Figure 3-8. SDS-PAGE (18%) gel of inclusion bodies. 1. Lane A represents the Precision Plus Ladder (Biorad), lane B the first wash of IBs, lane C the second wash of IBs, lane D MW ladder and lane E IBs 121-residue HTLV-1 PR. 2. Lane A represents the Precision Plus Ladder (Biorad), lane B before IPTG induction, lane C 3 h after IPTG induction and lane D. IBs 122-residue HTLV-1 PR.

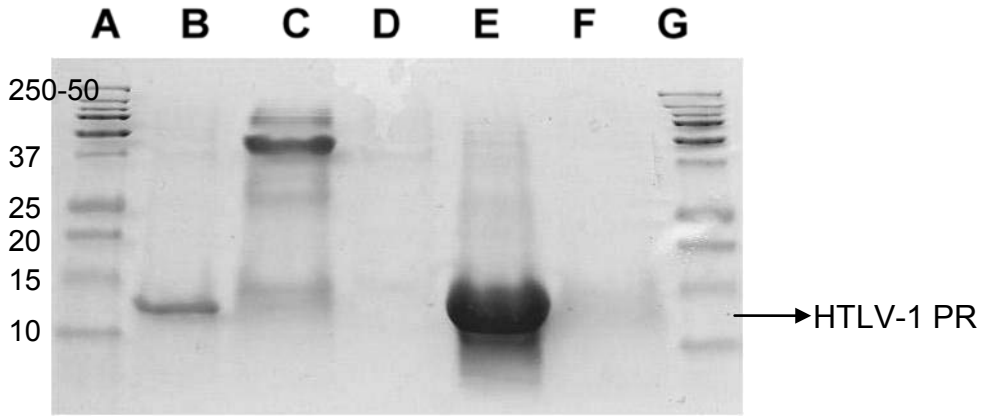

Figure 3-9. SDS PAGE (18%) gel picture of purification of 121-residue HTLV-1 PR. Lane A is the Precision Plus Ladder (Biorad), lane B is the Q column flow through, lane C is the Q column elution by 1 M NaCl, lane D is the SP column flow through, lane E is the SP column elution by 0.4 M NaCl, lane F is the SP column elution by 1 M NaCl, and the lane G the Precision Plus Ladder (Biorad).

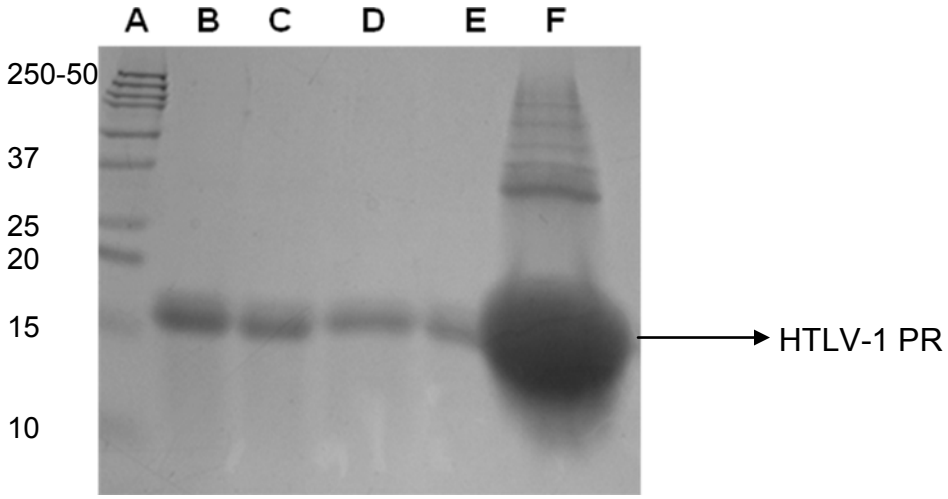

Figure 3-10. SDS-PAGE (18%) gel of dialysis of HTLV-1 PR against 20 mM PIPES, pH 7.0, containing 2 mM DTT, 1 mM EDTA, 150 mM NaCl and 10% glycerol at 25ºC. Lane A is the Precision Plus Ladder (Biorad), lane B dialysis after 3 h, lane C dialysis after 5 h, lane D dialysis after 8 h, lane E dialysis overnight, and F is the precipitation after dialysis.

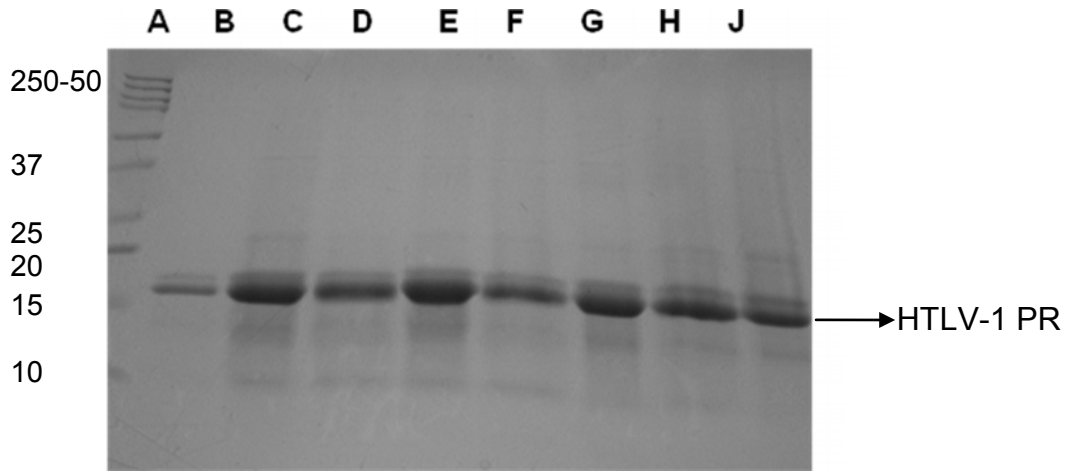

Figure 3-11. SDS-PAGE (18%) gel of dialysis of HTLV-1 PR against dialysis buffer-1 (50 mM sodium acetate buffer (pH 3.0) containing 100 mM NaCl) at 25 Cº and dialysis buffer-2 (50 mM sodium acetate buffer (pH 4.0) containing 100 mM NaCl). Lane A is the Precision Plus Ladder (Biorad), lane B is dialysis-1 after 3 h, lane C is dialysis-1 after 5 h, lane D is dialysis-1 after 8 h, lane E is dialysis-1 overnight; lane F is dialysis-1 after 3 h, lane G is dialysis-1 after 5 h, lane H is dialysis-1 after 8 h, lane J is dialysis-1 overnight.

A

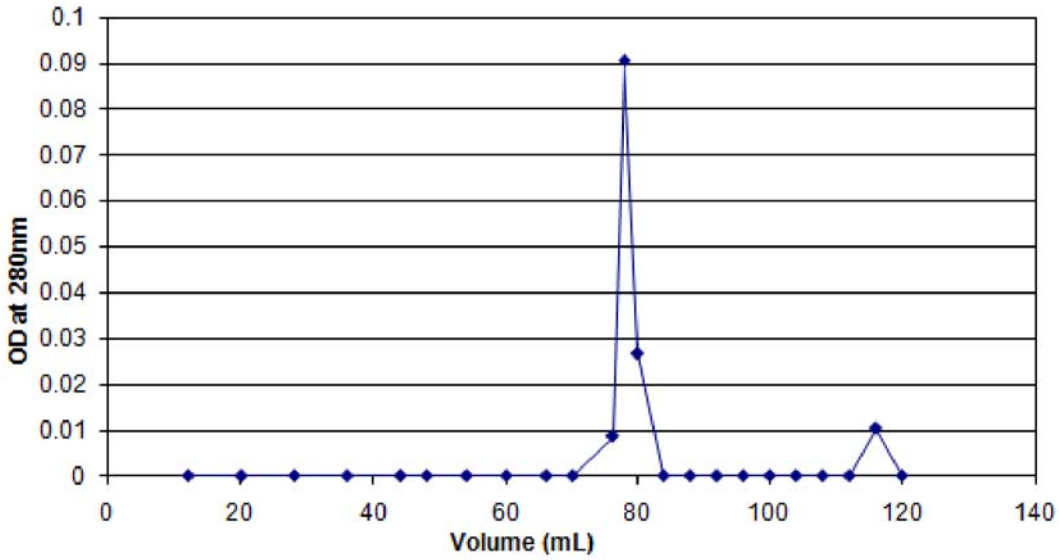

B

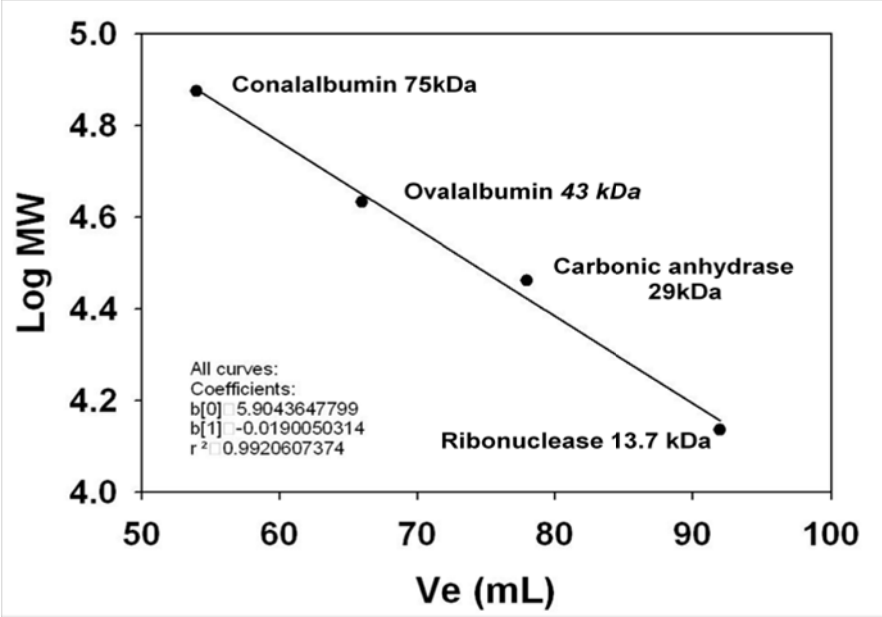

Figure 3-12. A. Graph of Size Exclusion Chromatography. (Each fraction has 2 mL) B. Calibration curve of Size Exclusion Column

CHAPTER 4
KINETIC CHARACTERIZATION AND INHIBITOR DISCOVERIES OF HTLV-1 PR

Truncated Forms of C-Terminal Region

There are additional amino acids at the C-terminal region of HTLV-1 protease when compared to other aspartic acid proteases such as HIV-1 PR. HTLV-1 PR is most similar to BLV-1 PR. (Figure 1-7) The function of this extra loop and its effect on enzyme activity is still unclear. In the literature, it is controversial as well. An *in vivo* study by Hayakawa et al. shows the last 5 amino acids at the C-terminal region are necessary for protease activity, although 5 amino acids prior to these 5 are not (*115*). These results might come from the cell components or other proteases in the cell, since the HTLV-1 PR was not isolated, purified and characterized. Herger et al. showed that 10 residues at the C-terminal region are not essential for full catalytic activity, since the full length and -10 residue have the same specificity constant (*116*). Controversially, a 60% decrease in the catalytic activity was determined by Li et al. comparing 116-residue and full length (125-residue) HTLV-1 PR (*27*). A recent study by Kadas et al. shows that 120-residue HTLV-1 PR has 3% percent activity, while 116-residue has only residual activity (*1*). The dimerization tendency and catalytic activity increase upon getting closer to full length (*1*).

We have investigated the effect of C-terminal residues at catalytic activity. We have tried to a find construct with full catalytic activity and a crystallizable form of HTLV-1 PR.

Kinetic Characterization of Various Constructs

116, 121, and 122-residues were used for kinetic characterization of HTLV-1 PR. (Figure 4-1) All the constructs were expressed and purified as described in Materials

and Methods. (Chapter 2) Final purity of each protease was verified by 18% SDS-PAGE (Figure 3-7). The purified constructs were concentrated with polysulfone membrane spin columns (mwco 10,000; GE Healthcare) to concentrations between 10-80 μM and were used for further enzyme characterization.

Turnover number of each construct was determined by using various substrate concentrations from 15-75 μM. Each substrate concentration has a different rate of reaction plotted and calculated by Sigma Plot software (Systat Software Inc.). (Figure 4-2) Kinetic constants determination by Lineweaver-Burk equation is shown in Figure 4-3. Even though no error bars exists in the figure; K_m value was reproduced many times in the same range. The coefficient of determination ($R^{2)}$ is the proportion of variability in a data set. Larger values for R^2 (close to 1) indicate that the data set fits into the equation. For each kinetic measurement, R^2 was kept equal or greater than 0.98 for accuracy of the data.

We have found that each construct has a distinct catalytic activity (Table 4-1). The substrate specificity constants (K_{cat}/K_m) are similar for various lengths of HTLV-1 PR, indicating that the C-terminal amino acids are not essential for full protease activity. HTLV-1 PR in full length has not been refolded properly in our research; therefore there is no kinetic data for this construct. Each construct was utilized in further inhibitor studies.

Inhibitor Discoveries

Even though HIV-1 PR has been extensively studied, HTLV-1 PR which shares many similarities has not been as well characterized (*81, 84, 117-123*). Despite the similarities of both retroviral proteases, their substrate and inhibitor specificity are very different from each other (*82, 94, 103*).

Different substrate concentrations (15-75 μM) were used to determine the inhibition constants of each inhibitor. Two different concentrations of inhibitor were used to determine the decrease in the rate of reaction for each substrate concentration and plotted by Sigma Plot software (Systat Software, Inc.). (Figure 4-4) K_m value was reproduced and R^2 was greater than 0.98.

Various aspartic acid protease inhibitors were tested to determine their inhibition effect on HTLV-1 PR. None of the clinically used HIV-1 PR inhibitors (obtained from NIAID) had any inhibition on HTLV-1 PR. (K_i>100 μM) 22 inhibitors from the laboratory of Anders Hallberg at Uppsala University, 18 compounds from the laboratory of Sergio Romeo at University of Milan, and 19 compounds from other collaborators were tested against HTLV-1 PR. All of these compounds were designed against plasmepsins. Only four of the Swedish inhibitors (available in Dunn lab) have shown inhibition of HTLV_1 PR with K_i values lower than 2 μM. Their structures and K_i values are shown in Figure 4-5 and possible H-bonding between the inhibitors and the active site were determined by Chimera software (UCSF) as shown in Figure 4-6 (*124, 125*).

Kinetic Characterization of Various Constructs and Small Molecule Analysis

By using the DOCK program (UCSF, San Diego), various inhibitors were docked in the active site of the HTLV-1 PR. 140,000 compounds available from the National Cancer Institute Developmental Therapeutics Program were used in docking experiments. These compounds obey Lipinski Rules of Five which are rules for druglikeness of a compound (*126, 127*). According to Lipinski, absorption or permeation of a drug is higher when there are less than 5 H-bond donors, 10 H-bond acceptors, the molecular weight (MWT) is lower than 500 and the calculated Log P (CLogP) is smaller than 5 (or MlogP.4.15) Energy binding values of the inhibitors were determined and

ranked by the DOCK program (UCSF, San Diego) (*108*). Top ranked inhibitors were purchased and tested to determine the inhibition on HTLV-1 PR as mentioned in the Method section.

Some of the top ranked small molecules identified by *in silico* screening were tested in inhibition assays and several have shown an inhibition effect on the protease. The inhibition constants range between 1-78 μM for the 116-residue HTLV-1 PR (Table 4-3). In general, the L40I mutant has lower inhibition constants (K_i), i.e., better binding, when compared to the double mutant (W98V/L40I) of HTLV-1 PR. The best inhibitor is Compound 1 with $K_i = 0.8 \pm 0.1$ μM. The possible H-bonding between Compound 1 and HTLV-1 PR is shown in Figure 4-7.

Five inhibitors were selected to determine inhibition constants for each construct. All of them have significantly better inhibition against the 116-residue HTLV-1 PR compared to any of the longer constructs. (Table 4-4)

Discussion

New therapies are needed to treat patients infected with HTLV-1. The viral target for most of the current treatments is unknown and most have many side effects. Due to the success seen with targeting the protease from HIV-1, we have focused our studies upon the protease from HTLV-1, which belongs to the same class of enzymes and shares structural and functional characteristics with HIV-1 PR. The specificity constants stay identical for various lengths of HTLV-1 PR, which indicates that the C-terminal amino acids are not essential for full protease activity. In an effort to look at the structural differences that may be present in this region and identify specific interactions between the active site residues and the inhibitor, crystallization trials are currently underway, both with and without inhibitors.

The compounds selected by the DOCK program have shown inhibition both in kinetic and cellular assays. Within the top ranked inhibitors, 13 of them gave inhibition constants ranging from 1 μM to 78 μM for the116-residue L40I HTLV-1 PR.

15, 3, 5, 7-tetraazatricyclo [3.3.1.1~3, 7~] decane is the most common group in the structure of small molecules. Molecules with an electronegative element (Cl, Br or I) attached to it seem to give better inhibition as in Compounds 2, 4, and 7. Alkenes attached to the 15, 3, 5, 7-tetraazatricyclo [3.3.1.1~3, 7~] decane molecule have lower inhibition. (Compound 3 and 8) Alcohol group has lower effect on inhibition compared to halogens comparing Compound 4, 7 and 8. Attaching a halogen decreases the inhibition constant for 35 fold, while attaching an alcohol group decreases for 4 fold. (Table 4-2)

The inhibition constants for these small molecules increase for the longer protease constructs. Higher inhibition constant for small molecules means small molecules have lower inhibition for longer constructs. Only Compound 1 has low inhibitions constants for each of the 3 constructs tested here. The selection was made based on the inhibition constants values of 116-residue HTLV-1 PR. The different inhibition constant might be based on the extra residues interactions with the inhibitors in the active site of HTLV-1 PR.

Table 4-1. Specificity constants of various constructs of HTLV-1 PR.

Residues	K_m (μM)	k_{cat} (s^{-1})	k_{cat}/K_m (s^{-1} M^{-1})
116	31±3.6	$7.5x10^{-4}$±$2x10^{-5}$	24±3
121	47±5.2	$9.0x10^{-4}$±$1x10^{-5}$	19±2
122	32.2±4.6	$6.5x10^{-4}$±$3x10^{-5}$	20±3

R^2>0.98

Table 4-2. Inhibition constants of 13 inhibitors against L40I and L40I/W98V mutated 116-residue HTLV-1 PR. The best of these, marked by asterisk (*), were used in subsequent experiments.

Inhibitor	Rankings	Numbers	Structures	L40I K_i (μM)	W98V/L40I K_i (μM)
667746*	5,7	1		0.8 ± 0.1	5.1 ± 0.4
168615*	6	2		1.1 ± 0.1	8.5 ± 0.4
10408	10	3		27 ± 2	9.3 ± 0.5
172855*	12	4		1.1 ± 0.1	5.6 ± 0.5
30049	13	5		4.5 ± 0.4	13 ± 1
35024	14	6		1.1 ± 0.1	5.7 ± 0.5

Table 4-2. continued

Inhibitor	Rankings	Numbers	Structures	L40I K_i (μM)	W98V/L40I K_i (μM)
177977*	19	7		8.4 ± 0.5	6.2 ± 0.4
5062	25	8		35 ± 4.0	45 ± 3.0
21235	26	9		35 ± 3.0	58 ± 5.0
348978	37	10		18 ± 1.0	35 ± 3.0
4436	41	11		9.3 ± 0.7	77 ± 9.0
23429	42	12		38 ± 2.0	38 ± 3.0
362403*	44	13		3.6 ± 0.2	5.7 ± 0.5

Table 4-3. K_i values of 5 compounds with various constructs of HTLV-1 PR

	Inhibition Constants K_i (μM)		
Compound	116 L40I	121 L40I	122 L40I
1	0.8 ± 0.1	23 ± 2.0	11 ± 1.0
2	1.1 ± 0.1	23 ± 1.0	>100
4	1.0 ± 0.1	>100	>100
7	8.4 ± 0.5	>100	89 ± 10
13	3.6 ± 0.2	14 ± 1.0	>100

R^2>0.98

P V I P L D P A R R P V I K A Q V D T Q T S H P K T I E A L L **D T G** A D M T V L P I A

L F S S N T P L K N T S V L G A G G Q T Q D H F K L T S L P V L I R L P F R T T P I

V L T S C L V D T K N N W A I I G R D A L Q Q C Q G V L Y L **P** E A K G **P P** V I L

Figure 4-1. HTLV-1 PR sequence. Residue 116 is shown in blue, residue 121 in orange and residue 122 in green.

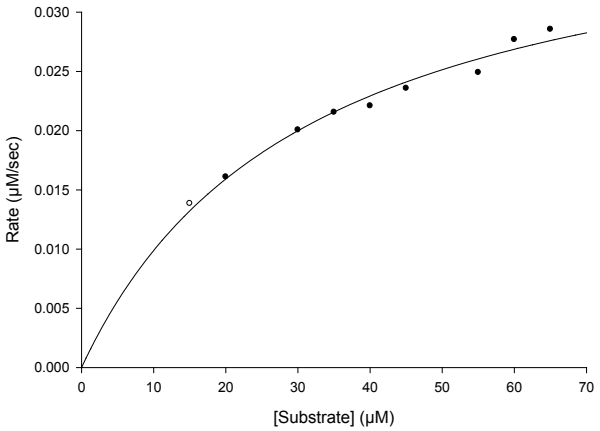

Km= 31.4± 3.6 µM

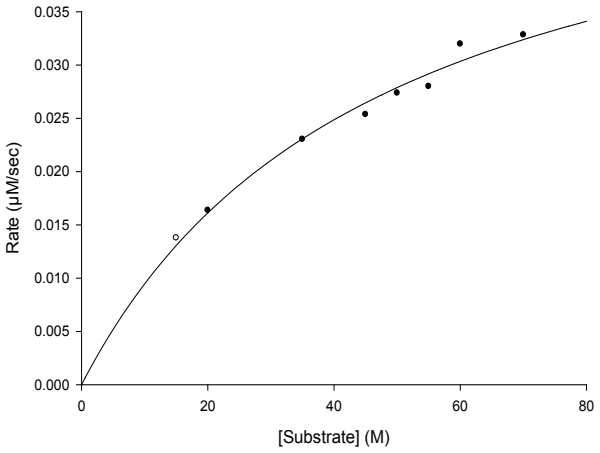

Km= 47.4± 5.2 µM

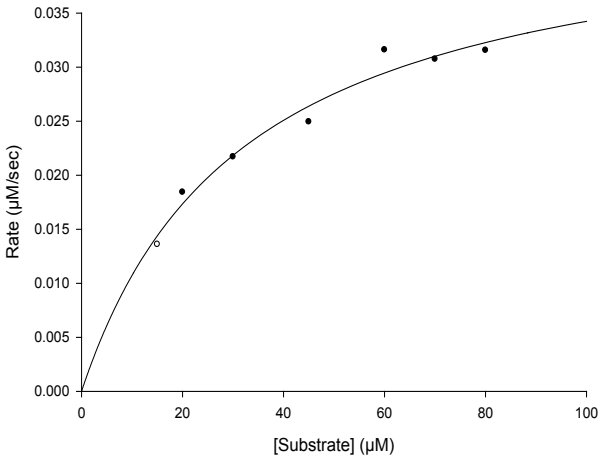

Km= 32.2± 4.6 µM

Figure 4-2. Kinetic constant determination by Michaelis Menten equation. A.116 B.121 C.122 (R^2>0.98)

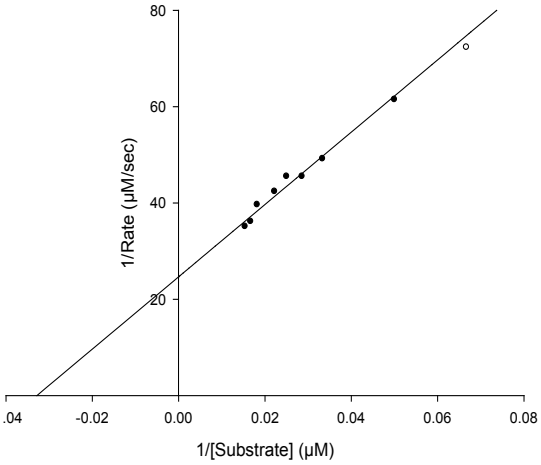

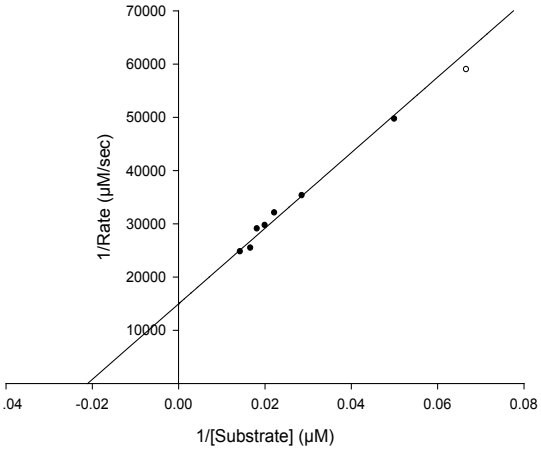

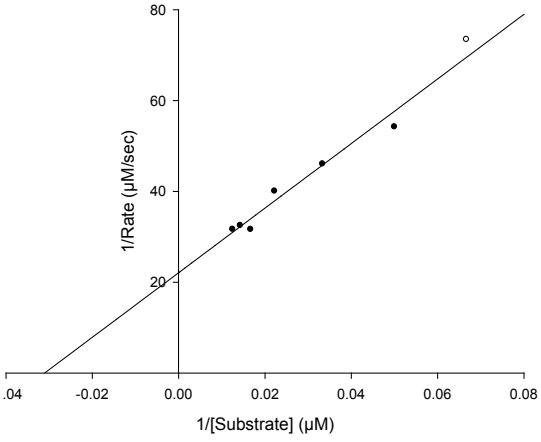

Figure 4-3. Kinetic constant determination by Lineweaver-Burk equation. A.116 B.121 C.122 (R^2>0.98)

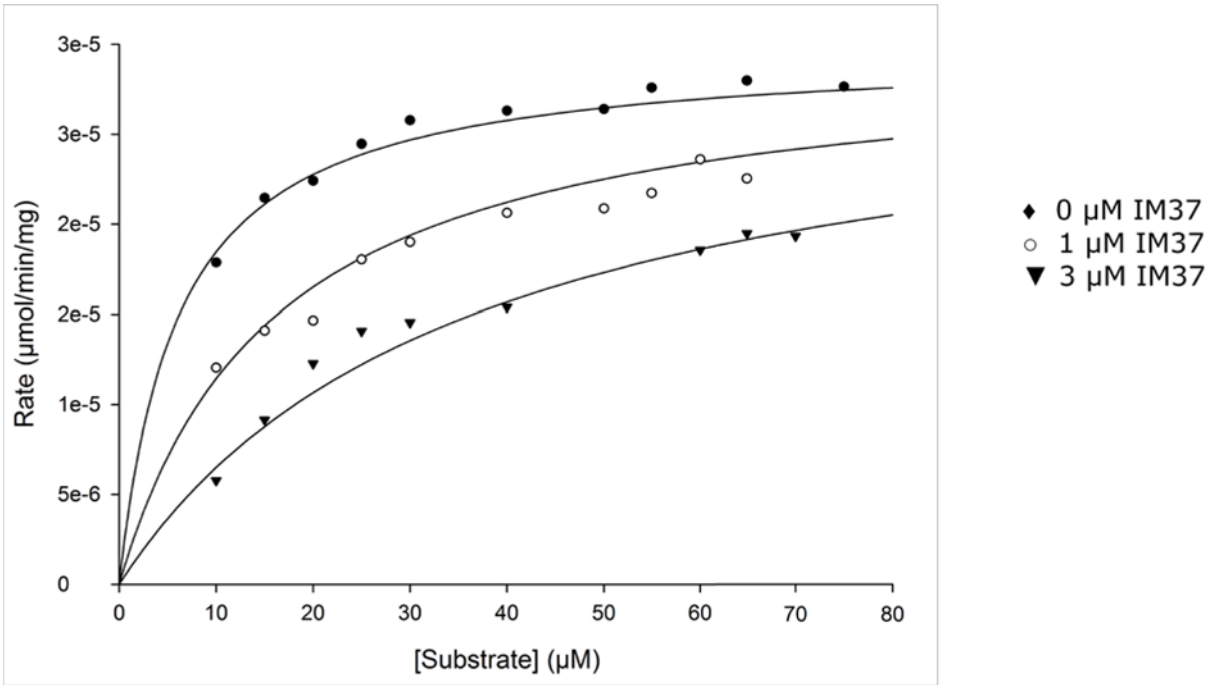

Figure 4-4. Inhibitor dissociation constant (Ki) Determination. Michaelis-Menten curve fit of rate (µmol/min/mg) versus substrate concentration (µM) with increasing inhibitor concentrations 0, 1, 3 µM. R^2>0.98

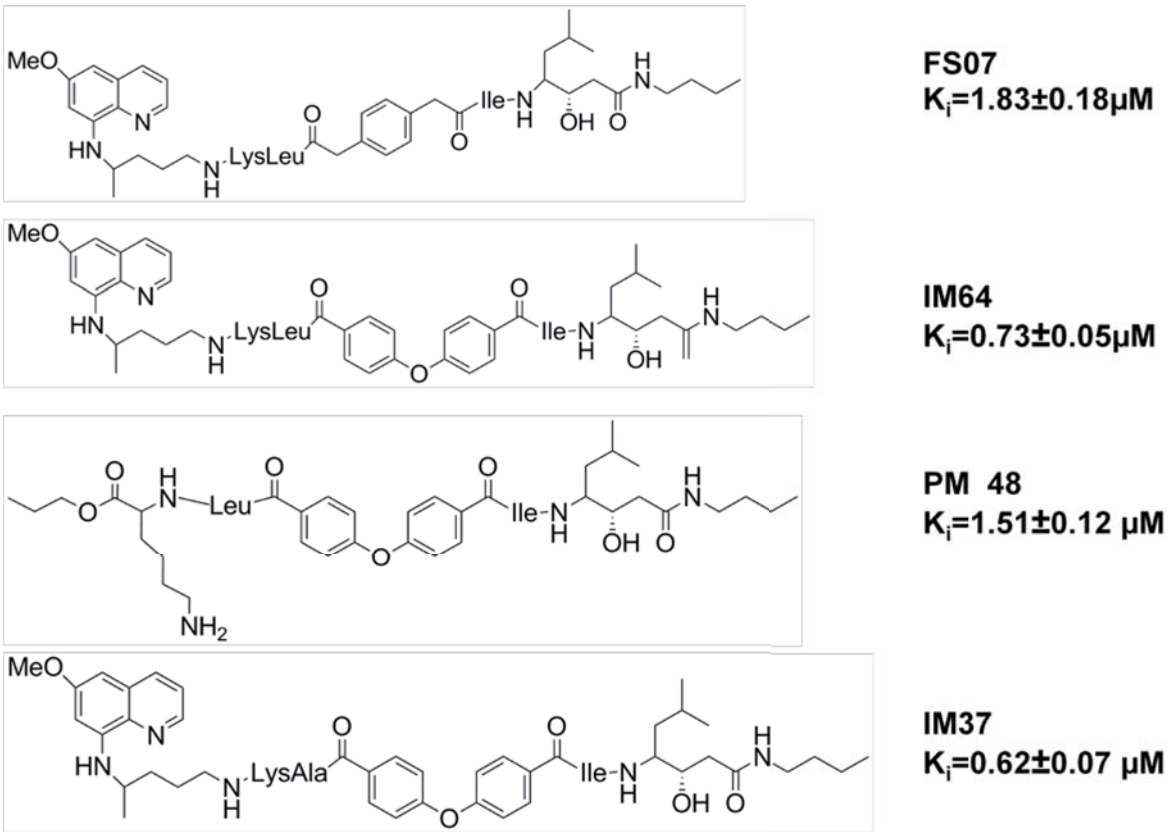

Figure 4-5. Structures of effective plasmepsin inhibitors.

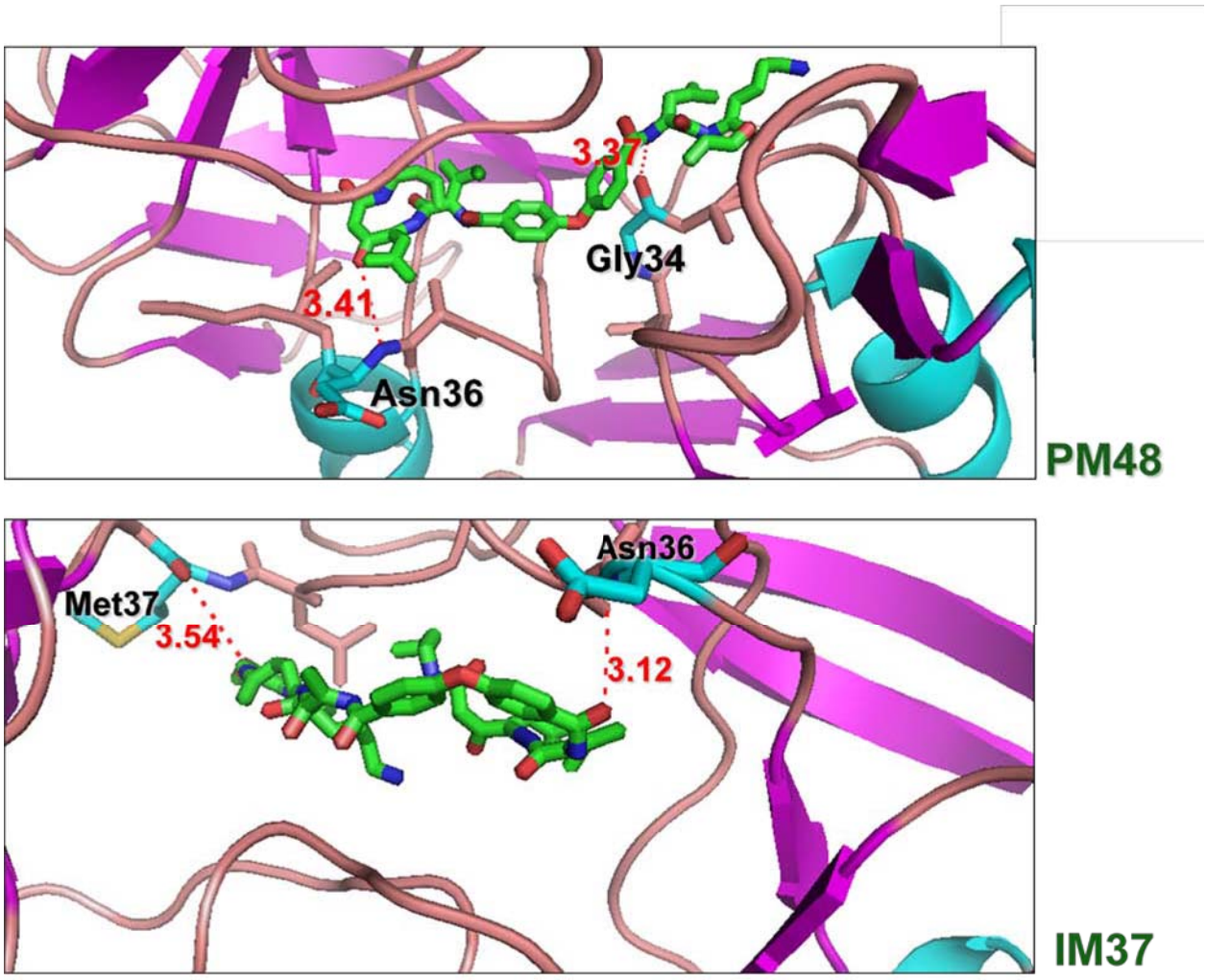

Figure 4-6. Possible H-bonding distances of PM48, IM37, FS07, IM64 in the active site of HTLV-1 PR determined by Pymol (UCSF) with the help of Dr. David Ostrov laboratory at University of Florida, Gainesville.

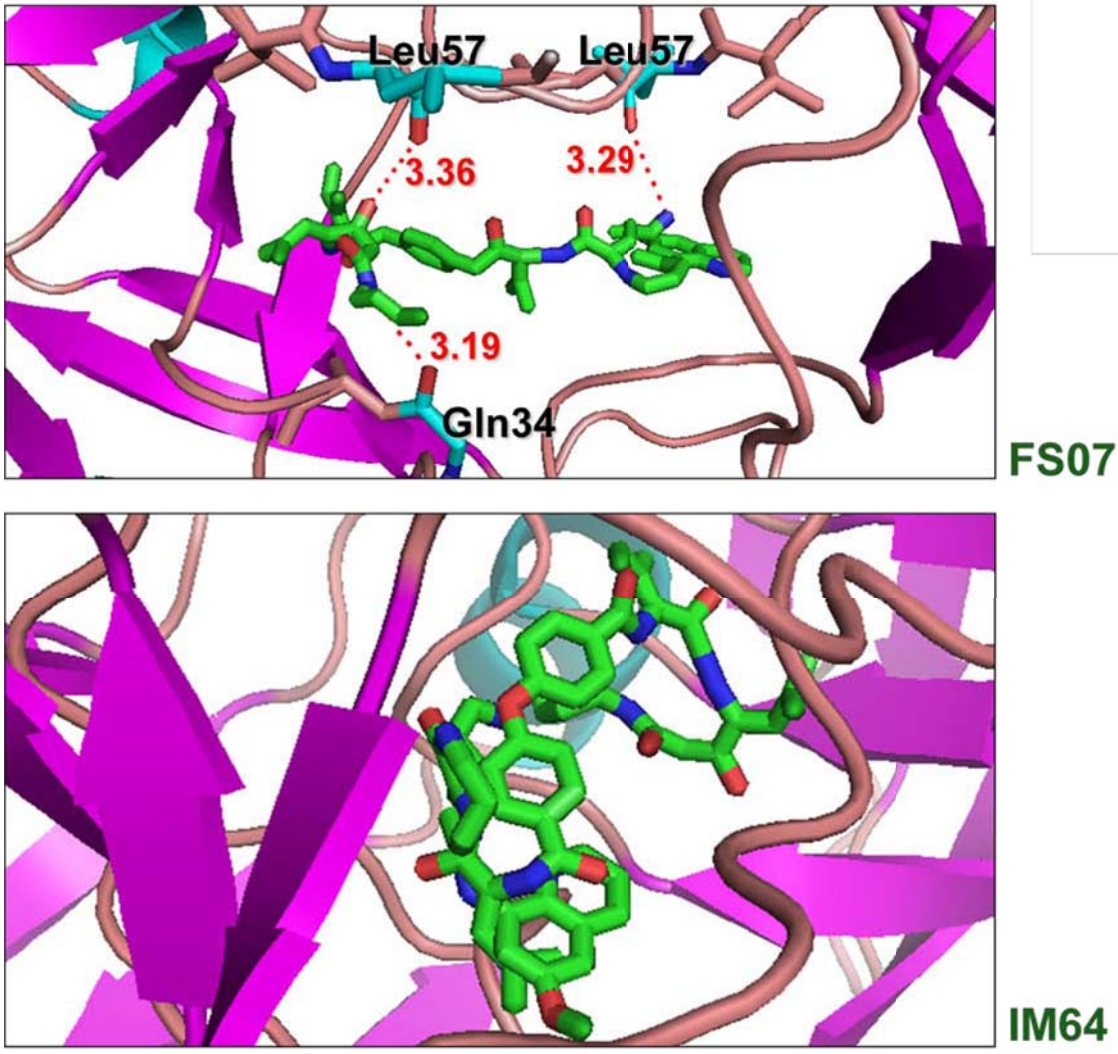

Figure 4-6. continued.

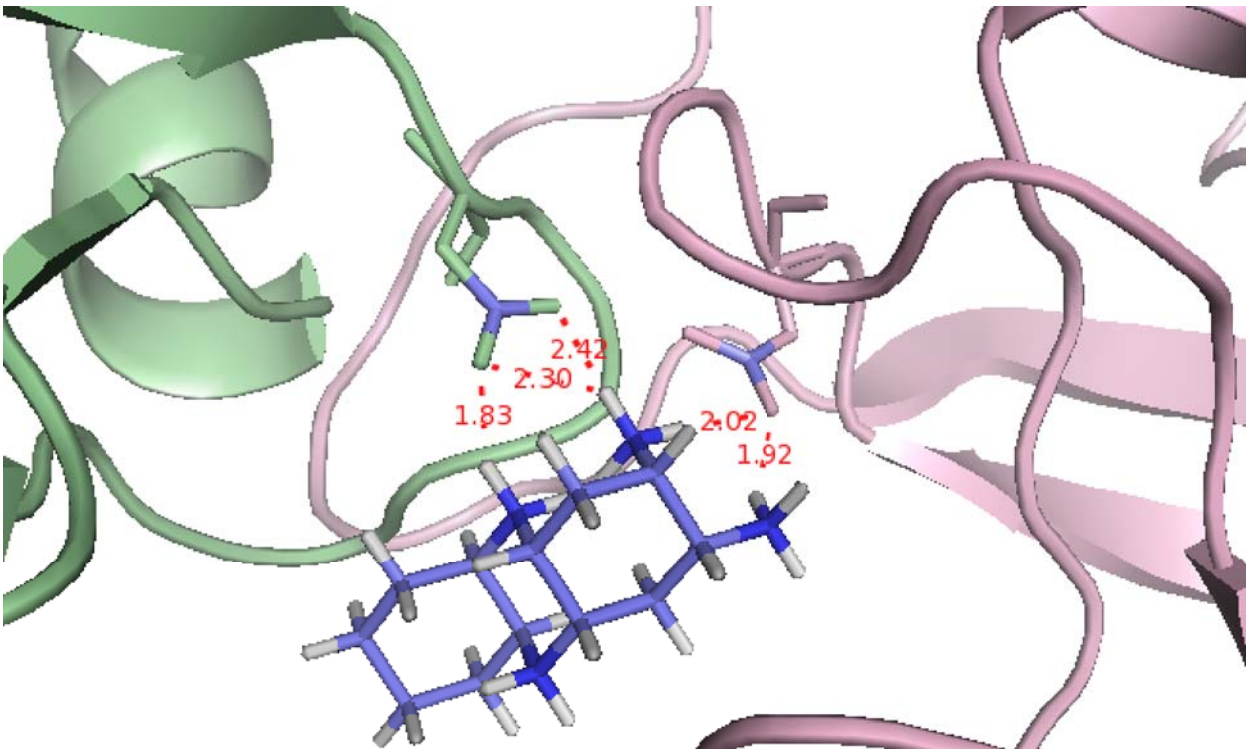

Figure 4-7. Possible H-bonding distances of Compound 1 and HTLV-1 PR determined by Pymol (UCSF) with the help of Dr. David Ostrov laboratory at University of Florida, Gainesville.

CHAPTER 5
THE EFFECT OF SMALL MOLECULES ON HTLV-1 INFECTED CELLS

Gag/Pol Processing

Gag and Gag/Pol processing take place after HTLV-1 virus buds out of the cell. This process is essential for viral maturation and cell to cell spread (*70*). PR is the functional necessary viral component for this processing; therefore blocking PR is an effective way to inhibit Gag/Pol processing (*70*). PR is encoded by the Pro gene which is an open reading frame (ORF) overlaps with both Gag and Pol ORFs (*69, 70, 128*). Pro region does not exist in all the retroviruses like HIV-1 and RSV; but it exist in HTLV-1, HTLV-2, Mouse Mammary Tumor Virus (MMTV) and Bovine Leukemia Virus (BLV) (*63, 65, 129-132*). Ribosomal shifting in the -1 direction is essential in all the retroviruses to align the various open reading frames (*133-135*). Two frameshifts are necessary for Gag, Pro, and Pol polyprotein synthesis of HTLV-1 (*75, 136*).

Targeting HTLV-1 PR, the inhibitors were expected to inhibit Gag processing of HTLV-1 (*111, 137*). MT-2 cells were used to test the inhibition effect of HTLV-1 protease inhibitors on HTLV-1 infected cells. MT-2 cell line was used for efficient HTLV-1 production (*138*). It is derived by co-culturing bone marrow $CD4^+$ T-lymphocytes of a healthy donor with leukemia cells of an ATL patient (*139, 140*).

The selected five best compounds were also used at various concentrations at multiple incubation times to test their antiviral activity. Gag protein precursor, a 53 kDa protein, yields MA (p19, 19 kDa), CA (p24, 24 kDa) and NC (p12, 12 kDa) proteins after proteolytic cleavage. The p19 (MA) antigen has been used for Western Blotting assays as explained in Chapter 2. In Figures 5-1, 5-2 and 5-3 the p53 (Gag) bands are at 53 kDa, p28 (MA precursor) are at 28 kDa, and p19 (MA) bands are at 19 kDa. All these

bands are present in each sample. The p28 protein, that is found to be linked with kinase activity of protein, is a combination of p19 and part of p24 (*141*). In each figure the thick band around 45 kDa appears after incubation of the cells with Compound 1 inhibitor. Beta-actin protein was used as a loading control for each sample shown in Figures 5-1, 5-2 and 5-3. None of the inhibitors show toxic effects within the cells at 4 h, 24 h, 2 days, or 6 days post-addition of the inhibitor.

The amount of p19 produced is shown to be reduced with the addition of inhibitor and the longer incubation times in ELISA assays. (Figure 5-4) In Figure 5-4B, the percent inhibition decreases within 48 hours of adding the inhibitor but there is still an inhibition effect on Gag processing. Even though no effect has been seen for C7 by Western Blotting, ELISA assay has shown some inhibition effect on the cells after 24 hours incubation.

Discussion

After determining inhibition constants of the computationally top ranked compounds, only five of them were tested in the *in vitro* cell assays. Their effect on Gag processing was observed. Out of five compounds, the best compound (Compound 1) that was determined to have the lowest inhibition constant (K_i), was the only compound that also showed distinctive bands in the Western Blot and ELISA assays. Even after 4 h of incubation resulted in MA-CA uncleaved product, this means the inhibitor effect starts before 4 h. (Figure 5-2) Reproducing the data at 24 h confirms inhibition of Gag processing. (Figure 5-1, Figure 5-2). 2 days and 6 days incubation results the same gene products at 45 kDa (MA-CA). (Figure 5-3) A similar effect was seen for HIV-1 PR with novel amino acid insertion; partially cleaved Gag products were seen in the Western Blotting (*142*). The ELISA P19 Antigen assays, which utilized the two best

inhibitor compounds identified by Western Blotting and kinetic analysis, support the Western Blotting data as shown in Figure 5-4. The amount of p19 protein was lower in the presence of Compound 1 compared to control cells (absence of any inhibitor) in the first or second day. (Figure 5-4A) The percent inhibition of Compound 1 at the first day is higher than at the second day. (Figure 5-4B) This result could mean in the case of drug usage, Compound 1 must be taken daily for efficient inhibition effect.

Compound 1, which was selected from the kinetic analysis for further testing, has also shown an inhibition effect on HTLV-1 infected cells, seeming to stop or slow down MA-CA cleavage. Inhibitor screening will continue to identify better compounds and crystal structures will be employed to develop possible drugs for HTLV-1.

A

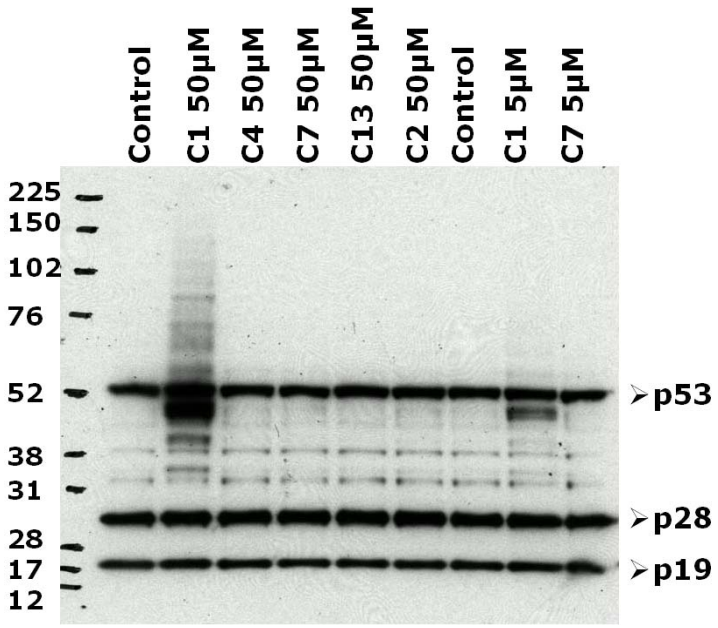

Figure 5-1. Western Blot of selected inhibitors incubated in MT-2 cells. First lane shows the molecular weight markers, second lane shows control cells without any compound. The rest of the lanes are 50 µM of Compound 1, Compound 4, Compound 7, Compound 13, Compound 2, control cells without any compound, 5 µM of Compound 1 and Compound 7 incubated in MT-2 cells for 24 hours, respectively. 20 µg protein has been loaded for 24 hours of incubation cells.

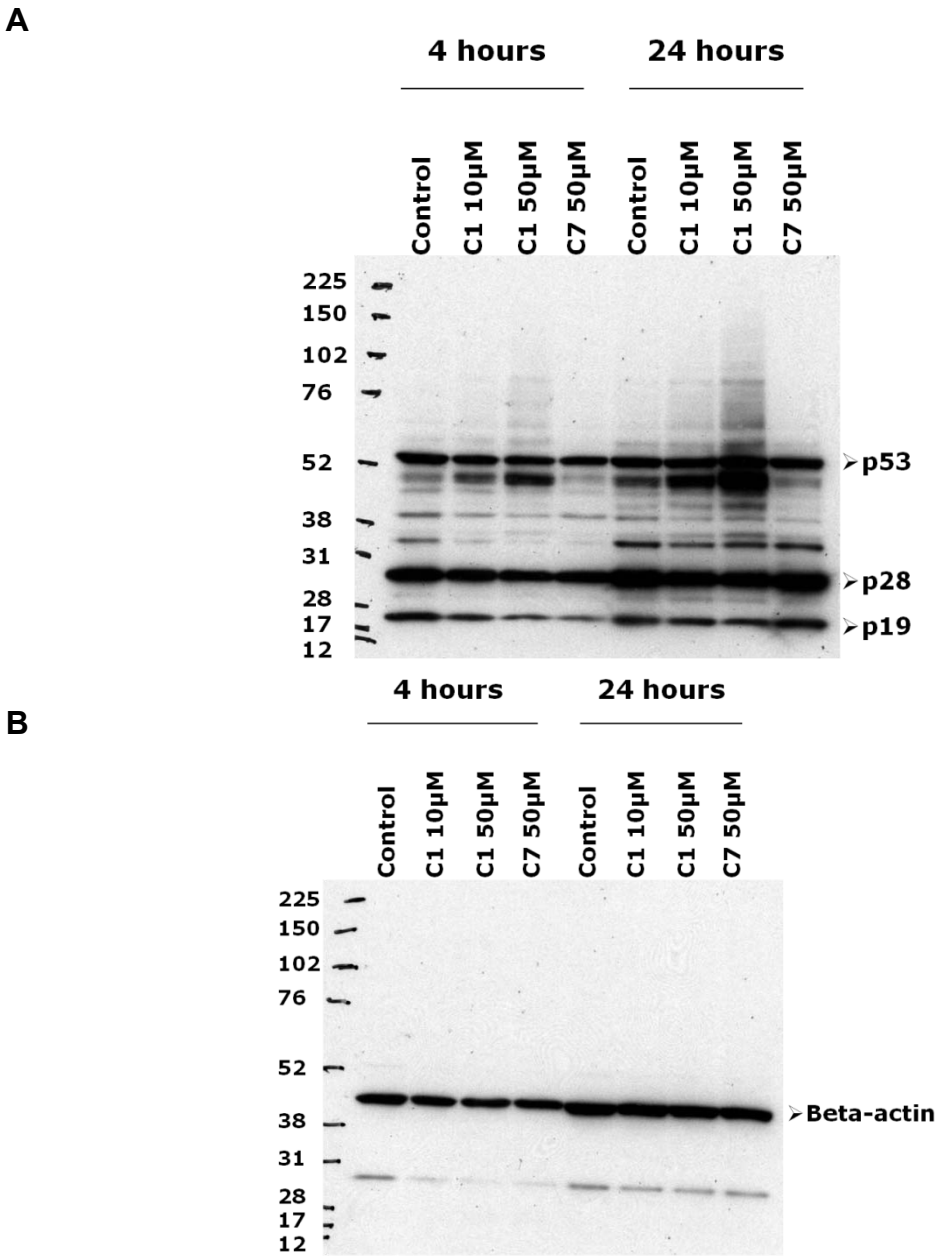

Figure 5-2. Western Blot of selected inhibitors incubated in MT-2 cells for 24 h. (A**)** First lane shows the molecular weight markers, second lane shows control cells without any compound. The rest of the lanes are 10 and 50 µM of Compound 1. Compound 7 50 µM incubated in MT-2 cells for 4 hours and 24 hours of incubation, respectively. 10 µg of protein has been loaded for 4 hours and 20 µg protein has been loaded for 24 hours of incubation cells. B) Beta-actin control loads of MT-2 cells. First lane shows molecular weight markers, second lane shows control cells without any compound. The rest of the lanes are 10 and 50 µM of Compound 1. Compound 7 50 µM incubated in MT-2 cells for 4 hours, 24 hours of incubation, respectively. 10 µg of protein has been loaded for 4 hours and 20 µg protein has been loaded for 24 hours of incubation cells.

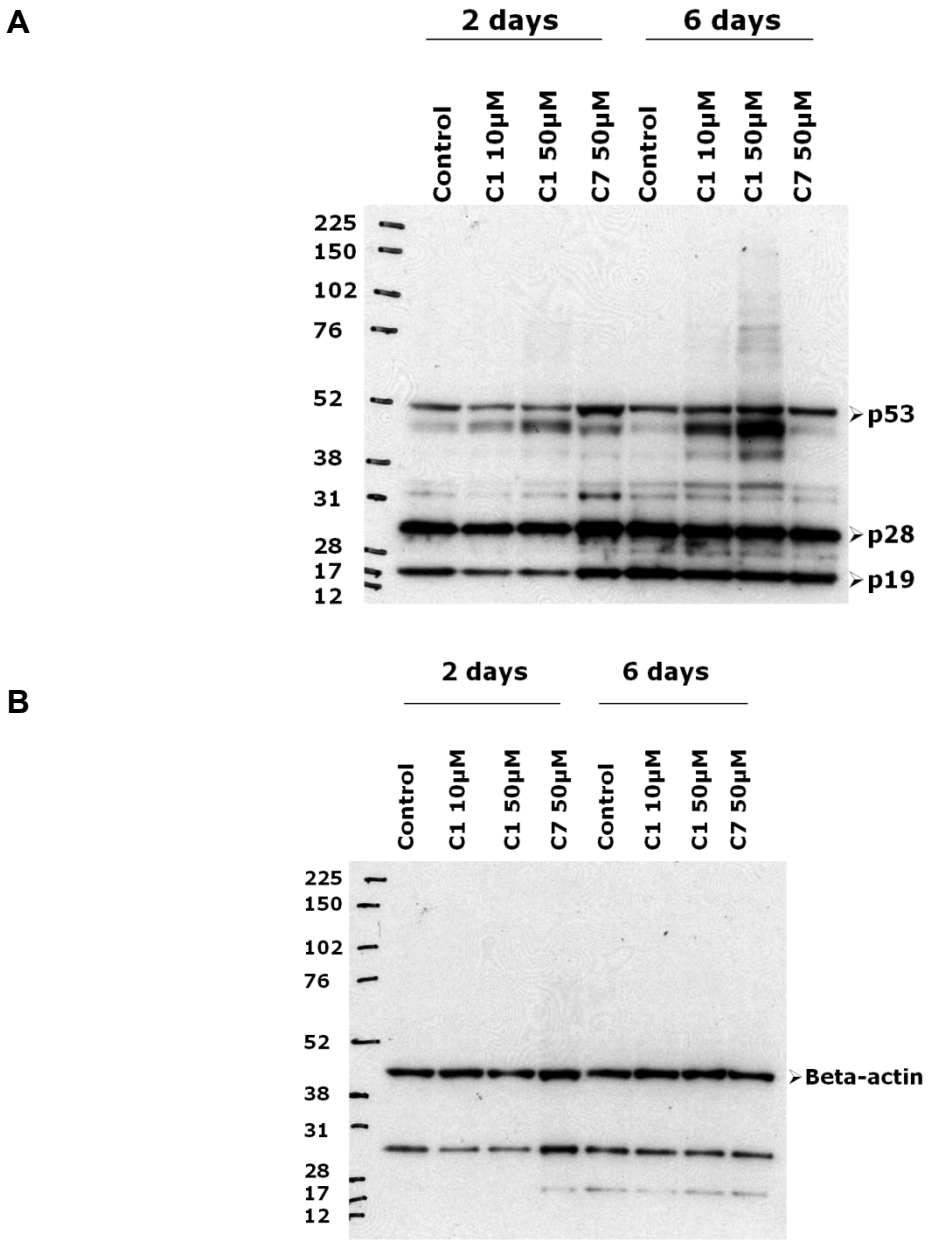

Figure 5-3. Western Blot of selected inhibitors incubated in MT-2 cells. (A**)** First lane shows the molecular weight markers, second lane shows control cells without any compound. The rest of the lanes are 10 and 50 µM of Compound 1. Compound 7 50 µM incubated in MT-2 cells for 2 and 6 days of incubation, respectively. B) Beta-actin control loads of MT-2 cells. First lane shows the molecular weight markers, second lane shows control cells without any compound. The rest of the lanes are 10 and 50 µM of Compound 1. Compound 7 50 µM incubated in MT-2 cells for 2 and 6 days of incubation, respectively. 10 µg of protein has been loaded.

A

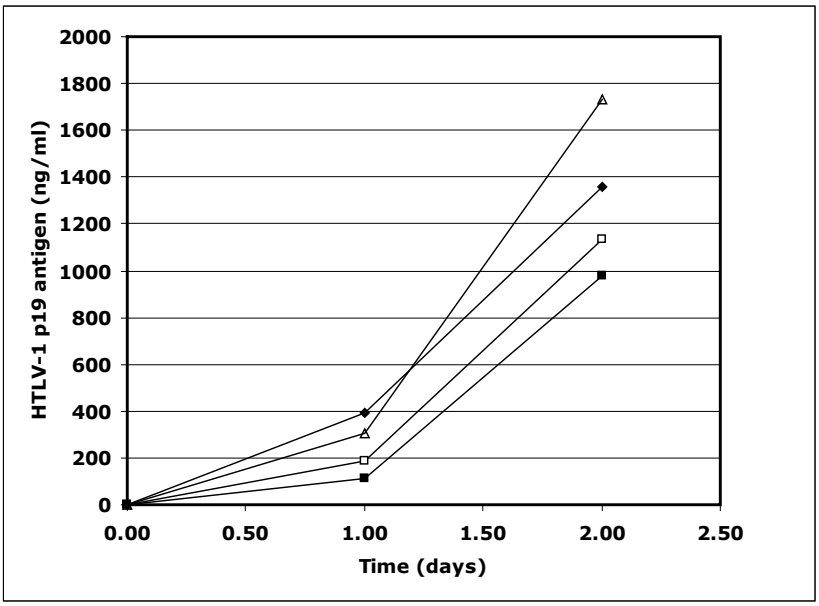

B

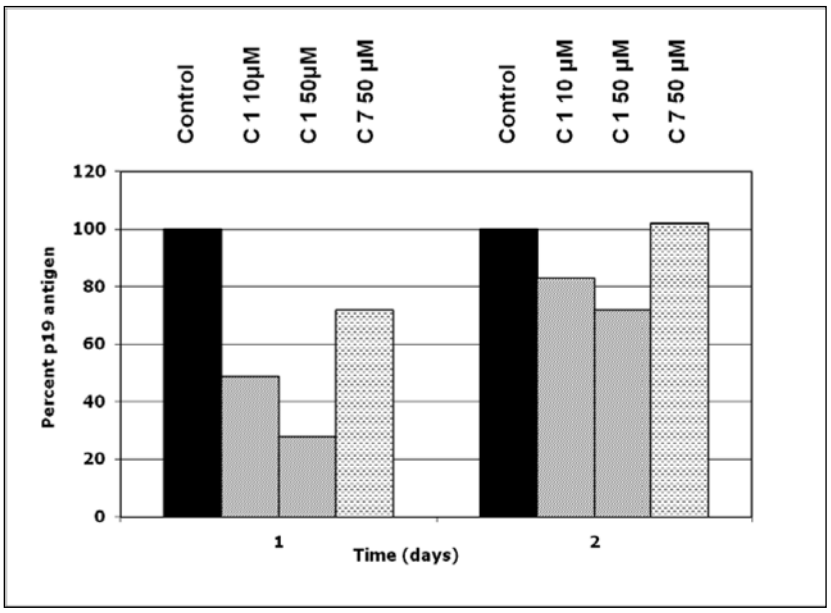

Figure 5-4. A. ELISA assay graph representation. P19 (MA) protein concentration in the cells with 1 and 2 days of incubation with Compound 110 and 50 µM, Compound 7 50 µM. Control cells are shown as quadrangle, 10 µM Compound 1 incubated cells are shown as open squares, 10 µM Compound 1 incubated cells are shown as squares and 50 µM Compound 7 incubated cells are shown as open triangles. B. ELISA assay bar representation. Percent P19 (MA) protein concentration in the cells with 1 and 2 days of incubation with Compound 1 ,10 and 50 µM, Compound 7 50 µM. (No error bars were indicated, because only one set of data was obtained.)

CHAPTER 6
DETERMINING FLAP CONFORMATION OF HTLV-1 PR BY ELECTRON PARAMAGNETIC RESONANCE SPECTROSCOPY

There are many methods that can be used to determine protein structure including X-ray crystallography, Nuclear Magnetic Resonance (NMR) Spectroscopy, and Electron Paramagnetic Resonance (EPR) Spectroscopy. Because HTLV-1 PR has flexible flap conformations, we have decided to use EPR to determine the flap confirmation of HTLV-1 PR beside the crystallography trials in our research. EPR, is a sensitive method for biological samples; examines the effects of the motion and polarity on the structure and has high accuracy. EPR is a very sensitive method, it can measure fast dynamic changes of a molecule (*143*). EPR was picked for our research based on the quantitative analysis of the flap distances. Using NMR with EPR can provide broad information about the structure of a biomolecule.

EPR, is also known as electron spin resonance (ESR) spectroscopy, measure the absorption of a paramagnetic substance when an external magnetic field applied in microwave radiation. Zeeman Effect is the interaction between the substance and the magnetic field. Zeeman effect splits these two unpaired electron in the presence of the magnetic field, these two spin states have degenerate magnetic moments (m_s= -1/2 and m_s= +1/2). (Figure 6-1) The energy difference between these two spin states is calculated by Zeeman equation:

$$\Delta E = h\nu = g\beta B \qquad (7\text{-}1)$$

Where ΔE is the energy difference, h is the Planck's constant (6.62606896×10^{-34} J.s), v is the microwave frequency, g is the splitting factor (≈2 for free electron), β is the Bohr magneton ($9.27400915 \times 10^{-24}$ J·T^{-1}), and B is the applied magnetic field (*144*). Enegy diagram is shown in Figure 6-1.

EPR has been used to determine the flap confirmation of HIV-1 PR by Fanucci and her co-workers (*117, 145, 146*). It was found that HIV-1 PR has a broad distribution of conformational change in the absence of the inhibitor, versus a narrow distribution in the presence of the inhibitor (*117, 146*). It is assumed HTLV-1 PR acts in a similar manner based on their genomic and sequence similarities. The flaps of HIV-1 PR have three conformations: open or semi-open forms with no inhibitor, and the closed form with inhibitor bound (*147*). This result was supported by NMR results showing large conformational changes at the flap region (*148-150*). Site-directed spin labeling (SDSL) is a method to label the specific sites of the macromolecules with spin probes and observe the dynamic changes for macromolecules. The approach to SDSL is introducing a nitroxide site chain at a specific site with using mutagenesis (*151*). Nitroxide is the name of the compounds used in the spin labeling. These compounds have $R_2NO^{\cdot}$ radicals after removing hydrogen at the hydroxyl groups. There are three commonly used spin labeling probes; the methanethiosulfonate spin label (MTSL), the iodoacetamido-proxyl spin label (IAP) and the maleimido-proxyl spin label (MSL). The methanethiosulfonate spin label (MTSL) is commonly used for site-specific labeling of proteins. It is sensitive to the motions of the protein backbone and secondary structure compared to other labels. The structure of MTSL and its bound structure to free cysteine is shown in Figure 6-2. The intrinsic motion of spin label, the backbone flexibility in cysteine residue region, and the overall tumbling of the molecule in the solution can be measured by EPR / SDSL.

Using EPR / SDSL, the free electron ($m_s = \pm 1/2$) on the MTSL spin label couples with the nuclear spin from nitrogen ($m_I = 1$). Based on 2I+1 rule, three energy transition

occur. Because MTSL binds to cysteine amino acid of a protein, any native cysteines are mutated to alanines and a cysteine in a desired region is introduced for analysis. Native cysteines were mutated to alanines at residue positions 90 and 109 for HTLV-1 PR. Based on HIV-1 PR mutations and used methods; three mutations were made (*146*). The glutamine at the 64^{th} position, which is equivalent to lysine at 55^{th} position of HIV-1 PR, was mutated to a cysteine for MTSL labeling. K55 was chosen based on the identical activity with the wild type, and the moiety of spin label cooperation (*146*). Mutations were made using the conditions described in the Site Directed Mutagenesis description in Chapter 2. The primers utilized for mutations are shown in Figure 6-3. It was confirmed that protease with the native cysteines mutated to alanines has the same catalytic properties as the wide type of HTLV-1 PR based on literature (*82, 103*). Protein expression, refolding, and purification methods were identical to those for wild type and purified protein was confirmed by 18% SDS-PAGE gel. (Figure 6-4 and 6-5) The next step is labeling the Cys 64 in the flap region of HTLV-1 PR with MTSL.

The distance between nitroxide spin labels can be measure by two methods. Continuous Wave (CW) method measures the distances based on dipolar interactions and extracts the distance 8-20 Å (*152*), or Double Electron Electron Resonance (DEER) method ,which is the pulsed EPR, measures the distances by producing a spin echo. DEER capable of measuring distances 20-70 Å. The distance between the two alpha carbons of the glutamines at 64^{th} position of HTLV-1 PR were determined by Chimera software (UCSF) to be 19 Å (*124*). (Figure 6-6) Because the distance between nitroxide spin labels is between 8-20 Å, CW is a better method to measure the conformational changes of flaps of HTLV-1 PR.

Our future work is to determine the molecular dynamics of the HTLV-1 PR flaps in the presence and absence of Compound 1 with using MTSL labeling and EPR spectroscopy.

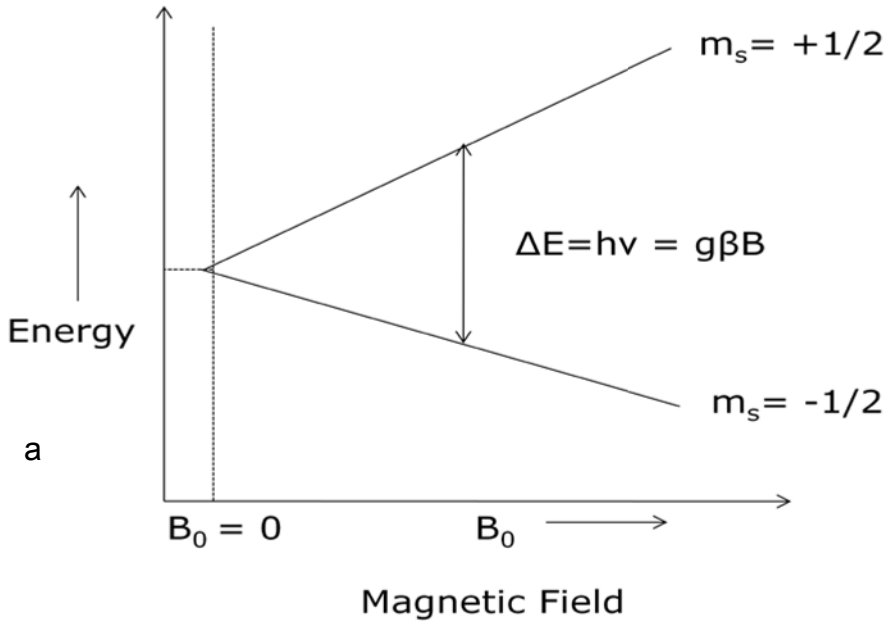

Figure 6-1. Energy diagram of a system with a free electron in the magnetic field.

a b

Figure 6-2. MTSL label structure a. unbound structure, b. structure of MTSL bound to cysteine.

>D32N
Upper CGAAGCTCTACTAAACACAGGAGCAGACATG
Lower CATGTCTGCTCCTGTGTTTAGTAGAGCTTCG

>**C90A**
Upper CCTATTGTTTTAACATCTGCGCTAGTTGATACC
Lower GGTATCAACTAGCGCAGATGTTAAAACAATAGG

>**C109A**
Upper GCCTTACAACAAGCGCAGGGCGTCCTGTACC
Lower GGTACAGGACGCCCTGCGCTTGTTGTAAGGC

>>**Q64C**
Upper GGGGGCCAAACCTGCGATCACTTTAAGCTCACC
Lower GGTGAGCTTAAAGTGATCGCAGGTTTGGCCCCC

Figure 6-3. Primers for D32N, C90A, C109A and Q64C mutations of HTLV-1 PR.

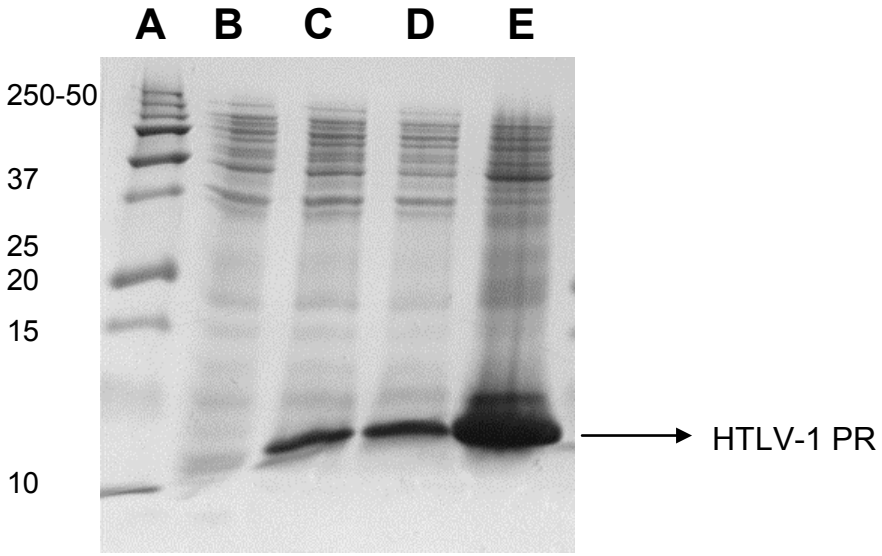

Figure 6-4. SDS Page gel of expression of triple mutated HTLV-1 PR. Lane A shows the Precision Plus Ladder (Biorad), lane B before IPTG induction, lane C 3 h after IPTG induction and lane D 6 h after IPTG induction and lane E is the inclusion bodies.

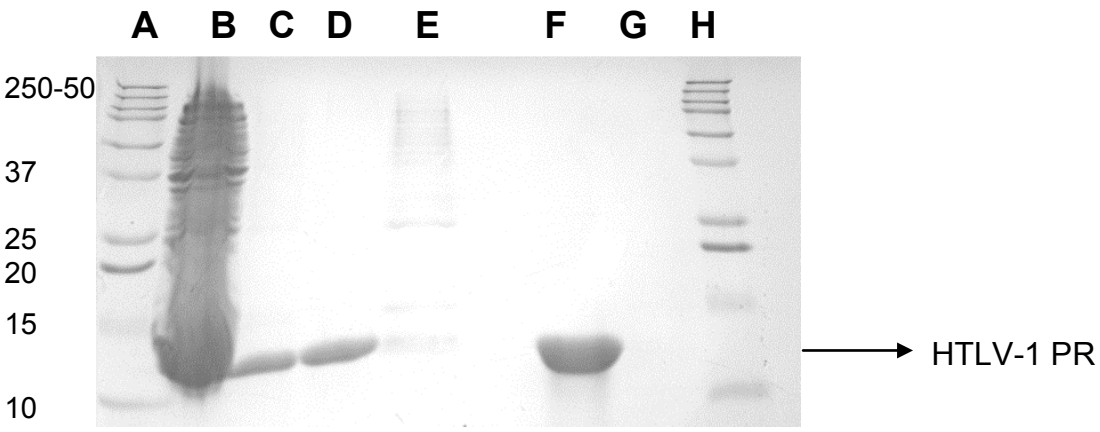

Figure 6-5. SDS Page gel picture of purification of of triple mutated HTLV-1 PR. Lane A shows the Precision Plus Ladder (Biorad), lane B Inclusion bodies, lane C Q column flow through, lane D Q column elution by 1 M NaCl, lane E SP column flow through, lane F SP column elution by 0.4 M NaCl, lane G SP column elution by 1 M NaCl, and the lane H the Precision Plus Ladder (Biorad).

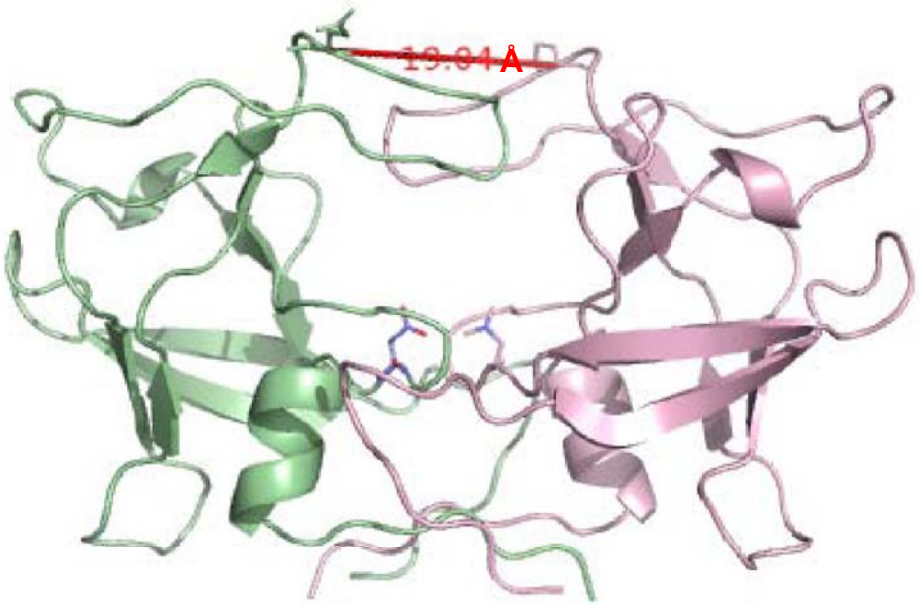

Figure 6-6. Distance between Cα of two Cys's of homodimer of HTLV-1 PR.

CHAPTER 7
CONCLUSIONS AND FUTURE WORK

HTLV-1 was isolated from a cutaneous lymphoma patient in 1980 by Gallo and it was proved to be the causative agent for ATL (*34, 153*). The Centers for Disease Control and Prevention have identified HTLV-1 as emerging pathogen (*154*). HIV-1 and HTLV-1 share many characteristics, but HIV-1 is more dangerous than HTLV-1 due to the effect of HIV-1 on the immune system (*155*). HTLV-1 infection has been reported in many regions of the world but is most prevalent in Southern Japan, the Caribbean basin, Central and West Africa, the Southeastern United States, Melanesia, parts of South Africa, the Middle East and India (*24*). Approximately 30 million people are infected by HTLV-1 worldwide, and although only 3-5% of the infected individuals evolve ATL in their life, the prognosis for those infected is still poor (*27*). The overall prognosis of ATL is still poor despite intensive chemotherapy (*45*). The median survival time of leukemia patients is 7-8 months (*156*). There is no specific drug treatment against HTLV-1. Many studies have been focused on drug design against HTLV-1, especially inhibitors for HTLV-1 PR, as PR as a drug target has been successful, especially in the case of AIDS treatment (*157-163*).

HTLV-1 PR is essential for viral replication and maturation. Therefore, it is a good target for drug design. First, conditions for expression, purification, refolding and kinetic characterization of HTLV-1 PR have been developed as mentioned in the Method chapter. HTLV-1 PR has a loop containing 10 extra amino acids at the C-terminal region only similar to BLV PR. It was determined that these 10 amino acids are not necessary for enzymatic activity. This research is significant to fully understand the enzymatic activity of HTLV-1 PR and the effects of the C-terminal residues on the activity.

Recombinant HTLV-1 PR has been used to identify inhibitors against HTLV-1 PR. *In silico* screening has been used for inhibitor discoveries using the crystal structure of 116-residue HTLV-1 PR. 140,000 small molecules were docked in the protease active site, and top ranked molecules were determined by DOCKv5.2 program. Several top ranked small molecules have been assayed in vitro by measuring the cleavage of the substrate A-P-Q-V-L*Nph-V-M-H-P-L, which mimics the natural MA/CA cleavage site, and was synthesized by the ICBR Core Facility at UF. Selected inhibitors have been used in *in vitro* cell culture assays to determine the effect in HTLV-1 infected cells. An inhibitor with the lowest inhibition constant has been discovered to inhibit Gag / Pol processing based on Western Blot and ELISA assays. Targeting HTLV-1 PR to treat HTLV-1 related disease is a very promising way based on the issues discussed throughout this dissertation. These results confirm the inhibition effect of the HTLV-1 PR inhibitors in the cells.

In addition to these studies, crystallization trials have been started for the HTLV-1 PR. The conditions from the literature and various modifications have been tried. First the conditions that yielded the obtained crystals used to determine the structure of HTLV-1 PR in Li et al. has been employed (*27*). Various pHs, salt concentration and precipitate concentrations have been tried, but only needle shaped crystals without any diffractions have been obtained. Hampton Research crystal screening kits and detergent kits have been used; in addition, the purified sample has been sent to Hampton Research to determine optimum conditions for crystal trials. No crystal structure has been obtained yet; new strategies will be tried to obtain a crystal structure while the set up crystal trays might produce crystals in time. Learning X-ray structure of

the full length HTLV-1 PR might provide a great insight to the inhibitor discoveries and treatment HTLV-1 related disease.

EPR studies are underway to determine flap conformation in the presence and absence of inhibitor. Necessary mutations and computational distance measurements have been made for EPR assays. Labeling and determination of flap conformational studies will continue using information of EPR studies of HIV-1 PR taking consideration of their structural similarities. The discoveries of the flap confirmation of HTLV-1 PR would expand the information about the binding of the inhibitors and their effect on the structures, as well as the effect of the C-terminal residues on the structure of the protease.

Expressing HTLV-1 PR in a soluble system would prevent folding and aggregation problems of HTLV-1 PR. Improving the folding properties by trying new strategies would help understanding the properties of full length of HTLV-1 PR. Obtaining information about the conformation of flaps can give details about the structure and the interactions between inhibitor and the protease. Determining crystal structure by X-ray crystallography or NMR would provide detailed information about enzyme active site, enzyme-inhibitor interactions.The best inhibitor that found by kinetic characterization can be improved after obtaining crystal structure of inhibitor bound HTLV-PR. It can be tried in animal model to observe the effect of the inhibitors. There have been a few animal models identified for HTLV-1 in the listed references (*164, 165*).

Understanding enzymology and structure of HTLV-1 PR is critical to design an inhibitor. Our *in vitro* assays help understanding enzymology of HTLV-1 PR, specifically effect of the last residues at the C-terminal region. The best inhibitor has effect in the

HTLV-1 infected cells. This work can lead a drug targeted at HTLV-1 PR to cure HTLV-1 infected patients.

APPENDIX:
SEQUENCE

CATATGCCAGTTATACCGTTAGATCCCGCCCGTCGGCCCGTAATTAAAGCCCAGG

TTGACACCCAGACCAGCCACCCAAAGACTATCGAAGCTCTACTAGATACAGGAGC

AGACATGACAGTC**ATC**CCGATAGCCTTGTTCTCAAGTAATACTCCCCTCAAAAAT

ACATCCGTATTAGGGGCAGGGGGCCAAACCCAAGATCACTTTAAGCTCACCTCCC

TTCCTGTGCTAATACGCCTCCCTTTCCGGACAACGCCTATTGTTTTAACATCTTG

CCTAGTTGATACCAAAAACAACTGGGCCATCATAGGTCGCGATGCCTTACAACAA

TGCCAGGGCGTCCTGTACCTCCCTGAGGCAAAAGGGCCGCCTGTAATCTTG**GGAT**

CC

Figure A-1. DNA sequence of full length HTLV-1 PR with a start methionine with a 5' NdeI site and a 3' BamH1 site for directional cloning into pET-11a.

P V I P L D P A R R P V I K A Q V D T Q T S H P K T I E

A L L D T G A D M T V L P I A L F S S N T P L K N T S V

L G A G G Q T Q D H F K L T S L P V L I R L P F R T T P

I V L T S C L V D T K N N W A I I G R D A L Q Q C Q G V

L Y L P E A K G P P V I L

Figure A-2. Protein sequence of full length HTLV-1 PR.

LIST OF REFERENCES

1. Kadas, J., Boross, P., Weber, I. T., Bagossi, P., Matuz, K., and Tozser, J. (2008) C-terminal residues of mature human T-lymphotropic virus type 1 protease are critical for dimerization and catalytic activity, *Biochem J 416*, 357-364.

2. Coffin, J. M. H., Stephen H.; Varmus, Harold E. (1997) *Retroviruses*, Cold Spring Harbor Laboratory Press, New York.

3. Voet J., V. D. (1990) *Biochemistry*.

4. Pique, C., Pham, D., Tursz, T., and Dokhelar, M. C. (1992) Human T-cell leukemia virus type I envelope protein maturation process: requirements for syncytium formation, *J Virol 66*, 906-913.

5. Rao, M. B., Tanksale, A. M., Ghatge, M. S., and Deshpande, V. V. (1998) Molecular and biotechnological aspects of microbial proteases, *Microbiol Mol Biol Rev 62*, 597-635.

6. Renoux-Elbe, C., Cheynier, R., and Wain-Hobson, S. (2002) Phylogeny derived from coding retroviral genome organization, *J Mol Evol 54*, 376-385.

7. Buchschacher, G. L., Jr. (2001) Introduction to retroviruses and retroviral vectors, *Somat Cell Mol Genet 26*, 1-11.

8. Murphy, F. A., C. M. Fauquet, D. H. L. Bishop, S. A. Ghabrial, A. W. Jarvis, G. P. Martelli, M. A. Mayo, and M. D. Summers. (1995) Virus taxonomy: classification and nomenclature of viruses: sixth report of the International Committee on Taxonomy of Viruses., *Archives of virology*.

9. Weiss, R. A. (1996) Retrovirus classification and cell interactions, *J Antimicrob Chemother 37 Suppl B*, 1-11.

10. Uchiyama, T., Yodoi, J., Sagawa, K., Takatsuki, K., and Uchino, H. (1977) Adult T-cell leukemia: clinical and hematologic features of 16 cases, *Blood 50*, 481-492.

11. Gessain, A., Barin, F., Vernant, J. C., Gout, O., Maurs, L., Calender, A., and de The, G. (1985) Antibodies to human T-lymphotropic virus type-I in patients with tropical spastic paraparesis, *Lancet 2*, 407-410.

12. Nishioka, K., Maruyama, I., Sato, K., Kitajima, I., Nakajima, Y., and Osame, M. (1989) Chronic inflammatory arthropathy associated with HTLV-I, *Lancet 1*, 441.

13. Mochizuki, M., Watanabe, T., Yamaguchi, K., Takatsuki, K., Yoshimura, K., Shirao, M., Nakashima, S., Mori, S., Araki, S., and Miyata, N. (1992) HTLV-I uveitis: a distinct clinical entity caused by HTLV-I, *Jpn J Cancer Res 83*, 236-239.

14. LaGrenade, L., Hanchard, B., Fletcher, V., Cranston, B., and Blattner, W. (1990) Infective dermatitis of Jamaican children: a marker for HTLV-I infection, *Lancet 336*, 1345-1347.

15. Morgan, O. S., Rodgers-Johnson, P., Mora, C., and Char, G. (1989) HTLV-1 and polymyositis in Jamaica, *Lancet 2*, 1184-1187.

16. Uchiyama, T. (1997) Human T cell leukemia virus type I (HTLV-I) and human diseases, *Annu Rev Immunol 15*, 15-37.

17. Mueller, N., Okayama, A., Stuver, S., and Tachibana, N. (1996) Findings from the Miyazaki Cohort Study, *J Acquir Immune Defic Syndr Hum Retrovirol 13 Suppl 1*, S2-7.

18. Murphy, E. L., Figueroa, J. P., Gibbs, W. N., Holding-Cobham, M., Cranston, B., Malley, K., Bodner, A. J., Alexander, S. S., and Blattner, W. A. (1991) Human T-lymphotropic virus type I (HTLV-I) seroprevalence in Jamaica. I. Demographic determinants, *Am J Epidemiol 133*, 1114-1124.

19. Mueller, N. (1991) The epidemiology of HTLV-I infection, *Cancer Causes Control 2*, 37-52.

20. Dumas, M., Houinato, D., Verdier, M., Zohoun, T., Josse, R., Bonis, J., Zohoun, I., Massougbodji, A., and Denis, F. (1991) Seroepidemiology of human T-cell lymphotropic virus type I/II in Benin (West Africa), *AIDS Res Hum Retroviruses 7*, 447-451.

21. Gessain, A., and de The, G. (1996) What is the situation of human T cell lymphotropic virus type II (HTLV-II) in Africa? Origin and dissemination of genomic subtypes, *J Acquir Immune Defic Syndr Hum Retrovirol 13 Suppl 1*, S228-235.

22. Andersson, S., Dias, F., Mendez, P. J., Rodrigues, A., and Biberfeld, G. (1997) HTLV-I and -II infections in a nationwide survey of pregnant women in Guinea-Bissau, West Africa, *J Acquir Immune Defic Syndr Hum Retrovirol 15*, 320-322.

23. Sarkodie, F., Adarkwa, M., Adu-Sarkodie, Y., Candotti, D., Acheampong, J. W., and Allain, J. P. (2001) Screening for viral markers in volunteer and replacement blood donors in West Africa, *Vox Sang 80*, 142-147.

24. Ferreira, O. C., Jr., Planelles, V., and Rosenblatt, J. D. (1997) Human T-cell leukemia viruses: epidemiology, biology, and pathogenesis, *Blood Rev 11*, 91-104.

25. Proietti, F. A., Carneiro-Proietti, A. B., Catalan-Soares, B. C., and Murphy, E. L. (2005) Global epidemiology of HTLV-I infection and associated diseases, *Oncogene 24*, 6058-6068.

26. Slattery, J. P., Franchini, G., and Gessain, A. (1999) Genomic evolution, patterns of global dissemination, and interspecies transmission of human and simian T-cell leukemia/lymphotropic viruses, *Genome Res 9*, 525-540.

27. Li, M., Laco, G. S., Jaskolski, M., Rozycki, J., Alexandratos, J., Wlodawer, A., and Gustchina, A. (2005) Crystal structure of human T cell leukemia virus protease, a novel target for anticancer drug design, *Proc Natl Acad Sci U S A 102*, 18332-18337.

28. Kannagi, M., Harashima, N., Kurihara, K., Utsunomiya, A., Tanosaki, R., and Masuda, M. (2004) Adult T-cell leukemia: future prophylaxis and immunotherapy, *Expert Rev Anticancer Ther 4*, 369-376.

29. Poiesz, B. J., Ruscetti, F. W., Gazdar, A. F., Bunn, P. A., Minna, J. D., and Gallo, R. C. (1980) Detection and isolation of type C retrovirus particles from fresh and cultured lymphocytes of a patient with cutaneous T-cell lymphoma, *Proc Natl Acad Sci U S A 77*, 7415-7419.

30. Gallo, D., Yeh, E. T., Moore, E. S., and Hanson, C. V. (1996) Comparison of four enzyme immunoassays for detection of human T-cell lymphotropic virus type 2 antibodies, *J Clin Microbiol 34*, 213-215.

31. Poiesz, B. J., Ruscetti, F. W., Mier, J. W., Woods, A. M., and Gallo, R. C. (1980) T-cell lines established from human T-lymphocytic neoplasias by direct response to T-cell growth factor, *Proc Natl Acad Sci U S A 77*, 6815-6819.

32. Gallo, R. C. T., M. M. (1996) Introduction. In: Human T-Cell Lymphotropic Virus Type I.

33. Hinuma, Y., Komoda, H., Chosa, T., Kondo, T., Kohakura, M., Takenaka, T., Kikuchi, M., Ichimaru, M., Yunoki, K., Sato, I., Matsuo, R., Takiuchi, Y., Uchino, H., and Hanaoka, M. (1982) Antibodies to adult T-cell leukemia-virus-associated antigen (ATLA) in sera from patients with ATL and controls in Japan: a nation-wide sero-epidemiologic study, *Int J Cancer 29*, 631-635.

34. Watanabe, T., Seiki, M., and Yoshida, M. (1984) HTLV type I (U. S. isolate) and ATLV (Japanese isolate) are the same species of human retrovirus, *Virology 133*, 238-241.

35. Wiktor, S. Z., Pate, E. J., Murphy, E. L., Palker, T. J., Champegnie, E., Ramlal, A., Cranston, B., Hanchard, B., and Blattner, W. A. (1993) Mother-to-child transmission of human T-cell lymphotropic virus type I (HTLV-I) in Jamaica: association with antibodies to envelope glycoprotein (gp46) epitopes, *J Acquir Immune Defic Syndr 6*, 1162-1167.

36. Kajiyama, W., Kashiwagi, S., Ikematsu, H., Hayashi, J., Nomura, H., and Okochi, K. (1986) Intrafamilial transmission of adult T cell leukemia virus, *J Infect Dis 154*, 851-857.

37. Okochi, K., Sato, H., and Hinuma, Y. (1984) A retrospective study on transmission of adult T cell leukemia virus by blood transfusion: seroconversion in recipients, *Vox Sang 46*, 245-253.

38. Kamihira, S., Nakasima, S., Oyakawa, Y., Moriuti, Y., Ichimaru, M., Okuda, H., Kanamura, M., and Oota, T. (1987) Transmission of human T cell lymphotropic virus type I by blood transfusion before and after mass screening of sera from seropositive donors, *Vox Sang 52*, 43-44.

39. Fujino, T., and Nagata, Y. (2000) HTLV-I transmission from mother to child, *J Reprod Immunol 47*, 197-206.

40. Derse, D., and Heidecker, G. (2003) Virology. Forced entry--or does HTLV-I have the key?, *Science 299*, 1670-1671.

41. Matsuoka, M., and Jeang, K. T. (2007) Human T-cell leukaemia virus type 1 (HTLV-1) infectivity and cellular transformation, *Nat Rev Cancer 7*, 270-280.

42. Igakura, T., Stinchcombe, J. C., Goon, P. K., Taylor, G. P., Weber, J. N., Griffiths, G. M., Tanaka, Y., Osame, M., and Bangham, C. R. (2003) Spread of HTLV-I between lymphocytes by virus-induced polarization of the cytoskeleton, *Science 299*, 1713-1716.

43. Franchini, G., and Streicher, H. (1995) Human T-cell leukaemia virus, *Baillieres Clin Haematol 8*, 131-148.

44. Tsukasaki, K., Utsunomiya, A., Fukuda, H., Shibata, T., Fukushima, T., Takatsuka, Y., Ikeda, S., Masuda, M., Nagoshi, H., Ueda, R., Tamura, K., Sano, M., Momita, S., Yamaguchi, K., Kawano, F., Hanada, S., Tobinai, K., Shimoyama, M., Hotta, T., and Tomonaga, M. (2007) VCAP-AMP-VECP compared with biweekly CHOP for adult T-cell leukemia-lymphoma: Japan Clinical Oncology Group Study JCOG9801, *J Clin Oncol 25*, 5458-5464.

45. Yasunaga, J., and Matsuoka, M. (2007) Leukaemogenic mechanism of human T-cell leukaemia virus type I, *Rev Med Virol 17*, 301-311.

46. Tsukasaki, K., Hermine, O., Bazarbachi, A., Ratner, L., Ramos, J. C., Harrington, W., Jr., O'Mahony, D., Janik, J. E., Bittencourt, A. L., Taylor, G. P., Yamaguchi, K., Utsunomiya, A., Tobinai, K., and Watanabe, T. (2009) Definition, prognostic factors, treatment, and response criteria of adult T-cell leukemia-lymphoma: a proposal from an international consensus meeting, *J Clin Oncol 27*, 453-459.

47. (2009-12-01) Guidelines for the use of antiretroviral agents in HIV-1-infected adults and adolescents, *Panel on Antiretroviral Guidelines for Adults and Adolescents*, 1-161.

48. Montessori, V., Press, N., Harris, M., Akagi, L., and Montaner, J. S. (2004) Adverse effects of antiretroviral therapy for HIV infection, *CMAJ 170*, 229-238.

49. Shimoyama, M., Ota, K., Kikuchi, M., Yunoki, K., Konda, S., Takatsuki, K., Ichimaru, M., Ogawa, M., Kimura, I., Tominaga, S., and et al. (1988) Chemotherapeutic results and prognostic factors of patients with advanced non-Hodgkin's lymphoma treated with VEPA or VEPA-M, *J Clin Oncol 6*, 128-141.

50. Kannagi, M., Ohashi, T., Harashima, N., Hanabuchi, S., and Hasegawa, A. (2004) Immunological risks of adult T-cell leukemia at primary HTLV-I infection, *Trends Microbiol 12*, 346-352.

51. Lane, M. (1979) Clinical problems of resistance to cancer chemotherapeutic agents, *Fed Proc 38*, 103-107.

52. Beck, W. T., Mueller, T. J., and Tanzer, L. R. (1979) Altered surface membrane glycoproteins in Vinca alkaloid-resistant human leukemic lymphoblasts, *Cancer Res 39*, 2070-2076.

53. Shen, D. W., Cardarelli, C., Hwang, J., Cornwell, M., Richert, N., Ishii, S., Pastan, I., and Gottesman, M. M. (1986) Multiple drug-resistant human KB carcinoma cells independently selected for high-level resistance to colchicine, adriamycin, or vinblastine show changes in expression of specific proteins, *J Biol Chem 261*, 7762-7770.

54. Tsuruo, T., Iida-Saito, H., Kawabata, H., Oh-hara, T., Hamada, H., and Utakoji, T. (1986) Characteristics of resistance to adriamycin in human myelogenous leukemia K562 resistant to adriamycin and in isolated clones, *Jpn J Cancer Res 77*, 682-692.

55. Borg, A., Yin, J. A., Johnson, P. R., Tosswill, J., Saunders, M., and Morris, D. (1996) Successful treatment of HTLV-1-associated acute adult T-cell leukaemia lymphoma by allogeneic bone marrow transplantation, *Br J Haematol 94*, 713-715.

56. Fukushima, T., Miyazaki, Y., Honda, S., Kawano, F., Moriuchi, Y., Masuda, M., Tanosaki, R., Utsunomiya, A., Uike, N., Yoshida, S., Okamura, J., and Tomonaga, M. (2005) Allogeneic hematopoietic stem cell transplantation provides sustained long-term survival for patients with adult T-cell leukemia/lymphoma, *Leukemia 19*, 829-834.

57. Takizawa, J., Aoki, S., Kurasaki, T., Higashimura, M., Honma, K., Kitajima, T., Momoi, A., Takahashi, H., Nakamura, N., Furukawa, T., and Aizawa, Y. (2007) Successful treatment of adult T-cell leukemia with unrelated cord blood transplantation, *Am J Hematol 82*, 1113-1115.

58. Grassmann, R., Aboud, M., and Jeang, K. T. (2005) Molecular mechanisms of cellular transformation by HTLV-1 Tax, *Oncogene 24*, 5976-5985.

59. Yasunaga, J., and Matsuoka, M. (2007) Human T-cell leukemia virus type I induces adult T-cell leukemia: from clinical aspects to molecular mechanisms, *Cancer Control 14*, 133-140.

60. Seiki, M., Inoue, J., Takeda, T., and Yoshida, M. (1986) Direct evidence that p40x of human T-cell leukemia virus type I is a trans-acting transcriptional activator, *EMBO J 5*, 561-565.

61. Chen, I. S., Slamon, D. J., Rosenblatt, J. D., Shah, N. P., Quan, S. G., and Wachsman, W. (1985) The x gene is essential for HTLV replication, *Science 229*, 54-58.

62. Tozser, J., and Weber, I. T. (2007) The protease of human T-cell leukemia virus type-1 is a potential therapeutic target, *Curr Pharm Des 13*, 1285-1294.

63. Mador, N., Panet, A., and Honigman, A. (1989) Translation of gag, pro, and pol gene products of human T-cell leukemia virus type 2, *J Virol 63*, 2400-2404.

64. Mitchell, M. S., Tozser, J., Princler, G., Lloyd, P. A., Auth, A., and Derse, D. (2006) Synthesis, processing, and composition of the virion-associated HTLV-1 reverse transcriptase, *J Biol Chem 281*, 3964-3971.

65. Nam, S. H., Copeland, T. D., Hatanaka, M., and Oroszlan, S. (1993) Characterization of ribosomal frameshifting for expression of pol gene products of human T-cell leukemia virus type I, *J Virol 67*, 196-203.

66. Seiki, M., Hattori, S., Hirayama, Y., and Yoshida, M. (1983) Human adult T-cell leukemia virus: complete nucleotide sequence of the provirus genome integrated in leukemia cell DNA, *Proc Natl Acad Sci U S A 80*, 3618-3622.

67. Boross, P., Bagossi, P., Weber, I. T., and Tozser, J. (2009) Drug targets in human T-lymphotropic virus type 1 (HTLV-1) infection, *Infect Disord Drug Targets 9*, 159-171.

68. Shuker, S. B., Mariani, V. L., Herger, B. E., and Dennison, K. J. (2003) Understanding HTLV-I protease, *Chem Biol 10*, 373-380.

69. Hattori, S., Kiyokawa, T., Imagawa, K., Shimizu, F., Hashimura, E., Seiki, M., and Yoshida, M. (1984) Identification of gag and env gene products of human T-cell leukemia virus (HTLV), *Virology 136*, 338-347.

70. Nam, S. H., and Hatanaka, M. (1986) Identification of a protease gene of human T-cell leukemia virus type I (HTLV-I) and its structural comparison, *Biochem Biophys Res Commun 139*, 129-135.

71. Jiang, F., Wisen, S., Widersten, M., Bergman, B., and Mannervik, B. (2000) Examination of the transcription factor NtcA-binding motif by in vitro selection of DNA sequences from a random library, *J Mol Biol 301*, 783-793.

72. Briggs, J. A., Simon, M. N., Gross, I., Krausslich, H. G., Fuller, S. D., Vogt, V. M., and Johnson, M. C. (2004) The stoichiometry of Gag protein in HIV-1, *Nat Struct Mol Biol 11*, 672-675.

73. Tozser, J., Zahuczky, G., Bagossi, P., Louis, J. M., Copeland, T. D., Oroszlan, S., Harrison, R. W., and Weber, I. T. (2000) Comparison of the substrate specificity of the human T-cell leukemia virus and human immunodeficiency virus proteinases, *Eur J Biochem 267*, 6287-6295.

74. Verdonck, K., Gonzalez, E., Van Dooren, S., Vandamme, A. M., Vanham, G., and Gotuzzo, E. (2007) Human T-lymphotropic virus 1: recent knowledge about an ancient infection, *Lancet Infect Dis 7*, 266-281.

75. Jacks, T., Townsley, K., Varmus, H. E., and Majors, J. (1987) Two efficient ribosomal frameshifting events are required for synthesis of mouse mammary tumor virus gag-related polyproteins, *Proc Natl Acad Sci U S A 84*, 4298-4302.

76. Nam, S. H., Kidokoro, M., Shida, H., and Hatanaka, M. (1988) Processing of gag precursor polyprotein of human T-cell leukemia virus type I by virus-encoded protease, *J Virol 62*, 3718-3728.

77. Rawlings, N. D., O'Brien, E., and Barrett, A. J. (2002) MEROPS: the protease database, *Nucleic Acids Res 30*, 343-346.

78. Liu, H., Muller-Plathe, F., and van Gunsteren, W. F. (1996) A combined quantum/classical molecular dynamics study of the catalytic mechanism of HIV protease, *J Mol Biol 261*, 454-469.

79. Pettit, S. C., Sanchez, R., Smith, T., Wehbie, R., Derse, D., and Swanstrom, R. (1998) HIV type 1 protease inhibitors fail to inhibit HTLV-I Gag processing in infected cells, *AIDS Res Hum Retroviruses 14*, 1007-1014.

80. Tozser, J., and Oroszlan, S. (2003) Proteolytic events of HIV-1 replication as targets for therapeutic intervention, *Curr Pharm Des 9*, 1803-1815.

81. Murphy, E. M., Jimenez, H. R., and Smith, S. M. (2008) Current clinical treatments of AIDS, *Adv Pharmacol 56*, 27-73.

82. Kadas, J., Weber, I. T., Bagossi, P., Miklossy, G., Boross, P., Oroszlan, S., and Tozser, J. (2004) Narrow substrate specificity and sensitivity toward ligand-binding site mutations of human T-cell Leukemia virus type 1 protease, *J Biol Chem 279*, 27148-27157.

83. Satoh, T., Li, M., Nguyen, J. T., Kiso, Y., Gustchina, A., and Wlodawer, A. Crystal structures of inhibitor complexes of human T-cell leukemia virus (HTLV-1) protease, *J Mol Biol 401*, 626-641.

84. Clemente, J. C., Robbins, A., Grana, P., Paleo, M. R., Correa, J. F., Villaverde, M. C., Sardina, F. J., Govindasamy, L., Agbandje-McKenna, M., McKenna, R., Dunn, B. M., and Sussman, F. (2008) Design, synthesis, evaluation, and crystallographic-based structural studies of HIV-1 protease inhibitors with reduced response to the V82A mutation, *J Med Chem 51*, 852-860.

85. Jaskolski, M., Miller, M., Rao, J. K., Leis, J., and Wlodawer, A. (1990) Structure of the aspartic protease from Rous sarcoma retrovirus refined at 2-A resolution, *Biochemistry 29*, 5889-5898.

86. Kervinen, J., Lubkowski, J., Zdanov, A., Bhatt, D., Dunn, B. M., Hui, K. Y., Powell, D. J., Kay, J., Wlodawer, A., and Gustchina, A. (1998) Toward a universal inhibitor of retroviral proteases: comparative analysis of the interactions of LP-130 complexed with proteases from HIV-1, FIV, and EIAV, *Protein Sci 7*, 2314-2323.

87. Kovalevsky, A. Y., Louis, J. M., Aniana, A., Ghosh, A. K., and Weber, I. T. (2008) Structural evidence for effectiveness of darunavir and two related antiviral inhibitors against HIV-2 protease, *J Mol Biol 384*, 178-192.

88. Rose, R. B., Rose, J. R., Salto, R., Craik, C. S., and Stroud, R. M. (1993) Structure of the protease from simian immunodeficiency virus: complex with an irreversible nonpeptide inhibitor, *Biochemistry 32*, 12498-12507.

89. Fechner, H., Blankenstein, P., Looman, A. C., Elwert, J., Geue, L., Albrecht, C., Kurg, A., Beier, D., Marquardt, O., and Ebner, D. (1997) Provirus variants of the bovine leukemia virus and their relation to the serological status of naturally infected cattle, *Virology 237*, 261-269.

90. Ha, J. J., Gaul, D. A., Mariani, V. L., Ding, Y. S., Ikeda, R. A., and Shuker, S. B. (2002) HTLV-I protease cleavage of P19/24 substrates is not dependent on NaCl concentration, *Bioorg Chem 30*, 138-144.

91. Luukkonen, B. G., Tan, W., Fenyo, E. M., and Schwartz, S. (1995) Analysis of cross reactivity of retrovirus proteases using a vaccinia virus-T7 RNA polymerase-based expression system, *J Gen Virol 76 (Pt 9)*, 2169-2180.

92. Schechter, I., and Berger, A. (1967) On the size of the active site in proteases. I. Papain, *Biochem Biophys Res Commun 27*, 157-162.

93. Ding, Y. S., Rich, D. H., and Ikeda, R. A. (1998) Substrates and inhibitors of human T-cell leukemia virus type I protease, *Biochemistry 37*, 17514-17518.

94. Daenke, S., Schramm, H. J., and Bangham, C. R. (1994) Analysis of substrate cleavage by recombinant protease of human T cell leukaemia virus type 1 reveals preferences and specificity of binding, *J Gen Virol 75 (Pt 9)*, 2233-2239.

95. Ding, Y. S., Owen, S. M., Lal, R. B., and Ikeda, R. A. (1998) Efficient expression and rapid purification of human T-cell leukemia virus type 1 protease, *J Virol 72*, 3383-3386.

96. Akaji, K., Teruya, K., and Aimoto, S. (2003) Solid-phase synthesis of HTLV-1 protease inhibitors containing hydroxyethylamine dipeptide isostere, *J Org Chem 68*, 4755-4763.

97. Nguyen, J. T., Zhang, M., Kumada, H. O., Itami, A., Nishiyama, K., Kimura, T., Cheng, M., Hayashi, Y., and Kiso, Y. (2008) Truncation and non-natural amino acid substitution studies on HTLV-I protease hexapeptidic inhibitors, *Bioorg Med Chem Lett 18*, 366-370.

98. Yamaguchi, K., Kiyokawa, T., Watanabe, T., Ideta, T., Asayama, K., Mochizuki, M., Blank, A., and Takatsuki, K. (1994) Increased serum levels of C-terminal parathyroid hormone-related protein in different diseases associated with HTLV-1 infection, *Leukemia 8*, 1708-1711.

99. Gessain, A., and de The, G. (1996) Geographic and molecular epidemiology of primate T lymphotropic retroviruses: HTLV-I, HTLV-II, STLV-I, STLV-PP, and PTLV-L, *Adv Virus Res 47*, 377-426.

100. Furnia, A., Lal, R., Maloney, E., Wiktor, S., Pate, E., Rudolph, D., Waters, D., Blattner, W., and Manns, A. (1999) Estimating the time of HTLV-I infection following mother-to-child transmission in a breast-feeding population in Jamaica, *J Med Virol 59*, 541-546.

101. Williams, A. E., Fang, C. T., Slamon, D. J., Poiesz, B. J., Sandler, S. G., Darr, W. F., 2nd, Shulman, G., McGowan, E. I., Douglas, D. K., Bowman, R. J., and et al. (1988) Seroprevalence and epidemiological correlates of HTLV-I infection in U.S. blood donors, *Science 240*, 643-646.

102. Laco, G. S., Fitzgerald, M. C., Morris, G. M., Olson, A. J., Kent, S. B., and Elder, J. H. (1997) Molecular analysis of the feline immunodeficiency virus protease: generation of a novel form of the protease by autoproteolysis and construction of cleavage-resistant proteases, *J Virol 71*, 5505-5511.

103. Louis, J. M., Oroszlan, S., and Tozser, J. (1999) Stabilization from autoproteolysis and kinetic characterization of the human T-cell leukemia virus type 1 proteinase, *J Biol Chem 274*, 6660-6666.

104. Marquardt, D. W. (1963) An algorithm for least squares estimation of nonlinear parameters, *J. Soc. Ind. Appl. Math. 11*, 431-441.

105. Kurenova, E. V., Hunt, D. L., He, D., Magis, A. T., Ostrov, D. A., and Cance, W. G. (2009) Small molecule chloropyramine hydrochloride (C4) targets the binding site of focal adhesion kinase and vascular endothelial growth factor receptor 3 and suppresses breast cancer growth in vivo, *J Med Chem 52*, 4716-4724.

106. Monga, M., and Sausville, E. A. (2002) Developmental therapeutics program at the NCI: molecular target and drug discovery process, *Leukemia 16*, 520-526.

107. Richards, F. M. (1977) Areas, volumes, packing and protein structure, *Annu Rev Biophys Bioeng 6*, 151-176.

108. Moustakas, D. T., Lang, P. T., Pegg, S., Pettersen, E., Kuntz, I. D., Brooijmans, N., and Rizzo, R. C. (2006) Development and validation of a modular, extensible docking program: DOCK 5, *J Comput Aided Mol Des 20*, 601-619.

109. Holbeck, S. L. (2004) Update on NCI in vitro drug screen utilities, *Eur J Cancer 40*, 785-793.

110. Haertle, T., Carrera, C. J., Wasson, D. B., Sowers, L. C., Richman, D. D., and Carson, D. A. (1988) Metabolism and anti-human immunodeficiency virus-1 activity of 2-halo-2',3'-dideoxyadenosine derivatives, *J Biol Chem 263*, 5870-5875.

111. Harada, S., Koyanagi, Y., and Yamamoto, N. (1985) Infection of HTLV-III/LAV in HTLV-I-carrying cells MT-2 and MT-4 and application in a plaque assay, *Science 229*, 563-566.

112. Oguariri, R. M., Brann, T. W., and Imamichi, T. (2007) Hydroxyurea and interleukin-6 synergistically reactivate HIV-1 replication in a latently infected promonocytic cell line via SP1/SP3 transcription factors, *J Biol Chem 282*, 3594-3604.

113. Imamichi, T., Murphy, M. A., Adelsberger, J. W., Yang, J., Watkins, C. M., Berg, S. C., Baseler, M. W., Lempicki, R. A., Guo, J., Levin, J. G., and Lane, H. C. (2003) Actinomycin D induces high-level resistance to thymidine analogs in replication of human immunodeficiency virus type 1 by interfering with host cell thymidine kinase expression, *J Virol 77*, 1011-1020.

114. Hayakawa, T., Misumi, Y., Kobayashi, M., Ohi, Y., Fujisawa, Y., Kakinuma, A., and Hatanaka, M. (1991) Expression of human T-cell leukemia virus type I protease in Escherichia coli, *Biochem Biophys Res Commun 181*, 1281-1287.

115. Hayakawa, T., Misumi, Y., Kobayashi, M., Yamamoto, Y., and Fujisawa, Y. (1992) Requirement of N- and C-terminal regions for enzymatic activity of human T-cell leukemia virus type I protease, *Eur J Biochem 206*, 919-925.

116. Herger, B. E., Mariani, V. L., Dennison, K., and Shuker, S. B. (2004) The 10 C-terminal residues of HTLV-I protease are not necessary for enzymatic activity, *Biochem Biophys Res Commun 320*, 1306-1308.

117. Kear, J. L., Blackburn, M. E., Veloro, A. M., Dunn, B. M., and Fanucci, G. E. (2009) Subtype polymorphisms among HIV-1 protease variants confer altered flap conformations and flexibility, *J Am Chem Soc 131*, 14650-14651.

118. Coman, R. M., Robbins, A. H., Fernandez, M. A., Gilliland, C. T., Sochet, A. A., Goodenow, M. M., McKenna, R., and Dunn, B. M. (2008) The contribution of naturally occurring polymorphisms in altering the biochemical and structural characteristics of HIV-1 subtype C protease, *Biochemistry 47*, 731-743.

119. Clemente, J. C., Coman, R. M., Thiaville, M. M., Janka, L. K., Jeung, J. A., Nukoolkarn, S., Govindasamy, L., Agbandje-McKenna, M., McKenna, R., Leelamanit, W., Goodenow, M. M., and Dunn, B. M. (2006) Analysis of HIV-1 CRF_01 A/E protease inhibitor resistance: structural determinants for maintaining sensitivity and developing resistance to atazanavir, *Biochemistry 45*, 5468-5477.

120. Clemente, J. C., Moose, R. E., Hemrajani, R., Whitford, L. R., Govindasamy, L., Reutzel, R., McKenna, R., Agbandje-McKenna, M., Goodenow, M. M., and Dunn, B. M. (2004) Comparing the accumulation of active- and nonactive-site mutations in the HIV-1 protease, *Biochemistry 43*, 12141-12151.

121. Goodenow, M. M., Bloom, G., Rose, S. L., Pomeroy, S. M., O'Brien, P. O., Perez, E. E., Sleasman, J. W., and Dunn, B. M. (2002) Naturally occurring amino acid polymorphisms in human immunodeficiency virus type 1 (HIV-1) Gag p7(NC) and the C-cleavage site impact Gag-Pol processing by HIV-1 protease, *Virology 292*, 137-149.

122. Pereira, A. S., Kenney, K. B., Cohen, M. S., Eron, J. J., Tidwell, R. R., and Dunn, J. A. (2002) Determination of amprenavir, a HIV-1 protease inhibitor, in human seminal plasma using high-performance liquid chromatography-tandem mass spectrometry, *J Chromatogr B Analyt Technol Biomed Life Sci 766*, 307-317.

123. Barrie, K. A., Perez, E. E., Lamers, S. L., Farmerie, W. G., Dunn, B. M., Sleasman, J. W., and Goodenow, M. M. (1996) Natural variation in HIV-1 protease, Gag p7 and p6, and protease cleavage sites within gag/pol polyproteins: amino acid substitutions in the absence of protease inhibitors in mothers and children infected by human immunodeficiency virus type 1, *Virology 219*, 407-416.

124. Pettersen, E. F., Goddard, T. D., Huang, C. C., Couch, G. S., Greenblatt, D. M., Meng, E. C., and Ferrin, T. E. (2004) UCSF Chimera--a visualization system for exploratory research and analysis, *J Comput Chem 25*, 1605-1612.

125. Morris, J. H., Huang, C. C., Babbitt, P. C., and Ferrin, T. E. (2007) structureViz: linking Cytoscape and UCSF Chimera, *Bioinformatics 23*, 2345-2347.

126. Lipinski, C. A. (2003) Chris Lipinski discusses life and chemistry after the Rule of Five, *Drug Discov Today 8*, 12-16.

127. Lipinski, C. A., Lombardo, F., Dominy, B. W., and Feeney, P. J. (2001) Experimental and computational approaches to estimate solubility and permeability in drug discovery and development settings, *Adv Drug Deliv Rev 46*, 3-26.

128. Heidecker, G., Hill, S., Lloyd, P. A., and Derse, D. (2002) A novel protease processing site in the transframe protein of human T-cell leukemia virus type 1 PR76(gag-pro) defines the N terminus of RT, *J Virol 76*, 13101-13105.

129. Jacks, T., Power, M. D., Masiarz, F. R., Luciw, P. A., Barr, P. J., and Varmus, H. E. (1988) Characterization of ribosomal frameshifting in HIV-1 gag-pol expression, *Nature 331*, 280-283.

130. Jacks, T., and Varmus, H. E. (1985) Expression of the Rous sarcoma virus pol gene by ribosomal frameshifting, *Science 230*, 1237-1242.

131. Moore, R., Dixon, M., Smith, R., Peters, G., and Dickson, C. (1987) Complete nucleotide sequence of a milk-transmitted mouse mammary tumor virus: two frameshift suppression events are required for translation of gag and pol, *J Virol 61*, 480-490.

132. Rice, N. R., Stephens, R. M., Burny, A., and Gilden, R. V. (1985) The gag and pol genes of bovine leukemia virus: nucleotide sequence and analysis, *Virology 142*, 357-377.

133. Hatfield, D., and Oroszlan, S. (1990) The where, what and how of ribosomal frameshifting in retroviral protein synthesis, *Trends Biochem Sci 15*, 186-190.

134. Hatfield, D. L., Levin, J. G., Rein, A., and Oroszlan, S. (1992) Translational suppression in retroviral gene expression, *Adv Virus Res 41*, 193-239.

135. Jacks, T. (1990) Translational suppression in gene expression in retroviruses and retrotransposons, *Curr Top Microbiol Immunol 157*, 93-124.

136. Lochelt, M., and Flugel, R. M. (1996) The human foamy virus pol gene is expressed as a Pro-Pol polyprotein and not as a Gag-Pol fusion protein, *J Virol 70*, 1033-1040.

137. Morozov, V. A., and Weiss, R. A. (1999) Two types of HTLV-1 particles are released from MT-2 cells, *Virology 255*, 279-284.

138. Nagy, K., Clapham, P., Cheingsong-Popov, R., and Weiss, R. A. (1983) Human T-cell leukemia virus type I: induction of syncytia and inhibition by patients' sera, *Int J Cancer 32*, 321-328.

139. Miyoshi, I., Kubonishi, I., Yoshimoto, S., Akagi, T., Ohtsuki, Y., Shiraishi, Y., Nagata, K., and Hinuma, Y. (1981) Type C virus particles in a cord T-cell line derived by co-cultivating normal human cord leukocytes and human leukaemic T cells, *Nature 294*, 770-771.

140. Miyoshi, I., Kubonishi, I., Yoshimoto, S., and Shiraishi, Y. (1981) A T-cell line derived from normal human cord leukocytes by co-culturing with human leukemic T-cells, *Gann 72*, 978-981.

141. Iino, T., Takeuchi, K., Nam, S. H., Siomi, H., Sabe, H., Kobayashi, N., and Hatanaka, M. (1986) Structural analysis of p28 adult T-cell leukaemia-associated antigen, *J Gen Virol 67 (Pt 7)*, 1373-1379.

142. Brann, T. W., Dewar, R. L., Jiang, M. K., Shah, A., Nagashima, K., Metcalf, J. A., Falloon, J., Lane, H. C., and Imamichi, T. (2006) Functional correlation between a novel amino acid insertion at codon 19 in the protease of human immunodeficiency virus type 1 and polymorphism in the p1/p6 Gag cleavage site in drug resistance and replication fitness, *J Virol 80*, 6136-6145.

143. Borbat, P. P., Costa-Filho, A. J., Earle, K. A., Moscicki, J. K., and Freed, J. H. (2001) Electron spin resonance in studies of membranes and proteins, *Science 291*, 266-269.

144. Weil, J. A., J. R. Bolton, et al. (1972) Electron Spin Resonance: Elementary Theory and Practical Applications

145. Blackburn, M. E., Veloro, A. M., and Fanucci, G. E. (2009) Monitoring inhibitor-induced conformational population shifts in HIV-1 protease by pulsed EPR spectroscopy, *Biochemistry 48*, 8765-8767.

146. Galiano, L., Bonora, M., and Fanucci, G. E. (2007) Interflap distances in HIV-1 protease determined by pulsed EPR measurements, *J Am Chem Soc 129*, 11004-11005.

147. Hornak, V., Okur, A., Rizzo, R. C., and Simmerling, C. (2006) HIV-1 protease flaps spontaneously open and reclose in molecular dynamics simulations, *Proc Natl Acad Sci U S A 103*, 915-920.

148. Ishima, R., Freedberg, D. I., Wang, Y. X., Louis, J. M., and Torchia, D. A. (1999) Flap opening and dimer-interface flexibility in the free and inhibitor-bound HIV protease, and their implications for function, *Structure 7*, 1047-1055.

149. Hamelberg, D., and McCammon, J. A. (2005) Fast peptidyl cis-trans isomerization within the flexible Gly-rich flaps of HIV-1 protease, *J Am Chem Soc 127*, 13778-13779.

150. Perryman, A. L., Lin, J. H., and McCammon, J. A. (2004) HIV-1 protease molecular dynamics of a wild-type and of the V82F/I84V mutant: possible contributions to drug resistance and a potential new target site for drugs, *Protein Sci 13*, 1108-1123.

151. Hubbell, W. L., McHaourab, H. S., Altenbach, C., and Lietzow, M. A. (1996) Watching proteins move using site-directed spin labeling, *Structure 4*, 779-783.

152. Rabenstein, M. D., and Shin, Y. K. (1995) Determination of the distance between two spin labels attached to a macromolecule, *Proc Natl Acad Sci U S A 92*, 8239-8243.

153. Yoshida, M., Miyoshi, I., and Hinuma, Y. (1982) A retrovirus from human leukemia cell lines: its isolation, characterization, and implication in human adult T-cell leukemia (ATL), *Princess Takamatsu Symp 12*, 285-294.

154. Satcher, D. (1995) Emerging infections: getting ahead of the curve, *Emerg Infect Dis 1*, 1-6.

155. Ewald, P. W. (1996) Guarding against the most dangerous emerging pathogens, *Emerg Infect Dis 2*, 245-257.

156. Matsushita, K., Matsumoto, T., Ohtsubo, H., Fujiwara, H., Imamura, N., Hidaka, S., Kukita, T., Tei, C., Matsumoto, M., and Arima, N. (1999) Long-term maintenance combination chemotherapy with OPEC/MPEC (vincristine or methotrexate, prednisolone, etoposide and cyclophosphamide) or with daily oral etoposide and prednisolone can improve survival and quality of life in adult T-cell leukemia/lymphoma, *Leuk Lymphoma 36*, 67-75.

157. Mueller, B. U. (1997) Antiviral chemotherapy, *Curr Opin Pediatr 9*, 178-183.

158. Morris-Jones, S., Moyle, G., and Easterbrook, P. J. (1997) Antiretroviral therapies in HIV-1 infection, *Expert Opin Investig Drugs 6*, 1049-1061.

159. McDonald, C. K., and Kuritzkes, D. R. (1997) Human immunodeficiency virus type 1 protease inhibitors, *Arch Intern Med 157*, 951-959.

160. Deeks, S. G., and Volberding, P. A. (1997) HIV-1 protease inhibitors, *AIDS Clin Rev*, 145-185.

161. Carpenter, C. C., Fischl, M. A., Hammer, S. M., Hirsch, M. S., Jacobsen, D. M., Katzenstein, D. A., Montaner, J. S., Richman, D. D., Saag, M. S., Schooley, R. T., Thompson, M. A., Vella, S., Yeni, P. G., and Volberding, P. A. (1997) Antiretroviral therapy for HIV infection in 1997. Updated recommendations of the International AIDS Society-USA panel, *JAMA 277*, 1962-1969.

162. Eron, J. J., Jr., Ashby, M. A., Giordano, M. F., Chernow, M., Reiter, W. M., Deeks, S. G., Lavelle, J. P., Conant, M. A., Yangco, B. G., Pate, P. G., Torres, R. A., Mitsuyasu, R. T., and Twaddell, T. (1996) Randomised trial of MNrgp120 HIV-1 vaccine in symptomless HIV-1 infection, *Lancet 348*, 1547-1551.

163. Markowitz, M., Saag, M., Powderly, W. G., Hurley, A. M., Hsu, A., Valdes, J. M., Henry, D., Sattler, F., La Marca, A., Leonard, J. M., and et al. (1995) A preliminary study of ritonavir, an inhibitor of HIV-1 protease, to treat HIV-1 infection, *N Engl J Med 333*, 1534-1539.

164. Kazanji, M. (2000) HTLV type 1 infection in squirrel monkeys (Saimiri sciureus): a promising animal model for HTLV type 1 human infection, *AIDS Res Hum Retroviruses 16*, 1741-1746.

165. Lairmore, M. D., Silverman, L., and Ratner, L. (2005) Animal models for human T-lymphotropic virus type 1 (HTLV-1) infection and transformation, *Oncogene 24*, 6005-6015.

BIOGRAPHICAL SKETCH

Ahu Demir was born in June of 1982 in Ankara, Turkey. She completed high school at Cumhuriyet High School in Ankara in June of 2000. Ahu began her undergraduate work in October of 2000 at the Hacettepe University, Ankara, majoring in Chemistry. Ahu began her research career under the tutelage of Dr. Adil Denizli, studying the folding of tRNAs for three years. Her senior year she worked for Mining Inc. as a laboratory technician, learning the atmosphere of an industrial work setting. In May 2004 Ahu graduated with a B.S. in Chemistry. In January 2005 Ahu joined the Chemistry Department in the College of Life and Science at the University of Florida in Gainesville, Florida. She started working with Dr. Steven Benner on 2005 until his leave. In February 2006 Ahu joined the laboratory of Distinguished Professor Dr. Ben M. Dunn. She spent four years characterizing novel proteins for Human T-cell Leukemia Virus-1 Protease, gaining invaluable research and teaching skills. She received her PhD from University of Florida in the fall of 2010.